AFRICA CENTER OF EXCELLENCE FOR WATER MANAGEMENT

ADDIS ABABA UNIVERSITY

REMOTE SENSING BASED EVAPOTRANSPIRATION MODELLING FOR IRRIGATION PERFORMANCE ASSESSMENT IN JEDEB WATERSHED, UPPER BLUE NILE BASIN, ETHIOPIA

BY:

YILKAL GEBEYEHU MEKONNEN (GSR/3929/13)

Supervisors: Dr Tena Alamirew and Dr Abebe Demissie Chukalla

A Dissertation Submitted to Africa Center of Excellence for Water Management, Addis Ababa University, in Partial Fulfillment of the Requirements for the Degree of Doctor of Philosophy in Water Management (Doctoral Program in Hydrology and Water Resources Management)

OCTOBER, 2024

ADDIS ABABA

AFRICA CENTER OF EXCELLENCE FOR WATER MANAGEMENT

ADDIS ABABA UNIVERSITY

REMOTE SENSING BASED EVAPOTRANSPIRATION MODELLING FOR IRRIGATION PERFORMANCE ASSESSMENT IN JEDEB WATERSHED, UPPER BLUE NILE BASIN, ETHIOPIA

BY:

YILKAL GEBEYEHU MEKONNEN (GSR/3929/13)

Supervisors: Dr Tena Alamirew and Dr Abebe Demissie Chukalla

A Dissertation Submitted to Africa Center of Excellence for Water Management, Addis Ababa University, in Partial Fulfillment of the Requirements for the Degree of Doctor of Philosophy in Water Management (Doctoral Program in Hydrology and Water Resources Management)

OCTOBER, 2024

ADDIS ABABA

Declaration of the Author

I, Yilkal Gebeyehu Mekonnen (GSR/3929/13), hereby declare that this research dissertation entitled **Remote Sensing based Evapotranspiration Modelling for Irrigation Performance Assessment in Jedeb Watershed, North Western Ethiopia** has been developed by me, original work and has not been submitted to any other institution for the award of any academic qualification. The content of the dissertation has not been plagiarized, and where works of other researchers have been used, they have been appropriately cited.

The following parts of this dissertation work have been published in a peer-reviewed journal:

1. Mekonnen, Y.G., Alamirew, T., Chukalla, A.D., Hunegnaw, A.T., Malede, D.A., 2024. Comparison of Google Earth Engine Machine Learning Algorithms for Mapping Smallholder Irrigated Areas in a Mountainous Watershed, Upper Blue Nile Basin, Ethiopia. Journal of the Indian Society of Remote Sensing 52. https://doi.org/10.1007/s12524-024-01846-w.
2. Mekonnen, Y.G., Alamirew, T., Tadesse, K.B., Chukalla, A.D., 2024. Monitoring small-scale irrigation performance using remote sensing in the Upper Blue Nile Basin, Ethiopia. Agricultural Water Management 300, 108928. https://doi.org/10.1016/j.agwat.2024.108928.
3. Mekonnen, Y.G., Alamirew, T., Malede, D.A., Pareeth, S., Bantider, A., Chukalla, A.D., 2024. Tailoring the surface energy balance algorithm for land-improved (SEBALI) model using high-resolution land/use land cover for monitoring actual evapotranspiration. *Agricultural Water Management*, 303, 109058. https://doi.org/10.1016/j.agwat.2024.109058
4. Mekonnen, Y.G., Alamirew, T., Chukalla, A.D., Malede, D.A., Yalew, S.G., Mengistu, A.F., 2024. Remote sensing in hydrology: A systematic review of its applications in the upper Blue Nile Basin, Ethiopia. *HydroResearch*. https://doi.org/10.1016/j.hydres.2024.09.002

Ph.D. Candidate's Name	Signature	Date
Yilkal Gebeyehu Mekonnen	_____	_____

Acknowledgments

First of all, I greatly thank the Almighty God, Creator and master of the Universe, for giving me health, endurance, and power to complete this study.

I sincerely appreciate my supervisors, Dr. Tena Alamirew and Dr. Abebe Demissie Chukalla, for their invaluable guidance throughout my research journey. Their expertise and unwavering support have been instrumental in shaping the direction and quality of my work.

I want to express my sincere thanks to Balew Yibel, Animut Enawgaw, and Alene Goshu for their invaluable help with hydrological data. I am thankful to Dr. Amare Bantider, Dr. Sajid Pareeth, Dr Kassahun Birhanu, Dr. Sileshi G. Yalew, and Dr Tsigemariam Bashe for the reviews provided. Their insights and expertise have been crucial in shaping the direction of my work.

I would also like to acknowledge my fellow students for their collaboration throughout this academic journey. My friends Dr Demelash Ademe, Alebel Melaku, and Yohannes Kebede, for their insightful discussions and courage, have enriched the intellectual environment of my research. Special recognition goes to Dr. Aramde Fetene, whose encouragement has been a guiding force since my undergraduate years, playing a significant role in my academic and professional development.

I am grateful to the Africa Center of Excellence for Water Management (ACEWM), Addis Ababa University, for the financial support that has enabled me to pursue this research. I am also so thankful to Debre Markos University for allowing and providing me with the opportunity to learn for the last four years.

Finally, I am deeply grateful to my family: my wife Nitsuh Worku, my little boy Abel Yilkal, my mother Adanech Mehari, brothers Dessie and Temesgen, and sisters Laway, Masresha, and Tirunesh for their support and love throughout this academic pursuit. Their encouragement has been a constant source of motivation, and I am indebted to them for their belief in my capabilities.

Dedication

This Ph.D. dissertation is dedicated to my late father, Ato Gebeyehu Mekonnen.

Table of Contents

List of Tables

List of Figures

Acronyms and Abbreviation

DEM	Digital Elevation Model
EC	Eddy Covariance
ET	Evapotranspiration
ETa	Actual Evapotranspiration
EMI	Ethiopian Meteorology Institute
GCP	Ground Control Points
GEE	Google Earth Engine
GIS	Geographic Information System
GPS	Global Positioning System
LULC	Land Use /Land Cover
LULCC	Land Use /Land Cover Change
MAE	Mean Absolute Error
MoWE	Ministry of Water and Energy
NSE	Nash-Sutcliffe coefficient of efficiency
PBias	Percentage of bias
R^2	Coefficient of Determination
RMSE	Root Mean Square Error
SAR	Synthetic Aperture Radar
SCS CN	Soil Conservation Service's Curve Number
SEBALI	Surface Energy Balance for Land – Improved
SRTM	Shuttle Radar Topographic Mission
SWAT+	Soil and Water Assessment Tool
WaPOR	Water Productivity Open-access Portal

Abstract

Accurate actual evapotranspiration (ETa) data, alongside irrigated area maps, are important for assessing temporal and spatial irrigation performance indicators, which are critical for improving water resource monitoring, management, and sustainability. This study compared machine learning algorithms on the Google Earth Engine platform (GEE) in irrigated area mapping, customized the surface energy balance for land–improved (SEBALI) model using high-resolution land use/cover (LULC) data and implementation in Python, and evaluated the performance of a small-scale irrigation scheme using remote sensing (RS) and ground truth data in northwestern Ethiopia over two irrigation seasons. The study used Sentinel-1, Sentinel-2, and Landsat 8 satellite data and European Centre for Medium-Range Weather Forecasts (ECMWF) Reanalysis v5 (ERA5) climatic data as the main inputs. The accuracy of irrigated area mapping was evaluated relative to the inputs and agroecology, and the accuracy was improved by incorporating monthly SAR and vegetation index data. Random forest was a consistent classifier in different agroecological zones and inputs. The Python version of the SEBALI model (SEBALIGEEpy) was validated over croplands using publicly available AmeriFlux flux tower eddy covariance data. In addition, the ETa from SEBALIGEEpy was compared with the ETa simulated using the Soil & Water Assessment Tool Plus (SWAT+) model, which was calibrated with observed discharge, and with the FAO's remote-sensing based Water Productivity Open Access Portal (WaPOR). The results show that SEBALIGEEpy provides more accurate evapotranspiration estimates with fewer missing records and has the potential to be used for agricultural water management. Thus, the performance indicators, including equity, adequacy, overall consumed ratio (OCR), and productivity, were evaluated using SEBALIGEEpy results and ground truth data. The scheme showed good equity, with coefficient of variation (CV) values of 1.90 and 1.63 for the two seasons, alongside satisfactory water distribution among fields and within the field. The overall consumed ratio (OCR) was 0.54 and 0.43 for the two seasons. The mean crop water productivity (CWP) of wheat estimated from SEBALIGEEpy was 2.49 kg/m^3. This study revealed the potential of using remote sensing to evaluate irrigation performance and water productivity per field within small-scale irrigation schemes.

Keywords: Google Earth Engine; Smallholder Irrigation; Machine Learning; Python; Remote Sensing; SEBALIGEEpy

1. INTRODUCTION

1.1. Background

Reliable spatial and temporal information on irrigated area extent, consumptive use or actual evapotranspiration (ETa), and water productivity (WP) is essential in agricultural water management at the field and irrigation scheme levels (Foster et al., 2020; Modanesi et al., 2022; Singh et al., 2020). However, direct measurement of ETa requires continuous updates, advanced instrumentation, and methods and is extremely time-consuming and expensive. Estimating ETa and WP is difficult since they are controlled by various climatic factors, human activities, and watershed ecohydrological processes (Zhao et al., 2020).

Advances in remote sensing capabilities have helped researchers collect expensive and challenging representative spatial and temporal data for watershed-scale modeling (Dile et al., 2018). It can be coupled with the water-energy balance, allowing the estimation of irrigation volumes (Zappa et al., 2021). It also enables accurate mapping of irrigated areas for precise water allocation, improving our understanding of the water budget and improving crop and hydrological model simulations (Chawla et al., 2020). Remote sensing methodologies are considered innovative tools for monitoring irrigation schemes to improve land and water productivity amid the growing competition for land and water resources (Chukalla et al., 2022).

Satellite-based ETa estimation approaches are based on solving the surface energy balance equation with varying levels of complexity. The surface energy balance algorithm for land (SEBAL) (Bastiaanssen et al., 1998a, 1998b), surface energy balance systems (SEBS) (Su, 2002), two-source energy balance approach (TSEB) (Norman et al., 1995), mapping evapotranspiration at high resolution and with internalized calibration (METRIC) (Allen et al., 2007), and simplified surface energy balance (SSEB) (Senay et al., 2013, 2007) are among the most commonly used algorithms. Among these models, SEBAL-improved (SEBALI) (Mhawej et al., 2020a, 2020b) is the latest improvement over the most commonly used SEBAL and METRIC models.

The use of remote sensing data for hydrometeorological studies allows for a more distributed representation of the catchment than the standard in situ network of sensors. Processing remote sensing information over a large area and a wide range of temporal coverages requires considerable computational time in the case of complex spatiotemporal analysis at fine resolution. For this

reason, the open-access GEE platform, which offers a wide range of preprocessed datasets from various sources, can be used for this type of analysis (Gorelick et al., 2017). The GEE platform has been used for a wide range of hydrological studies at the global and local levels, including actual evapotranspiration estimation (Abunnasr et al., 2022; Allen et al., 2015; Jaafar et al., 2022; Laipelt et al., 2021; Mhawej and Faour, 2020; Senay et al., 2022), irrigated area mapping (Deines et al., 2019; Ketchum et al., 2020; Magidi et al., 2021; Zhang et al., 2022; Zurqani et al., 2021), land use/land cover change analysis (Bathe and Patil, 2024; Biswas et al., 2023; Deng et al., 2019; Farhan et al., 2024; Svoboda et al., 2022), irrigation performance assessment (Poudel et al., 2021), drought monitoring (Bayissa et al., 2021, 2017; Khan et al., 2021), wetland mapping (Hird et al., 2017; Long et al., 2021), flood monitoring (Liu et al., 2018), soil erosion assessment (Aldiansyah and Wardani, 2024; Elnashar et al., 2021; Sentani et al., 2024; Sud et al., 2024; Wang and Zhao, 2020) and reservoir monitoring (Kansara et al., 2021).

The estimation of water productivity using remote sensing requires the estimation of crop yield (Elshaikh et al., 2018). To estimate the crop yield across an irrigation scheme, the volume of biomass produced and a detailed irrigated area map with the crops grown are necessary (Sawadogo et al., 2020). Irrigated area mapping approaches have been developed in parallel with the advancement of remote sensing technology in terms of radiometric, spatial, and spectral resolutions and computing capabilities. The availability of synthetic aperture radar (SAR) data offers new opportunities for irrigation monitoring by allowing observations under any weather condition (Gao et al., 2018). Recent studies on irrigation mapping have focused on the synergistic use of machine learning methods and high-resolution remote sensing data (Massari et al., 2021).

Platforms such as GEE increase the capabilities of scientific analysis and visualization of geospatial datasets, addressing the challenges of big data analysis (Gorelick et al., 2017). Open-access remote sensing data from GEE has a large collection of datasets for earth science and satellite imagery, both current and historical, that can be used as a key tool for water use monitoring in irrigated agriculture with weak in situ water use monitoring infrastructure.

This research aimed to evaluate the performance of machine learning algorithms for mapping irrigated areas and customize the automated SEBALIGEE model using high-resolution land cover data to enhance its performance for small agricultural fields in the Jedeb watershed. The SEBALIGEE model was rewritten in Python to broaden its accessibility and facilitate integration

with existing libraries and tools. This study assessed the performance of the SEBALIGEE model by comparing its estimates with the SWAT+ model calibrated with observed streamflow data from the Jedeb watershed. The ETa estimates were also validated with eddy covariance (EC) data from AmeriFlux sites over agricultural lands and compared with WaPOR data from the Koga irrigation scheme. Furthermore, the performance of the Shumbrit irrigation scheme was assessed by integrating remote sensing and in situ measurements.

1.2. Statement of the Problem

Anthropogenic pressure and climate change affect water resource availability, demanding efficiency of crop yield per unit of water consumed (Ghorbanpour et al., 2022; Malede et al., 2022b). The performance of irrigation schemes in Ethiopia is far below expectations, as measured by various relevant indicators, and schemes do not function at their optimal capacity (Agide et al., 2016; Amede, 2015; Awulachew and Ayana, 2011; Gebul, 2021). Improving water management requires assessing an irrigation scheme's performance using reliable and up-to-date information about the land and water resources used in irrigated agricultural areas (Chukalla et al., 2022; Zurqani et al., 2021). However, the majority of agricultural water use is usually not properly monitored, or a limited assessment of irrigation water consumption is performed (Foster et al., 2020).

Remote sensing is becoming a viable alternative for agricultural water management, offering innovative solutions to enhance the efficiency and sustainability of irrigation practices in the digital era (Bwambale et al., 2022; Ferreira et al., 2021; Manivasagam, 2024; Sawadogo et al., 2020). However, the implementation of remote sensing-based methodologies faces several challenges, including variations in the spatial and temporal resolutions of inputs, low accuracy due to cloud cover, limitations in data processing expertise and computational resources, and a lack of in situ irrigation water measurements for validation (Ajaz et al., 2019; Blatchford et al., 2020b; Gupta et al., 2022). Additionally, monitoring smallholder irrigated areas using remote sensing is challenged by the dynamic spatiotemporal patterns of sowing, harvesting, and irrigation application (Vogels et al., 2020). Moreover, the performance of models for ETa estimation (a key component in irrigation monitoring) varies on the basis of input data, model structure, and parameter estimation methods, which is challenging to verify in fragmented smallholder-dominated areas with limited

data availability (Bai, 2023). These challenges underscore the need for innovative approaches to overcome data limitations and improve irrigation monitoring in these areas.

GEE provides a scalable and low-cost solution to fill widespread gaps in monitoring irrigation water use, bypassing the technical, socioeconomic, and political challenges that have constrained in situ metering (Foster et al., 2020; Mhawej and Faour, 2020; Poudel et al., 2021). The GEE platform overcomes the limitations of local computing infrastructure, making advanced remote sensing and data analysis accessible (Amani et al., 2020). In Ethiopia, the GEE has been used for various hydrological studies. For example, Vogels et al. (2020) quantified monthly irrigation water consumption at the field level using MODIS evapotranspiration products in the Central Rift Valley. Kansara et al. (2021) monitored water level changes by filling the Grand Ethiopian Renaissance Dam (GERD) reservoir using Sentinel-1 SAR time-series data and classifying water pixels from June 2017 to September 2020. Abebe et al. (2021) used the GEE platform to map land use and land cover changes from 1986, employing a random forest algorithm for a holistic environmental flow assessment at the Gumara River, Lake Tana subbasin. Despite these advancements, research on applying GEE for small-scale irrigation scheme monitoring needs to be explored.

1.3. Research Questions

On the basis of the problems stated, this study strived to answer the following research questions:

1. Which machine learning algorithm of the GEE is more accurate for mapping small-scale irrigation in Ethiopian highlands?
2. How accurately does the SEBALI algorithm estimate actual evapotranspiration?
3. How capable is remote sensing for assessing the irrigation performance of a small-scale irrigation scheme?
4. What are the spatial and temporal variations in the agricultural performance of small-scale irrigation schemes in the Jedeb watershed?

1.4. Research Objectives

To address the problems mentioned in the previous research questions, the major goal of this research is, therefore, to assess the potential of earth observation satellites for agricultural water management in the data-scarce Upper Blue Nile highlands of Ethiopia.

The specific objectives of this study are as follows:

- To evaluate image classification algorithms in the GEE platform to map irrigated areas,
- To validate the SEBALI model's performance in estimating actual evapotranspiration on irrigated croplands,
- To evaluate the spatiotemporal agricultural performance of a small-scale irrigation scheme.

1.5. Significance of the study

The findings of this study and the freely available code base will be important to policymakers, irrigation managers, and researchers as a baseline by providing an irrigation extent mapping methodology at a 10 m resolution that can be scaled up to a target area. Additionally, the automated high-resolution ETa compatible with smallholder irrigation or any watershed for different hydrological and agricultural water management applications can be extracted by simply providing a boundary or extent of the area of interest. Moreover, this study has broadened the applicability of the SEBALI model by rewriting it in Python, increasing its accessibility and facilitating integration with other libraries and tools. The study also provided a framework to assess the performance of a small-scale irrigation scheme with limited data availability using the GEE platform, which is essential for sustainable land and water management, especially where field data are too scarce.

1.6. Scope and Limitations of the Study

The scope of this study was limited to evapotranspiration modeling and performance assessment of irrigation schemes in the Jedeb River watershed. This research is one of the first attempts to operationalize the SEBALI model for assessing the irrigation performance of small-scale irrigation schemes. While adapting the model and assessing irrigation performance, the study did not consider the scheme's hydraulic aspects and service delivery. Hydrometeorological and spatial data

were used in the Jedeb River watershed for hydrological modeling to evaluate the performance of the SEBALI model in estimating ETa. This study was limited to evaluating the SEBALI model from 2015/16 to 2021/2022 and monitoring irrigation performance for the 2021/22 and 2022/23 irrigation seasons. Additionally, the study was limited to the biophysical aspects, and a socioeconomic performance assessment still needs to be performed. This is due to the availability of Sentinel-2 satellite images, which are used as the major input in the modeling process.

1.7. Structure of the Dissertation

This study investigated the use of remote sensing in agricultural water resource management in the Jedeb watershed, Upper Blue Nile/Abbay River Basin of Ethiopia, a region critical for the country's agricultural sustainability. This dissertation has been organized from chapters 1 to 5.

Chapter 1 introduces the topic and illustrates current research issues and the importance of remote sensing in agricultural water management. It also presents the research questions, general and specific objectives, significance, scope, and limitations of the study.

Chapter 2 reviews the relevant literature on remote sensing applications in Abbay/Upper Blue Nile hydrology, machine learning algorithms for irrigated area mapping, the use of GEE and remote sensing for actual evapotranspiration and water productivity, remote sensing-based irrigation performance assessment, and the challenges of using remote sensing in hydrology and water resource management.

Chapter 3 describes the study area, including location, topography, climate, hydrology, LULC, soil, geological information, and irrigation development. It also discusses the data sources and methods applied for irrigated area mapping, evapotranspiration modeling, and irrigation performance assessment.

Chapter 4 presents the results and discussion for each objective of the study conducted.

Chapter 5 presents the conclusion and highlights the recommendations for further research.

2. LITERATURE REVIEW

2.1. Remote Sensing Applications in Upper Blue Nile Hydrology and Water Management

The management of water resources requires continuous monitoring of the dynamics of water availability, use, and vulnerability across different spatial and temporal dimensions (Alemu et al., 2022; Chawla et al., 2020). However, water resource management is challenged by data scarcity worldwide, especially in arid and high-altitude regions such as the Upper Blue Nile (UBN) Basin, where in situ hydrometeorological monitoring networks are found in towns along main roads (Dile et al., 2018). The UBN basin is vulnerable to extreme climatic conditions and faces increasing pressure from the growing population projected to continue to expand significantly (Allam et al., 2016; Seyoum, 2018). With increasing human activities in the basin and increasing water and land demand for agriculture and industry, effective management is necessary (Salama et al., 2022). The UBN basin is one of the most data-scarce basins, and the lack of long-term hydroclimatic data is a major research challenge (Abera et al., 2017; Dile et al., 2018). This scarcity of ground observation data poses a significant challenge for accurately assessing current water conditions and conducting comprehensive planning, which includes predicting the future impacts of potential developments and climate change (Worqlul et al., 2017). As such, remote sensing data are increasingly contributing, particularly in research studies.

Remote sensing plays a critical role in hydrological studies, particularly in inaccessible areas with limited ground-based observations due to constraints in infrastructure and resources. It offers real-time and cost-effective information, capturing the spatiotemporal dynamics of water balance components (Chawla et al., 2020; Dile et al., 2020; Duan et al., 2021). A wealth of satellite missions have been launched, offering datasets covering every geoscience sphere and providing massive amounts of data for studying hydrology. The open-access availability of Landsat data since 2008 has transformed hydrological analyses, enabling significantly large coverage and higher-resolution studies and advancing scientific and practical advancements (Wulder et al., 2022). The recent freely available high-resolution Sentinel 1 and 2 satellites have further increased the application of remote sensing in hydrology, enabling smarter decisions and fostering water sustainability (Sheffield et al., 2018; Zeng et al., 2023).

Remote sensing has been extensively utilized in various hydrological applications in the UBN basin, including estimating rainfall amounts (Andualem et al., 2020; Ayehu et al., 2018; Bayissa et al., 2017; Belete et al., 2020; Fenta et al., 2014; Taye et al., 2023), the LULCC (Assefa et al., 2022; Dubeau et al., 2017; Teferi et al., 2010), ET modeling (Alemu et al., 2015a; Allam et al., 2016), drought assessment (Bayissa et al., 2021, 2019, 2017; Taye et al., 2020), estimating aerosol optical depth (Getachew et al., 2020), monitoring soil moisture (Ayehu et al., 2020), forecasting floods (Gashu et al., 2023), estimating water quality (Ayana et al., 2015), assessing irrigation performance (Bashe et al., 2023; Mekonnen et al., 2024), and planform change (Abebe and Mulat, 2021).

Performance evaluation of satellite rainfall products have been conducted at different scales, including the Nile (eastern) basin level (Abdelmoneim et al., 2020; Abdelwares et al., 2020; Senay et al., 2014); the UBN basin level (Bayissa et al., 2017; Sahlu et al., 2016); subbasin level, including Lake Tana and South Gojjam (Malede et al., 2022a); and the watershed level, including Gilgel Abay (Bitew and Gebremichael, 2011; Habib et al., 2014; Worqlul et al., 2018), Beles (Worqlul et al., 2018), Koga (Bitew and Gebremichael, 2011), and Ribb (Belete et al., 2020). Notably, the Gilgel Abay watershed is the most studied watershed in the basin. Performance was assessed using three methods: direct comparison with rain gauge observations (point to pixel or area) (Ayehu et al., 2018; Malede et al., 2022a; Taye et al., 2023), integration into a hydrologic model for rainfall-runoff simulation (Belayneh et al., 2020; Belete et al., 2020; Bitew and Gebremichael, 2011; Lakew et al., 2020, 2017; Worqlul et al., 2018), drought assessment models (Bayissa et al., 2021, 2017), and machine learning methods (Alquraish and Khadr, 2021; Nourani et al., 2021; Wegayehu and Muluneh, 2023). The easiest and most commonly used method is a point-to-pixel or area approach.

Studies have indicated a predicted increase in agricultural and urban land and a decrease in natural forest land throughout the UBN basin. The expansion of cultivated land and declines in woodland coverage, urbanization, and deforestation have led to increased erosion, sedimentation, and flooding, affecting water resource availability and socioeconomic development (Tekleab et al., 2014; Woldesenbet et al., 2017). Changes in LULC have also altered the water balance, affecting rainfall, evaporation, and runoff and influencing surface runoff generation and groundwater flow (Leta et al., 2022; Malede et al., 2022c).

Remote sensing-based ET has been studied in the UBN basin (Alemu et al., 2015b, 2014; Allam et al., 2016; Ayana and Srinivasan, 2019; Bastiaanssen et al., 2014; Blatchford et al., 2020a; Dile et al., 2020; Hu and Mo, 2022; Nooni et al., 2019; Salama et al., 2022; Senay et al., 2009; Tegegne et al., 2021; Zeng et al., 2022). Senay et al. (2009) studied the water balance dynamics in the Nile basin using daily ET estimates using the VegET model. Alemu et al. (2014) used the operational simplified surface energy balance (SSEBop) (Senay et al., 2013) and MODIS Global Terrestrial Evapotranspiration (MOD16) (Mu et al., 2011) to characterize the variation in ET and investigate its relationship with vegetation productivity in the Nile Basin for 2002–2011. Dile et al. (2020) evaluated Advanced Very High-Resolution Radiometer (AVHRR) ET (Zhang et al., 2010) and MOD16 ET estimates for hydrological applications using SWAT in ten mesoscale watersheds in the UBN basin. Zeng et al. (2022) used Penman–Monteith-Leuning (PML) (Zhang et al., 2019) and SSEBop products to study the contributions of natural factors and human activities to ET using the random forest regressor (RFR) algorithm. The Global Land Evaporation Amsterdam Model (GLEAM) ET product was also used to analyze spatiotemporal variations in ET over the Nile Basin (Nooni et al., 2019). The products assessed have a temporal resolution of daily to decadal and a spatial resolution of 30 m to 0.25° (27.8 km at the equator). Bashe et al. (2023) used the surface energy balance algorithm for land (SEBAL) model to assess irrigation performance in the Koga irrigation scheme.

Various methods have been employed to validate ETa estimates, including random forest regression (Zeng et al., 2022), measurements from a lysimeter system (McNamara et al., 2021), the Budyko curve (ET Budyko) as a reference (Weerasinghe et al., 2020), and water balance models (Ayana and Srinivasan, 2019; Blatchford et al., 2020a; Dile et al., 2020; Weerasinghe et al., 2020). Validation was also performed through comparisons with independent field measurements (Tegegne et al., 2021) and FLUXNET data from other sites in the Nile basin (Nooni et al., 2019). Scale mismatch, canopy heterogeneities, and measurement problems are identified as causes of inconsistency (Blatchford et al. 2020). Compared with remote sensing ET products such as MOD16 and SSEBop, simulated monthly ET (Ayana and Srinivasan 2019). The AVHRR ET performed better than the MOD16 actual ET in replicating the SWAT-simulated actual ET (Dile et al., 2020). PMLv2 and WaPORv2.1 were identified as the best-performing products (McNamara et al., 2021). It is widely acknowledged that higher-resolution products generally outperform coarser-resolution products (Weerasinghe et al., 2020).

Soil moisture is crucial in the prediction of productivity and management of both rainfed and irrigated agriculture, particularly in smallholder irrigation schemes (Sinshaw et al., 2020; Wu et al., 2014). Water balance models can be integrated with soil information derived from satellite images to monitor soil moisture with acceptable accuracy (Damtie et al., 2022). Soil moisture assessment using remote sensing has been performed in the UBN basin using different approaches and models (Abiy and Melesse, 2017; Ayehu et al., 2019; Damtie et al., 2022; Sinshaw et al., 2020). Abiy and Melesse (2017) assessed the spatial and temporal changes in soil moisture in the Lake Tana subbasin using downscaled GRACE data. The study suggested a general decrease in soil moisture and groundwater storage over time. Ayehu et al. (2019) developed a residual soil moisture prediction model using stepwise cluster analysis using a combination of Sentinel-1 SAR, MODIS NDVI, and DEM data as input parameters. Sinshaw et al. (2020) used the SWAT hydrological model along with Sentinel 2 satellite images and modified the normalized difference water index (MNDWI) combined with the OPtical TRApezoid Model (OPTRAM) model to estimate soil moisture. Damtie et al. (2022) used the water cloud model (WCM) model and Sentinel 1A data to estimate soil moisture.

2.2. Machine Learning Algorithms for Irrigated Area Mapping

Reliable information on the distribution of irrigated cultivated land is essential for grain yield estimation, water resource management, and drought risk assessment and for enhancing medium- to long-term land and water resource planning (Basukala et al., 2017; Ren et al., 2021; Xie and Lark, 2021; Zhu et al., 2024). Official reports on irrigated areas are unreliable because of inconsistent and inaccurate data collection methods and are often unavailable for public use (Ajaz et al., 2019). In addition, reports are not updated periodically, as enormous costs and time are required to enumerate irrigated land regularly (Massari et al., 2021). Satellite remote sensing is considered among the most effective means of earth observation and comprehensive information acquisition technology for mapping the extent of irrigation in an area (Xu et al., 2024).

Mapping small-scale irrigated agriculture in a complex landscape with fragmented cultivated plots managed by smallholder farmers in places such as Ethiopia is challenging (Mohammedshum et al., 2023; Vogels et al., 2019a). Doubts about the reliability of irrigated area mapping arise from variations in accuracy resulting from the spectral signature overlap between irrigated and non-

irrigated fields, methods, and datasets used for classification (Bwambale et al., 2022; Zhang et al., 2022). Irrigated areas can be mapped using single date or time series images during crop growth. Using a single date image is unreliable because it does not account for the spatial and temporal variations in planting dates (Gao et al., 2018). Studies have shown that temporally dense time series images improve classification accuracy (Demarez et al., 2019). The accuracy of mapping with optical time series is reduced in high-altitude and mountainous areas with contrasting climates because of high cloud cover (Demarez et al., 2019; Gao et al., 2018; Khatami et al., 2020). One possible way to overcome this challenge is to use a fusion of SAR data capable of penetrating clouds with optical imagery. The fusion of different datasets improved classification accuracy, as demonstrated in earlier studies (Bazzi et al., 2021; Demarez et al., 2019; Pageot et al., 2020; Zurqani et al., 2021). SAR is particularly important because of its sensitivity to changes in moisture content and is not affected by weather conditions or illumination (Bazzi et al., 2021; Massari et al., 2021; Modanesi et al., 2022). The use of vegetation indices, a combination of various vegetation indices, and the incorporation of ancillary precipitation and slope data improved the accuracy of irrigated area mapping (Abera et al., 2021; Deines et al., 2019; Magidi et al., 2021; Xiang et al., 2019; Zurqani et al., 2021).

Advancements in cloud-based spatial data management systems such as the Google Earth Engine (GEE) (Gorelick et al., 2017) have improved the speed and accuracy of irrigated area mapping (Deines et al., 2019; Ketchum et al., 2020; Magidi et al., 2021; Xie and Lark, 2021; Zhang et al., 2022; Zurqani et al., 2021). GEE allows rapid data processing without high-performance personal computers or much data storage space (Ferreira et al., 2021). Despite the improvements and widespread application of machine learning algorithms, conflicting results have been reported in studies comparing classification methods (Maxwell et al., 2018; Modanesi et al., 2022), thereby demanding a thorough evaluation of the accuracy and uncertainties of the classification algorithms.

Studies on mapping smallholder irrigated areas in many sub-Saharan African countries are limited and often underestimate the actual extent of smallholder irrigation. A case in point is Ethiopia (Chandrasekharan et al., 2021; Conlon et al., 2022; Mohammedshum et al., 2023; Vogels et al., 2019a, 2019b; Yimer et al., 2024). Yimer et al. (2024) used Sentinel-1 time series to map irrigated areas in the Bilate and Gumara watersheds using random forest classification. Abera et al. (2021) used SAVI and NDVI to distinguish irrigated and non-irrigated croplands in the Lake Tana Basin.

By applying the random forest (RF) algorithm and object-based image analysis using SPOT6 imagery, Vogels et al. (2019a) separated smallholder irrigation and large-scale irrigation in the Central Rift Valley. The International Water Management Institute (IWMI) conducted country-wide irrigated area mapping using Landsat 8, MODIS NDVI, CHIRPS precipitation, NDWI, and slope (Chandrasekharan et al., 2021). The existing studies have used limited and inconsistent algorithms, indices, and data sources. The accuracy of machine learning algorithms for mapping irrigated areas has yet to be thoroughly examined for smallholder farms, particularly mountainous areas. Therefore, it is necessary to evaluate the performance of machine learning classification algorithms concerning the inputs and spatiotemporal variations (Basheer et al., 2022; Conlon et al., 2022).

2.3. Remote Sensing based Actual Evapotranspiration Estimation using the Google Earth Engine Platform

Agricultural water management at the field and scheme levels requires spatiotemporal quantification of consumptive water use or actual evapotranspiration (ETa) (Anapalli et al., 2019). However, measuring ETa in the field is challenging because of the complex nature of the phenomenon, which is influenced by several factors, such as climatic conditions, human activities, and the ecohydrological processes of a watershed (Wanniarachchi and Sarukkalige, 2022). Additionally, field measurements of ETa are costly and limited in spatial and temporal coverage. Therefore, improving the practicality and accuracy of ETa estimation, such as via the use of emerging remote sensing technologies, is vital for sustainable agricultural water management. These enhancements ease water allocation in irrigation with reasonable accuracy and improve crop and hydrological model simulations (Elshaikh et al., 2018; Zappa et al., 2021).

Recent developments in remote sensing have eased the estimation of ETa by overcoming the limitations of expensive ground-based techniques and providing high-resolution spatial and temporal data with extensive coverage (Abiodun et al., 2018; Elsayed et al., 2022). A considerable number of evapotranspiration (ET) models have been developed to estimate ETa using remote sensing imagery and the surface energy balance principle. However, these models require extensive data storage and substantial computational resources (Mhawej and Faour, 2020).

Google Earth Engine (GEE) has enabled the implementation of various evapotranspiration (ET) models at high spatial and temporal resolutions. It achieves this goal by providing improved access to global imagery, geophysical, and climate datasets, resulting in faster data processing through its powerful computing resources and analysis tools (Gorelick et al., 2017; Pan et al., 2023). Different evapotranspiration models have been applied using the GEE platform (Abunnasr et al., 2022; Allen et al., 2015; Jaafar et al., 2022; Laipelt et al., 2021; Mhawej and Faour, 2020; Senay et al., 2022).

The accuracy of the ETa estimate is notably affected by the spatial resolution of the landcover dataset used, as it is a key parameter in determining the values attributed to biophysical properties (Abiodun et al., 2018; Fan et al., 2020). Higher-resolution landcover data allow a more detailed and realistic representation of the distributions and characteristics of different landcover classes, which in turn improves the estimation of ETa (Dile et al., 2020; Radeloff et al., 2024). Conversely, low spatial resolution landcover datasets can introduce significant uncertainties in ETa estimation, particularly for smallholder farmers and mountainous regions (Li et al., 2021). The MODIS land cover dataset is not capable of discriminating agricultural land used for hot/cold pixel selection because of subpixel heterogeneity, where a significant amount of sloping land is cultivated (Eggen et al., 2016; Leroux et al., 2014). Thus, the use of a higher-resolution landcover dataset is critical for accurately modeling agricultural water management in smallholder farming systems.

2.4. Assessment of Irrigation Performance via Remote Sensing

Water scarcity in irrigation areas is a concern, particularly in sub-Saharan Africa, where the combination of limited irrigation infrastructure and poor management contributes to inefficient water use and low water productivity (Eshete et al., 2020; Gebul, 2021; Sawadogo et al., 2020; Wamala et al., 2023). Only 18% of the irrigation projects in sub-Saharan Africa deliver over 75% of their planned irrigated area (Higginbottom et al., 2021). Addressing water scarcity can be achieved by improving irrigation efficiency, enabling more water available in fields to grow crops, thereby increasing overall performance and productivity (Abera et al., 2019; Pereira et al., 2012). Assessing the performance of existing irrigation systems is instrumental in realizing Sustainable Development Goals (SDGs 1 and 2), which state “end poverty in all its forms everywhere” and “end hunger, achieve food security and improved nutrition, and promote sustainable agriculture” (Poudel et al., 2021; Redicker et al., 2022).

Ensuring the sustainability of irrigated agriculture requires a thorough assessment of irrigation schemes' water management and increasing on-farm water use efficiency (Fernandez et al., 2020). This involves employing reliable and cost-effective methods to evaluate their performance in terms of irrigation service delivery and land and water resource use, as well as identifying areas for necessary interventions (Elshaikh et al., 2018; Eshete et al., 2020). The traditional approach to assess the performance of irrigation schemes relies on labor-intensive, costly, and time-consuming data measurements from field campaigns subjected to interference from the local population. Additionally, challenges arise from inadequate data quality and poor record-keeping systems (Eshete et al., 2020; Fernandez et al., 2020; Mamba and Shongwe, 2022; Sawadogo et al., 2020; Taghvaeian et al., 2018; Wamala et al., 2023).

Remote sensing data have been increasingly used as a cost-effective method for assessing irrigation performance globally (Ahadi et al., 2013; Ahmad et al., 2009; Akhtar et al., 2018; Awan et al., 2011; Bashe et al., 2023; Bastiaanssen and Bos, 1999; Chukalla et al., 2022; Karimi et al., 2019; Santos et al., 2010; Zwart and Leclert, 2010). Remote sensing offers an efficient means of evaluating irrigation performance, providing comprehensive spatial and temporal coverage, which is particularly beneficial for data-scarce regions such as Sub-Saharan Africa (Blatchford et al., 2020b). Remote sensing data, combined with little ground-based information, can provide valuable insights into the functioning of irrigation systems, identify areas of inferior performance, and guide improvements in water management practices (FAO and World Bank, 2022; Karatas et al., 2009).

In Ethiopia, efforts have been made to assess the performance of smallholder irrigation systems, mainly focusing on operational performance, such as the hydraulic performance of these schemes, through direct field measurements (Abera et al., 2019; Alemie et al., 2023; Awulachew and Ayana, 2011; Ayele et al., 2021; Haileslassie et al., 2016). However, the potential of remote sensing data for performance studies for evaluating small-scale irrigation schemes remains largely unexplored, with only a limited exploration of this approach (Bashe et al., 2023; Blatchford et al., 2020b). Remote sensing products, such as the FAO database to monitor water productivity through open access remotely sensed derived data (WaPOR), have been applied to analyze water productivity and performance assessment in irrigation schemes (Chukalla et al., 2022). However, the widely available WaPOR datasets at resolutions of 100 m and 250 m cannot capture irrigation variability and heterogeneity in the small-scale fields that dominate African agriculture. These datasets are

not recommended for plots smaller than 2 ha (Blatchford et al., 2020b). Thus, alternative high-resolution remote sensing ETa estimation methods are needed to assess the performance of fragmented small-scale irrigation fields. In addition, such assessment efforts require considering the infrastructure requirements for time series analysis, such as data storage and processing power, posing significant challenges.

2.5. Challenges of Using Remote Sensing Data in Hydrology and Water Management

Even though remote sensing is a desirable alternative to data-scarce regions such as the UBN basin, it faces several challenges. The absence of in situ data is needed for the validation and calibration of remote sensing estimates (Agutu et al., 2019; Seyoum, 2018). Additionally, there is a shortage of high-quality ground weather data (Wegayehu and Muluneh, 2023), resulting in inaccurate satellite precipitation estimation (Taye et al., 2023) and inaccessible scant in situ observations in high mountainous terrain (Bartsotas et al., 2018; Bayissa et al., 2021). Furthermore, there is limited availability of direct observations of data such as ET across Africa (Weerasinghe et al., 2020). The discontinuity of ground data due to topography and conflict limits the accuracy and consistency of measurements in remote areas (Belayneh et al., 2020).

Remote sensing data usage encounters various challenges, including limited spatial and temporal resolution, susceptibility to atmospheric interference, and the inability to penetrate dense cloud cover. These issues are further compounded by difficulties in detecting small-scale features, sensor inherent limitations, and distinguishing between land cover types with similar signatures. (Tamiru and Wagari, 2022; Tesfaye et al., 2023). Mixed land use can introduce inaccuracies in remote sensing data (Gumindoga et al., 2014). Measuring subsurface features and processes is another challenge (Agutu et al., 2019; Khaki and Awange, 2020). Remote sensing struggles with real-time data capture and penetrating dense vegetation, as highlighted by Anteneh et al. (2022) and Duguma & Duguma (2022). It cannot measure certain atmospheric variables, such as humidity and surface and subsurface runoff (Abera et al., 2017). The limited spatial resolution also affects measurement precision and the capability to provide detailed information on water quality or composition (Kansara et al., 2021). Near real-time monitoring is also hampered by limited spatial and temporal resolutions (Bayissa et al., 2021).

Expertise in remote sensing data interpretation and analysis is essential (Leta et al., 2022), but the interpretation of complex features poses difficulties, potentially leading to errors and inaccuracies (Andualem and Demeke, 2019; Duguma and Duguma, 2022). The acquisition and processing of high-resolution imagery is costly and time-consuming (Mekonnen et al., 2018). The limited availability of satellite images for certain periods and reliance on combining different data sources for analysis are additional challenges (Bewket, 2002). Some products suffer from minimal temporal coverage (Weerasinghe et al., 2020).

Uncertainties in sensor-derived parameters and a scale mismatch between remote sensing and ground measurements are critical issues (Blatchford et al., 2020a; Dile et al., 2020). Reliance on assumptions and parameterization in ET estimation methods for data interpretation introduces uncertainties and measurement problems in heterogeneous landscapes (Alemu et al., 2014; Blatchford et al., 2020a), and potential biases and uncertainties exist in satellite retrieval algorithms (Abdelmoneim et al., 2020; Gebremichael et al., 2010). Consequently, the accuracy and performance of remote sensing products vary across regions and seasons (Abera et al., 2016; Ahmad et al., 2020).

Integrating remote sensing with in situ data in hydrological studies provides a more comprehensive understanding of hydrological processes, enhancing the accuracy of models and improving the spatial and temporal coverage of hydrological variables (Abera et al., 2016; Ahmed et al., 2011; Ayehu et al., 2019; Lubczynski et al., 2024; Zou et al., 2017). Integration mechanisms include bias correction, data fusion from various sources, machine learning, and statistical downscaling (Jiang and Wang, 2019; Worqlul et al., 2018). However, the challenges include data compatibility due to differences in measurement techniques and formats, spatial and temporal mismatches, error propagation and uncertainty, and the choice of suitable data integration approach and hydrological model, which present additional research challenges (Ibrahim et al., 2024; Lakew, 2020).

3. MATERIALS AND METHODS

3.1. Study Area Description

3.1.1. Location and topography

This study focused on the Jedeb watershed, which originates at 3936 m and extends to the Temcha River at 1486 m above sea level. The watershed covers 867 km² across the Sinan, Machakel, Debre Elias, and Gozamin districts of the East Gojjam Zone of the Amhara Regional State of Ethiopia (Figure 3.1). The area of the watershed above the Yewula gauging stations is approximately 305 km². The Jedeb watershed is located around the northwest part of Debre Markos town and 302 km from Addis Ababa. The upstream part of the watershed is characterized by mountainous and highly separated terrain with steep slopes, whereas undulating topography and gentle slopes characterize the central and downstream parts (Asrade et al., 2024; Getnet and Mulu, 2021).

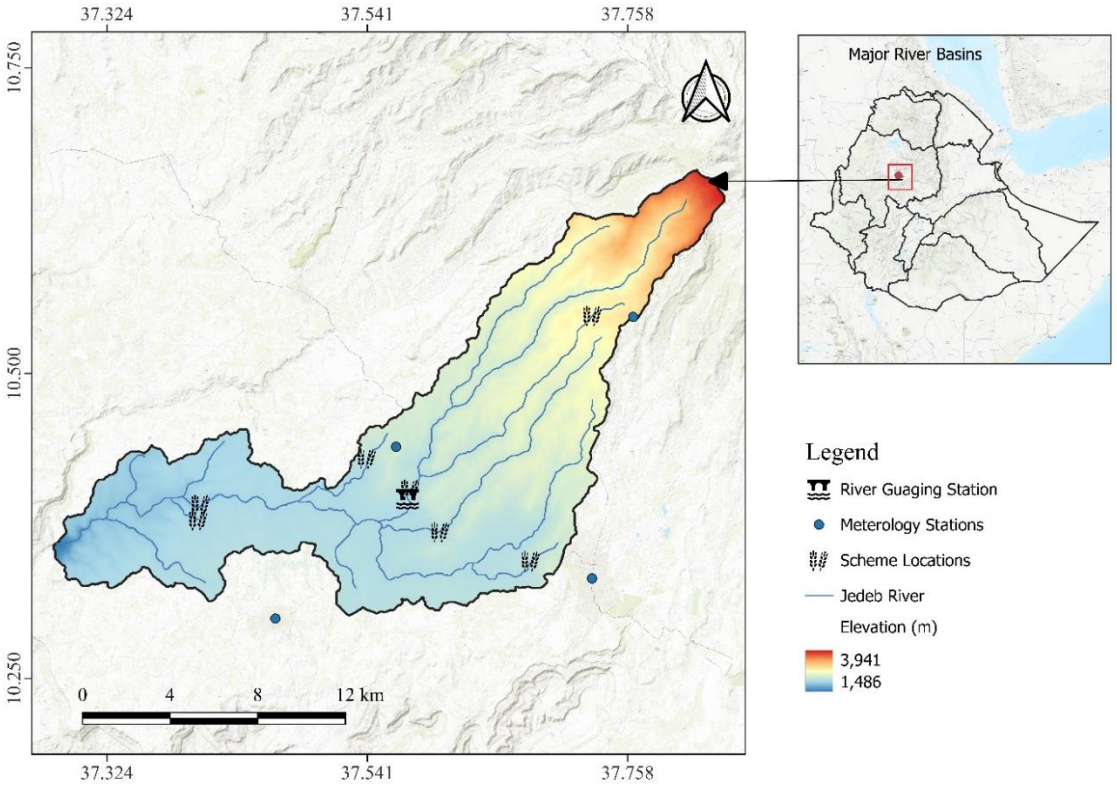

Figure 3-1. Location map of the Jedeb watershed with meteorological and hydrological gauging stations

3.1.2. Climate and hydrology

The climate of the Jedeb watershed belongs to the subtropical climate regime characterized by a highly uneven seasonal precipitation distribution (Figure 2.2). The area includes all traditionally classified agroecological zones: “wurch”, “dega”, and “woyna dega”. The area has three distinct seasons: the main rainy season, “Kiremit” (June--September), the dry spell “Bega” (October--February), and a short rainy period, “Belg” (March-May). The main rainy season, from June to September, accounts for more than 75% of the annual rainfall. The two rainy seasons in the region, the small Belg rains in spring and the main kiremt rains in summer have significant implications for agriculture (Ademe et al., 2021). The area's long-term mean annual minimum and maximum temperatures are 10.44°C and 24.27°C, respectively. The long-term mean annual rainfall of the watershed is 1371 mm, and the mean annual discharge in the Jedeb catchment is 7.9 m^3/s (Tekleab et al., 2015).

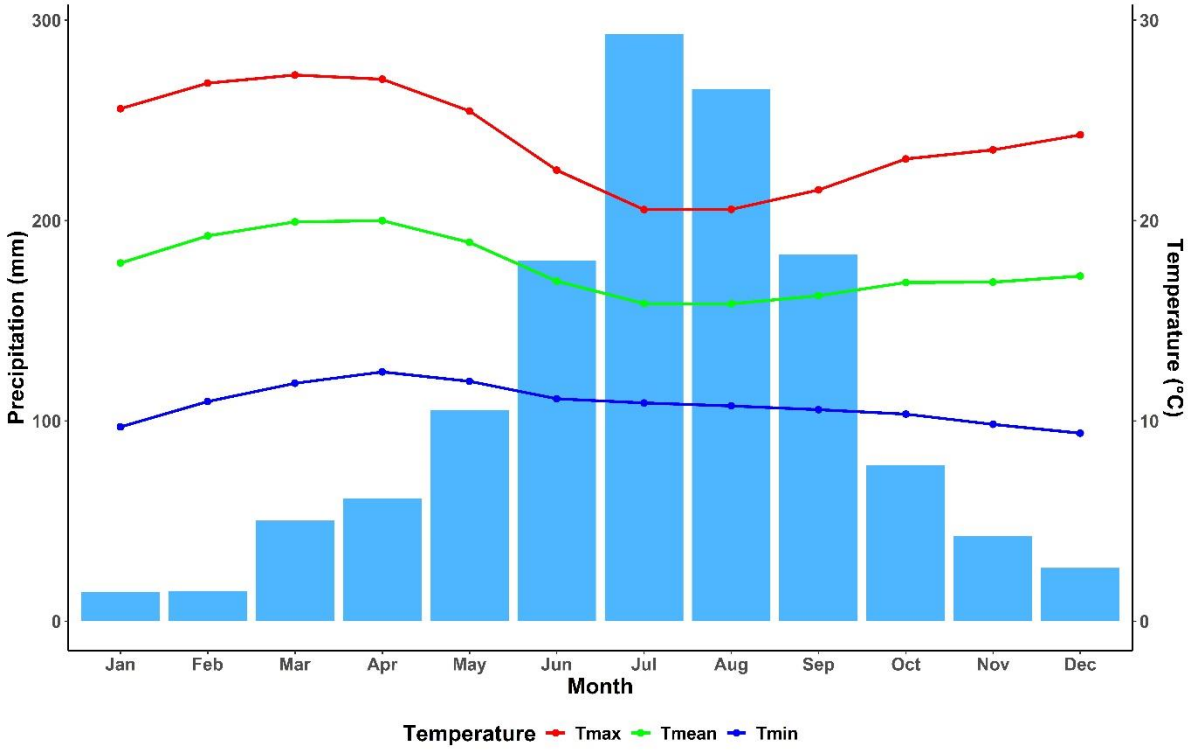

Figure 3-2. Monthly maximum (Tmax), minimum (Tmin), and mean (Tmean) temperatures and mean rainfall in the Jedeb River watershed (1992--2022) generated from the climate data obtained from EMI

3.1.3. Land Use and Land Cover

The Jedeb watershed comprises mainly rainfed crops (43.84%) and rangeland (38.61%), with forests covering 8.49% and irrigated land covering 5.74% of the watershed. Bare land covers 2.51%, built-up areas cover 0.74%, and water bodies cover only 0.07% (Mekonnen et al., 2024). The watershed faces severe land degradation problems, such as overgrazing, deforestation, climate variability, and unsustainable agricultural practices (Getnet and Mulu, 2021).

3.1.4. Soil and geological information

The major soil types in the Jedeb watershed are luvisols, nitosols, and vertisols. Chromic vertisols cover 319 km² (36.76%), followed by pellic vertisols cover 264 km² (30.48%), eutric nitisols cover 163 km² (18.81%), and chromic luvisols cover 92 km² (10.62%). The less common soils include leptosols 16 km² (1.79%) and chromic cambisols 9 km² (0.98%) (Figure 2.3). The soil textures primarily consist of loam (84.85%), clay (5.12%), and sandy loam (10.03%) (Asrade et al., 2024). The geological formations include Precambrian (0.12%), Cretaceous–Jurassic (14.64%), Tertiary extrusive, and intrusive (85.24%) formations (Manderso et al., 2023).

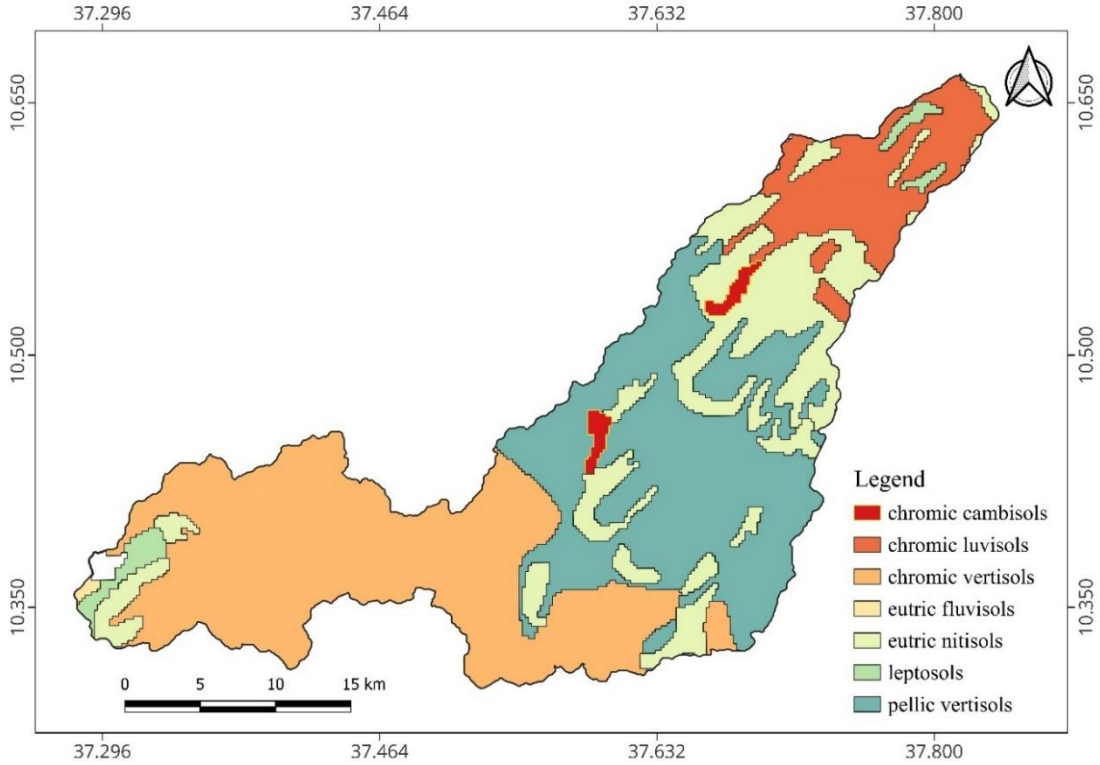

Figure 3-3. Major soil types in the Jedeb watershed

3.1.5. Irrigation development

Agriculture is predominantly crop–livestock mixed systems on small, independent farms averaging 0.5 hectares, with farmers growing tef, maize, and wheat, supplemented by barley and potato for local use (Simane et al., 2013). The area experiences intense land pressure due to an increasing population and an agriculture-based economy entirely dependent on smallholder, low-input–output agriculture (Ademe et al., 2021). Irrigation development is crucial for enhancing agricultural productivity, reducing dependence on rain-fed farming, and contributing to poverty alleviation (Amede, 2015; Awulachew et al., 2007). In the Jedeb watershed, seven small-scale irrigation schemes have been built, and from December to May, potato, maize, onion, garlic, cabbage, and wheat are produced using irrigation. (Table 2.1). The Shimburit small-scale irrigation scheme is considered for the irrigation performance assessment study.

The Shimburit micro earth fill dam irrigation scheme was constructed on the Shimburit River, a tributary of the Jedeb River at 10.38° N latitude and 37.40° E longitude northwest of Debre Markos town at approximately 56 km in the Debre Elias district, East Gojjam zone of the Amhara Regional State, Ethiopia (Figure 2). The scheme covers a total area of 425 ha and a command area of 270 ha and was designed for 25 years. The scheme was constructed in 2015 and benefits 780 households with parcel sizes ranging from 0.125 to 1 ha. The water supply to farmers is managed by government development agents every seven days and controlled through water user associations, and the irrigation method used by farmers is furrow. Over 88% of the irrigated area was covered by wheat during the study period in the Shimburit irrigation scheme.

Table 3.1. Small-Scale Irrigation Schemes in the Jedeb Watershed

Scheme Name	Structure	Location (Decimal Degree)		Command Area (ha)
		Latitude (N)	Longitude (E)	
Afkira	Weir	10.43	37.54	40
Jedeb 04	Weir	10.39	37.40	66
Yewula	Weir	10.41	37.58	192
Kulech	Weir	10.37	37.60	117
Atmina	Weir	10.54	37.73	25
Wonka	Weir	10.35	37.68	30
Shimburit	Dam	10.38	37.37	325

3.2. Data and Sources

Various spatial datasets have been utilized, including Sentinel 2 surface reflectance and Sentinel 1 SAR satellite images, Landsat 8 surface reflectance data, reanalysis data, digital elevation models, surface reflectance data, land cover data, ground truth data, crop production data and hydroclimatic data. The irrigated area classification was performed using Sentinel-2 multispectral and Sentinel-1 SAR images available on the GEE platform. Sentinel-2 provides multispectral imagery in 13 spectral bands with a spatial resolution of 10–60 meters. A total of 31 atmospherically corrected surface reflectance (Level 2A) scenes with cloud cover of less than 20% were used. To minimize the impact of clouds further, median images were used to avoid clouds. All bands except the coastal aerosol (band 1) were used in the classification process. The Sentinel-1 C-band Synthetic Aperture Radar Ground Range Detected (SAR GRD), which is ortho-corrected, was used. Seventeen scenes from a descending orbit, vertical transmit/vertical receive (VV), and vertical transmit/horizontal receive (VH) polarizations were obtained during the irrigation season from November 2021 to May 2021. The slope of an area significantly influences the accuracy of irrigation classification by affecting the choice of irrigation methods, land development processes, design of irrigation systems, plant adaptation, and drainage requirements (Hagos et al., 2022). Irrigated land is generally flat and uses furrow irrigation from an earthen dam, weir diversion, and pumps. Thus, the NASADEM digital elevation model (DEM) (NASA JPL, 2020) was used to extract the slope.

The temporal relationships of rainfed and irrigated areas with rainfall patterns are significantly different (Chandrasekharan et al., 2021). The accuracy of irrigation mapping is limited by the amount of rainfall received during the irrigation season (Bwambale et al., 2022). Therefore, Climate Hazards Group InfraRed Precipitation with Station (CHIRPS) (Funk et al., 2015) data, which demonstrated better performance than alternative products at monthly and seasonal timescales (Malede et al., 2022b), were used.

A field campaign to obtain the ground truth data was performed during the 2021/22 irrigation season using the KoboCollect app (the mean accuracy of the GPS points collected was 4.3 m). In data-poor locations, high-resolution PlanetScope quarterly composite base maps of the season were used for additional training point generation (Planet Team, 2017). The Central Statistics Agency's religious institution's location data were used to locate natural forests in the area. A total

of 1,929 ground truth points were collected, and the distribution of samples for each class was determined by area coverage and heterogeneity (Table 3.2).

Table 3.2. Definitions of land use and land cover (LULC) classes

Code	Class	Description	Samples
1	Bare land	Land with exposed soil, sand, or rocks	106
2	Built-up	Settlements and other man-made structures	90
3	Rainfed Crop	Farming areas that rely on rainfall for water	400
4	Forest	Natural (church) forests, eucalyptus, and other plantations	353
5	Irrigated area	Crops, fruit trees, and grasslands irrigated by river diversion and pumps	425
6	Rangeland	Grazing fields with grass and scattered shrubs	532
7	Water	Reservoir and river	23

Various spatial datasets, including Landsat 8 surface reflectance, reanalysis of climate data, digital elevation model, surface reflectance, and land cover, have been utilized to automate evapotranspiration estimation via SEBALIGEE and SEBALIGEEpy. Landsat 8 Operational Land Imager (OLI) and Thermal Infrared Sensor (TIRS) atmospherically corrected surface reflectance and land surface temperature image collection with the highest data quality available (Level 2 Tier 1) were used to derive the normalized difference vegetation index (NDVI), albedo, and leaf area index (LAI).

The European Centre for Medium-Range Weather Forecasts Reanalysis v5 – Land (ERA5-Land) provides high-resolution information on 50 surface variables from 1950 to the present (Muñoz-Sabater et al., 2021). The monthly aggregate dewpoint temperature, surface temperature, and wind speed at a spatial resolution of 0.1° (~10 km) were used. The 90-m Shuttle Radar Topographic Mission (SRTM) version 4 digital elevation model (DEM) (Jarvis et al., 2008) was used to calculate the altitude and slope for SEBALIGEE/SEBALIGEEpy and to generate hydrological response units (HRUs) combined with land use and soil data in the SWAT+ model. The soil data were collected from the Ministry of Water and Energy of Ethiopia and are based on the FAO soil classification system (FAO-ISRIC, 1990). The daily Moderate Resolution Imaging Spectroradiometer (MODIS) land surface reflectance (MOD09GAv061) dataset (Vermote and Wolfe, 2021) at a 1 km resolution was used to estimate the mean monthly cloud cover, ranging from 0 for cloudy areas to 1 for cloudless sky conditions, and to calculate sunshine hours. Another

product of MODIS, the annual global land cover type (MCD12Q1v061) dataset with 500 m resolution (Friedl and Sulla-Menashe, 2022), was used to identify agricultural lands for hot/cold pixel identification in the SEBALIGEE model. However, the MCD12Q1 land cover with a single pixel covering 2.5 ha is too coarse to capture the heterogeneity of small-scale agriculture, such as Ethiopia, with an average farm size of 0.95 ha and approximately 40% less than 0.5 ha (FAO, 2016; Headey et al., 2014). Thus, the SEBALIGEEpy model utilizes high-resolution annual dynamic world land cover data derived from Sentinel-2 satellite imagery using deep learning (Brown et al., 2022), where a 10 m resolution is more likely to capture detailed variations among fields for hot and cold pixel selection.

Using high-resolution land use data increases the accuracy of ETa estimation through better HRU representation in hydrological models (Dile et al., 2020b). Therefore, a 10 m resolution landcover with 90% overall accuracy and a kappa coefficient (agreement between the observed and classified data indicating the reliability of the classified image) of 0.87, incorporating Sentinel 1 and 2 satellite imagery prepared using GEE using a random forest algorithm (Mekonnen et al., 2024a), was used for the SWAT+ model. Additionally, the monthly ETa and decadal land cover classification product with 30 m resolution from the FAO's Water Productivity through Open access of Remotely sensed derived datasets (WaPOR version 2.1) (FAO, 2020) were used for comparison with the SEBALIGEEpy ETa of crops in the Koga irrigation scheme.

The SWAT+ hydrological model uses hydroclimatic data to simulate various water balance processes. Daily meteorological data (rainfall, maximum and minimum temperatures, relative humidity, sunshine hours, and wind speed) for 30 years (1992–2022) at the Debre Markos, Dembecha, Debre Elias, and Rob Gebeya meteorological stations were used. The observed discharge data (1994--2004) for Jedeb at the Yewula gauging station were used for calibration and validation. Meteorological and discharge data were collected from the Ethiopian Meteorology Institute (EMI) and the Ministry of Water and Energy (MoWE).

The FAO's portal to monitor water productivity through open access remotely sensed derived data (WaPOR version 2.1) covers Africa and the Near East regions in near-real time from 2009 until the end of 2023 (FAO, 2020). WaPOR version 2.1 datasets are available at the continental scale (Level 1 at 250 m), country scale (Level 2 at 100 m), and project level (Level 3 at 30 m). The methodology used for computing the ETa of WaPOR is based on the ETLook method

(Bastiaanssen et al., 2012). WaPOR v2.1 Level 3, given its higher spatial resolution than levels 1 and 2, is suitable for irrigation water management in smallholder areas. The WaPOR database version 2 provides ETa, evaporation, transpiration, interception, net primary productivity, total biomass production, gross and net biomass productivity, phenology, and land cover classification.

Point-based and distributed data were collected and estimated to assess the irrigation performance of the Shimburit small-scale irrigation scheme. Remote sensing should be used alongside traditional methods, such as in situ monitoring, for improved accuracy, with associated costs considered by planners (Foster et al., 2020). The Shimburit design documents were collected from the East Gojjam Zone Water Irrigation and Energy Office. Scheme-level assessments may not accurately reflect the actual performance of an irrigation system at the field level, and comparisons of ETa across an entire area, including both cropped and non-cropped areas, can be misleading (Akhtar et al., 2018). Therefore, of the 518 wheat growers, 41 farmers with farm sizes larger than 0.30 ha who had grown wheat for two consecutive seasons (2021/22 and 2022/23) were selected for field-level analysis. Thus, irrigated fields were delineated using the latest Google Earth Pro high-resolution image with small-scale irrigation expert and global positioning system (GPS) points collected with the Kobo Toolbox application using a smartphone. The daily discharge data, crop growth data, growing season data, field size data, and harvested amounts were collected from the Yegidad *Kebele* Agriculture Office.

Table 3.3. Summary of the datasets used

Dataset	Spatial Resolution	Temporal Resolution	Temporal Coverage	Dataset Provider
Sentinel 2	10 m	5 days	03/2017 – to date	ESA
Sentinel 1	10 m	6 days/12 days	2014 – to date	ESA
CHIRPS	5 km	Daily	1981 – to date	UCSB/CHG
WaPOR	30 m	Monthly		FAO
EC		Monthly	2017 – 2018	AmeriFlux
Discharge		Monthly		MoWE
Meteorology		Daily	1992 – 2022	EMI
SRTM DEM	30 m			USGS
Landsat 8	30 m	16 days	03/2013 – to date	USGS
GPS points			2021/22	Field Collection
Production			2021/22 – 2022/23	DA office

3.3. Comparison of GEE Machine Algorithms for Mapping Smallholder Irrigated Areas

3.3.1. Image preprocessing and classification

Cloud masking was applied to the Sentinel-2 images using the quality assessment (QA60) band. Temporal aggregation from satellite data over a certain period allows for effectively utilizing multitemporal data for land cover mapping (Carrasco et al., 2019). Thus, the median Sentinel-2 image during the irrigation season was used. Principal component analysis (PCA) was applied to reduce the dimensionality of the data and identify the directions of maximum variance to improve the classification (Vidal et al., 2016). Studies have shown that spectral indices can effectively capture the patterns of various crops and land uses (Abera et al., 2021; Demarez et al., 2019). The monthly NDVI (Tucker, 1979) time series from November to May was calculated using the GEE platform. The SAVI (Huete, 1988) is more accurate in identifying irrigated pixels (Abera et al., 2021), as the NDVI is more affected by the shading and moisture content of the soil (Neale et al., 2021). NDRE (Gitelson and Merzlyak, 1994) has been proven to be more helpful in optimizing harvest times and capturing irrigation irregularities, as it is sensitive to foliar pigments (Jorge et al., 2019; Pageot et al., 2020). NDWI (Gao, 1996) captures spatiotemporal patterns in surface moisture status, reducing confusion between irrigated crops and non-irrigated fields (Ouattara et al., 2020). Therefore, to get the most out of each index, a combination of monthly NDVI, SAVI, NDRE, and NDWI was used in the irrigation season (Equations (3.1)–(3.4)).

$$NDVI = \frac{\rho NIR - \rho Red}{\rho NIR + \rho Red} \quad 3.1$$

$$SAVI = \frac{\rho NIR - \rho Red}{\rho NIR + \rho Red} \quad 3.2$$

$$NDRE = \frac{\rho NIR - \rho VRE}{\rho NIR + \rho VRE} \quad 3.3$$

$$NDWI = \frac{\rho Green - \rho NIR}{\rho Green + \rho NIR} \quad 3.4$$

While Sentinel-1 GRD scenes in the GEE catalog have undergone thermal noise correction, radiometric calibration, and terrain correction preprocessing steps, additional processing is recommended for optimal use. This includes additional border noise correction, multi-look refined Lee filter speckle filtering using a 5 × 5 kernel, and terrain normalization, as suggested by Mullissa

et al. (2021). The mean of the irrigation season and monthly mean of VV and VH were also prepared.

In recent years, machine learning algorithms have been widely used to map irrigated areas (Ketchum et al., 2020; Magidi et al., 2021; Zurqani et al., 2021). The commonly used algorithms, CART (Breiman et al., 1984), GTB (Friedman, 2001), RF (Breiman, 2001), and SVM (Cortes and Vapnik, 1995) classifiers in the GEE, are used for the 2021/2022 irrigation season. CART is a decision classification tree method that simplifies decision-making and regression analyses by recursively separating nodes based on predetermined thresholds, dividing input data into subsets, and generating trees using all but one of those subsets (Basheer et al., 2022). RF is an ensemble classifier that uses multiple decision trees by sampling from the training dataset with replacement, and at each tree node, a random subset of variables is tested to partition the data into more homogeneous subsets on the basis of the variable yielding the highest increase in data purity. The final classification is determined by a majority vote from all the trees, with the label assigned by the majority of trees becoming the final result (Li et al., 2022). RF is widely used in irrigated area mapping (Magidi et al., 2021; Mohammedshum et al., 2023; Mpakairi et al., 2023; Zurqani et al., 2021). GTB involves the iterative combination of weak learner ensembles, gradually minimizing the loss function to make stronger predictions (Biswas et al., 2023; Friedman, 2001). The SVM classifier generates an optimal hyperplane that separates multiple classes and focuses exclusively on the training samples closest in the feature space to the optimal boundary between the classes (Maxwell et al., 2018). For this study, the linear kernel of the SVM classifier was found to be accurate.

Variable importance scores are used to identify important input variables to capture irrigation patterns accurately over time and space (Xu et al., 2019). The variable importance score was calculated for the GEE-supported variable importance calculation for the CART, GTB, and RF algorithms. The relative importance score was calculated for the CART, GTB, and RF algorithms via the built-in *explain()* function of GEE to understand how useful each feature is in predicting the defined classes. The calculated importance scores are expressed as percentages for a better comparison among different algorithms.

Four sets of images were used: the seasonal median of Sentinel-2 data referenced as “optical only”; the seasonal median of Sentinel-2 data and the monthly vegetation indices referenced as “optical

with vegetation indices"; the seasonal median of the optical and seasonal and monthly mean of SAR data referenced as "optical and SAR"; and the optical, SAR and vegetation indices with auxiliary data (mean rainfall and slope) referenced as "optical, SAR, vegetation indices and auxiliary data".

Each classification algorithm was evaluated in terms of overall accuracy (OA), the kappa coefficient, the producer's accuracy (PA), and the user's accuracy (UA) (Congalton, 1991; Foody, 2002) (Equations (3.5–3.8)) calculated from a confusion matrix implemented in GEE. Each classifier was trained with 70% and validated with 30% of the reference GCPs. To understand the classifiers' performance in different contexts, the accuracy was assessed across the two major agroecological zones ("Dega" and "Woyna Dega"), where irrigation calendars vary slightly. The parameters were adjusted to avoid overfitting until the difference between the training and validation overall accuracies was less than 5%.

$$Overall\ Accuracy\ (OA) = \frac{Number\ of\ Correctly\ Classified\ Samples}{Number\ of\ Total\ Samples} \quad 3.5$$

$$kappa\ (k) = \frac{Overall\ Acuuracy - Estimated\ Chance\ Agreement}{1 - Estimated\ Chance\ Agreement} \quad 3.6$$

$$UA = \frac{Number\ of\ Correctly\ Classified\ Samples\ in\ each\ Class}{Number\ of\ Samples\ Classified\ to\ that\ Class} \quad 3.7$$

$$PA = \frac{Number\ of\ Correctly\ Classified\ Samples\ in\ each\ Class}{Number\ of\ Samples\ from\ Reference\ Data\ in\ each\ Class} \quad 3.8$$

3.4. Adapting the SEBALI Evapotranspiration Model for Smallholder Irrigation

Making the SEBALIGEE model, which was originally based on JavaScript and is available in additional programming languages such as Python, can broaden its accessibility to a wider range of users and applications. Python is one of the most popular programming languages widely used in the hydrologic/atmospheric sciences and geospatial data analysis (Irving, 2019). On the other hand, JavaScript-based GEE applications can be difficult to operationalize because of their dependency on a specific development environment. Therefore, there is a significant advantage in rewriting the SEBALIGEE JavaScript code in Python to increase the model's applicability within the broader scientific community in water management. By providing SEBALIGEE in Python, the maintenance effort required for the model can be significantly reduced, allowing easy implementation of new processes using its extensive Python library designed for remote sensing and hydrological analysis (Stacke and Hagemann, 2021). For example, the geemap package (Wu,

2020) simplifies landcover mapping a dynamic world (Brown et al., 2022). Additionally, the GEE Python API can be easily integrated with ArcGIS Pro and QGIS, as each software uses Python as the scripting language.

In this study, we used corrected OpenET (Volk et al., 2023) eddy covariance flux tower ETa data over agricultural lands and recent records (2017--2018) to evaluate the performance of SEBALIGEEpy (Table 3.4). The calculated footprint area for each eddy covariance flux tower after Chu et al. (2021) was used to extract the ETa from the SEBALIGEE and SEBALIGEEpy results for comparison.

Table 3.4. Description of the eddy covariance flux tower sites used

Site ID	Lat	Long	Records	Climate	DOI
US-Bi1	38.0992	-121.4993	01/2017-12/2018	Csa	10.17190/AMF/1480317
US-Bi2	38.1091	-121.5351	05/2017-12/2028	Csa	10.17190/AMF/1419513
US-Ro5	44.6910	-93.0576	03/2017-12/2018	Dfa	10.17190/AMF/1419508
US-Ro6	44.6946	-93.0578	03/2017-12/2018	Dfa	10.17190/AMF/1419509

Csa stands for Mediterranean, mild with a dry, hot summer, and Dfa stands for Humid Continental: humid with severe winter, no dry season, and hot summer.

SEBALIGEEpy results were compared with the water balance ETa from the SWAT+ model in the Jedeb watershed and remote sensing-based WaPOR level 3 ETa data in the Koga irrigation scheme. This comparison was performed over seven irrigation seasons from 2015/2016 to 20201/22 in the Upper Blue Nile Basin, Ethiopia. The Koga irrigation scheme, which is located in the Mecha district of the Amhara Region, is a large-scale irrigation scheme that supports smallholder farmers and is geographically located between 11.33°N and 11.50°N (latitude) and 37.05°E and 37.15°E (longitude), with an average elevation of 1,980 m above sea level. The area receives a mean annual rainfall of 1420 mm and an average temperature of 20°C (Yihune et al., 2022). The irrigation scheme is supplied with water from the Koga dam, which has a storage capacity of 83 million m3 and a reservoir surface area of 1750 ha. The Koga irrigation scheme has a command area of 7000 ha, which is divided into 12 blocks. The main crops grown in the scheme include wheat, potato, maize, cabbage, garlic, onion, and green peppers (Bashe et al., 2022; Lewoyehu et al., 2023).

3.4.1. SEBALI and SEBALIGEE ETa estimation

The surface energy balance for land-improved (SEBALI) model is an enhanced version of the SEBAL model developed by Bastiaanssen et al. (1998a, 1998b) (1998) without soil-related inputs (Mhawej et al., 2020a, 2020b). The main improvements in SEBALI over SEBAL include a reduced number of inputs, automated selection of hot/cold pixels providing better internal calibration, and the use of atmospherically corrected satellite images for the NDVI and albedo (Mhawej et al., 2020a). SEBALI uses the well-established surface energy equation, where the latent heat flux as a proxy for ETa is calculated as a residual of net radiation (Rn), soil heat flux (G), and sensible heat flux (H) (Equation 3.9).

$$\lambda ET = R_n - G - H \quad 3.9$$

The soil-related inputs of the SEBAL model are generally lacking in many countries around the globe and are difficult to characterize from either modeling or remote sensing. Thus, SEBALI eliminates the need for soil-related information, and these parameters via the water stress approach to characterize vegetation moisture conditions and enables SEBALI to assess seasonal and annual ET and biomass production (Allam et al., 2021; Mhawej et al., 2020a) (Equation 3.10).

$$Ws = \frac{LE}{LE+H} \quad 3.10$$

where Ws is the water stress factor (Yuan et al., 2007), LE is the latent heat flux in W⁄m^2 corresponding to the instantaneous ET, and H is the sensible heat flux (W⁄m^2).

An enhancement in SEBALI compared with SEBAL involves adopting Hot/Cold pixel selection specifically over agricultural regions, as suggested by the METRIC model (Allen et al., 2007), resulting in improved internal calibration of the model (Mhawej et al., 2020a). The JavaScript-based SEBALIGEE model uses a 500 m resolution MODIS land cover dataset and was calibrated and validated in five countries using Eddy Covariance ET datasets (Mhawej and Faour, 2020).

3.4.2. SEBALIGEEpy model

This study made changes to the JavaScript SEBALIGEE model to improve its performance and applicability. The model was translated to Python, and dynamic LULC (10 m resolution) (Brown et al., 2022) was used as a source of land cover instead of the 500 m resolution MODIS land cover

dataset, which represents a mix of different land cover types in heterogeneous areas, such as the Ethiopian highlands. The MODIS land cover type (MCD12Q1) dataset could not discriminate croplands due to subpixel heterogeneity in Sub-Saharan Africa (Leroux et al., 2014), and the ETa results were too low and unrealistic in the Upper Blue Nile Basin when the SEBALIGEE model, which uses MCD12Q1, was used. For example, in the Koga irrigation scheme, over seven consecutive seasons, the maximum ETa is 35.04 mm/month for SEBALIGEE, 120.67 mm/month for SEBALIGEEpy, and 99.31 mm/month for WaPOR, with mean seasonal ETa values of 114 mm, 542 mm, and 463 mm, respectively. The calendar python library is used to set the number of dates in the month instead of filling in the number of dates for each month in the code. The code can also be accessed and implemented using Google Colab without additional installation or by adding the geemap package to ArcGIS Pro. The monthly outputs from SEBALIGEEpy include ETa, albedo, NDVI, LST (Land Surface Temperature), LAI, and LULC which can be saved into Google Drive or directly to a local disk.

3.4.3. SWAT+ hydrological model based ETa estimation

SWAT+ is an updated version of the widely used soil and water assessment tool (SWAT) hydrological model that works as an extension of QGIS, offering a flexible spatial representation of interactions and processes within a watershed (Bieger et al., 2017). Using soil, land cover, and slope data, 86 unique HRUs (the smallest units used to calculate the hydrological properties of a watershed) were generated using the dominant HRU method. The Penman–Monteith method (Allen et al., 1998) was used to calculate reference evapotranspiration, and the Soil Conservation Service (SCS) curve number (CN) method (NRCS, 2004) was used for surface runoff estimation. The flow through the catchment area was routed using the Muskingum routing method (Gill, 1978). The SWAT+ model uses the water balance equation (Equation 3.11) to estimate the hydrological processes of a catchment (Neitsch et al., 2011).

$$SW_t = SW_0 + \sum_{i=1}^{t}(R_{day} - Q_{surf} - ET_a - w_{seep} - Q_{gw} \quad 3.11$$

where SW_t represents the final soil moisture content, SW_0 represents the initial soil moisture content, R_{day} represents precipitation on day i, $Q_{surf\ represents}$ surface runoff on day i, ETa represents evapotranspiration on day i, w_{seep} represents deep percolation and bypass flow exiting the soil profile bottom on day i, and Q_{gw} represents the amount of return flow on day i.

The sensitivity analysis, calibration, and validation of the SWAT+ model (version 60.5.4) were performed using the observed streamflow data with the SWAT+ Toolbox (version 1.0.5). Parameter selection was based on sensitivity analysis using the Sobol method and the literature. The percolation coefficient (perco), available water capacity of the soil layer (AWC), and SCS runoff curve number (cn2) are the most sensitive parameters.

Table 3.5. List of calibrated parameters, their initial ranges, and fitted values for the SWAT+ model

Parameter	Description	Change Type	Min	Max	Fitted or Adjustment Value
perco	Percolation coefficient	Replace	0	1	0.98
awc	Available water capacity of the soil layer (mm_H2O/mm)	Relative	0.01	1	+0.50
cn2	SCS runoff curve number	Percentage	35	95	11%
bd	Soil bulk density (mg/cm^3)	Relative	0.9	2.5	+0.04
revap_min	Threshold depth of water in the shallow aquifer (m)	Relative	0	50	-5.0
esco	Soil evaporation compensation factor	Replace	0	1	0.85
alpha	Baseflow alpha factor (days)	Relative	0	1	+0.03
k	Saturated hydraulic conductivity (mm/hr)	Percentage	0.0001	2000	38%
cn3_swf	Pothole evaporation coefficient	Replace	0	1	0.96
revap_co	Groundwater 'revap' coefficient	Relative	0.02	0.2	+0.02

The model was calibrated with observed streamflow data from 1994--2001, and upon achieving satisfactory agreement, it was validated for 2002--2004 using the same set of parameters. The built-in objective functions in the SWAT+ toolbox Nash–Sutcliffe efficiency (Nash and Sutcliffe, 1970), percent bias (PBias), and root mean square error (RMSE) were used to evaluate model performance. NSE quantifies the agreement between simulated and observed values, with 1 indicating perfect agreement and values ≤ 0 suggesting that the observed average is a better predictor than the model is by estimating the relative magnitude of residual variance compared with the measured data variance (Dile et al., 2020). PBias measures the average bias of the simulated values compared with the observed values, with positive values indicating

overestimation, negative values indicating underestimation, and values closer to zero indicating better model performance (Moriasi et al., 2007). The root mean square error (RMSE) is a common metric in hydrology used to assess model performance by quantifying the average magnitude of differences between simulated and observed values, with lower values indicating better agreement. After calibration and validation with monthly streamflow data, the SWAT+ model demonstrated good performance in simulating the observed streamflow. The model captured the general streamflow pattern but overestimated the magnitude of the streamflow. Generally, the NSE values during the calibration and validation periods exceeded 0.75, which is considered very good model performance (Figure 3.4). Based on the SWAT+ results, the water balance is highly influenced by ETa (628 mm), accounting for approximately 48% of the 1310 mm precipitation, whereas surface runoff accounts for 19% (250 mm). This result is consistent with earlier research on the water balance in the Abbay Basin, which revealed that ETa accounts for 49.50% of precipitation, whereas surface runoff contributes 22.43% of precipitation to streamflow (Takele et al., 2022).

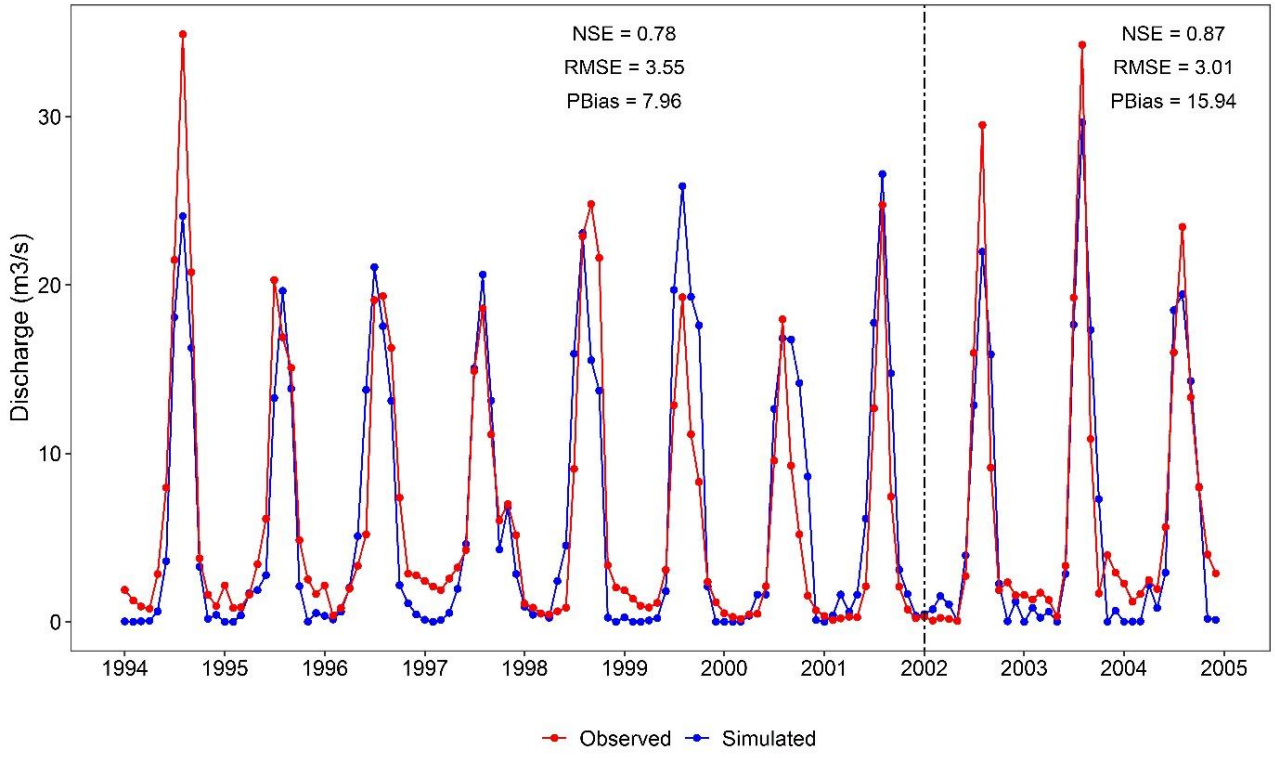

Figure 3.4. Observed and simulated streamflow of the Jedeb River at the Yewula gauging station for the calibration (1994–2001) and validation (2002–2004) period using the SWAT+ model.

3.4.4. Validation of SEBALIGEEpy ETa estimates

The RMSE, mean absolute error (MAE), and coefficient of determination (R^2) were used to identify the systemic bias in the ETa datasets. R2 indicates the proportion of variance in observed data explained by the model, ranging between 0 and 1, with higher values denoting less error, and typically values above 0.5 show acceptable agreement between subject variables (Dile et al., 2020; Moriasi et al., 2007). MAE measures the average absolute difference between the predicted and actual values, which helps identify the accuracy and reliability of the model used (Angelini et al., 2021). NSE and PBias are not used to evaluate ETa due to NSE sensitivity to large values caused by the squared difference, and PBias is disproportionately influenced by a few outliers (Dile et al., 2020; Gupta et al., 2009).

3.5. Remote Sensing based Irrigation Performance Assessment

In three main steps, irrigation performance indicators are derived from the SEBALI evapotranspiration model and field data. First, monthly reference evapotranspiration (ETo), actual evapotranspiration (ETa), and water productivity (WP) were estimated using the SEBALIGEEpy model. Second, the seasonal ETa, seasonal crop evapotranspiration (ETc), and seasonal productivity are calculated from monthly layers between the start of the season (SOS) and the end of the season (EOS). ETc is derived from reference evapotranspiration (ETo) and the crop coefficient (Kc) of wheat, which was predominantly grown during the 2021/22 and 2022/23 irrigation seasons. Finally, the irrigation performance indicators are analyzed by integrating CHIRPS satellite precipitation data, SEBALI seasonal outputs, and ground-based harvest index and discharge data.

Several performance indicators have been developed to quantify irrigation performance using satellite remote sensing that can be applied across different scales, with input data requirements varying on the basis of the scale and complexity of the assessment (Bashe et al., 2023; Chukalla et al., 2022; Wamala et al., 2023). In this study, adequacy (relative evapotranspiration, relative water supply), equity (CV of evapotranspiration), the depleted fraction, the overall consumed ratio, and productivity (production per hectare and crop water productivity) were employed. These performance indicators were selected based on data availability and are further explained below. Indicators that involve water volume recorded at the scheme level include the overall consumed

ratio (OCR), depleted fraction (DF), and relative water supply (RWS), along with adequacy, equity, and productivity assessed at the field level.

The adequacy indicator serves to quantify the sufficiency of water delivery to a designated command area, meeting the specified requirements, evaluating the reduction in ETa, and representing the degree of agreement between actual water use and crop water requirement (CWR) (Akhtar et al., 2018; Wamala et al., 2023). Relative evapotranspiration (RET) and relative water supply (RWS) were used to evaluate adequacy. These indicators were selected based on the ease of data collection and the applicability of remote sensing data.

RET is a seasonal ETa ratio to ETo (Equation 3.12) applied to identify regions experiencing crop stress and water shortages throughout the irrigation season (Poudel et al., 2021). Adequacy is categorized as good for the range of $0.8 < RET \leq 1$, acceptable for the range of $0.68 < RET \leq 0.8$, and poor for $RET \leq 0.68$ (Akhtar et al., 2018; Karimi et al., 2019).

$$RET = \frac{ET_a}{ET_o} \quad 3.12$$

The RWS was used as an indicator of the adequacy of irrigation water delivery, comparing the supplied water with crop water demand, indicating whether there is enough irrigation water supply or not (Alemie et al., 2023; Usman et al., 2020). The RWS assesses the delivery performance of irrigation water and is estimated as follows (Equation 5.13):

$$RWS = \frac{V_c + P_g}{ET_c} \quad 3.13$$

RWS represents the relative water supply, Vc represents the volume of irrigation delivered (mm), and Pg represents the gross precipitation amount. The performance is classified as inadequate or water-stressed if the RWS is less than 0.9, optimal if the RWS falls between 0.9 and 1.2, and excess if the RWS exceeds 1.2 (Haj-Amor et al., 2018).

Equity in irrigation water distribution is a crucial aspect of irrigation management that assesses the evenness of consumption among fields or users within an irrigation scheme (Chukalla et al., 2022; Elnmer et al., 2018; Kharrou et al., 2013). Equity is classified as good when the coefficient of variation (CV) ranges from 0 to 10%, fair from 10 to 25%, and poor when it exceeds 25% (Chukalla et al., 2022; Karimi et al., 2019).

The depleted fraction serves as an indicator for assessing the gross water balance of irrigable areas, reflecting variations in actual water utilization by crops and quantifying disparities in the water balance across the study area (Karatas et al., 2009; Sawadogo et al., 2020). The depleted fraction quantifies the amount of water lost during transportation or due to low application efficiency (Awan et al., 2011). It is estimated as follows (Equation 3.14):

$$DF = \frac{ET_a}{P_g + V_c} \quad 3.14$$

where DF is the depleted fraction, Pg is the gross rainfall (mm), and Vc is the volume of irrigation delivered (mm). The irrigation supply data for the main canal were used. The acceptable range for the DF varies from 0.6 to 1.1 (Bastiaanssen et al., 2001), whereas the critical value falls between 0.5 and 0.7 (Bashe et al., 2023).

The overall consumed ratio (OCR) is a performance indicator used to assess the efficiency of irrigation systems that quantifies the degree to which crop irrigation requirements are met (Abera et al., 2019; Bastiaanssen et al., 2001). The OCR is calculated as follows (Equation 3.15):

$$OCR = \frac{ET_c - P_e}{V_c} \quad 3.15$$

where OCR is the overall consumed ratio, ETc is the crop evapotranspiration, Pe is the effective precipitation, and Vc is the volume of water supplied to the command area in mm. The effective rainfall was calculated using the U.S. Department of Agriculture's Soil Conservation Service formula. The amount of water supplied to the command area (Vc) was measured by the float method at the outlet of the Shimburit dam. If the OCR values are >1, the scheme has a deficit to meet CWR and excess water is released if the OCR is <1 (Abera et al., 2019).

Land productivity (LP) is defined as biomass production or actual crop yield per unit of land (Chukalla et al., 2022), whereas water productivity (WP) is described as the gain in biomass or marketable crop yield during the growing season per unit of water used by the crop through evapotranspiration (Bastiaanssen and Bos, 1999; Fernandez, 2023; Fernandez et al., 2020). Water productivity is estimated using SEBALIGEE, an open-source system that uses the Google Earth Engine to estimate evapotranspiration rates, biomass production, and water productivity. Biomass water productivity (WPb) is derived by dividing total biomass production by the amount of irrigation water consumed or actual evapotranspiration (ETa), expressed in kg/m^3 (Safi et al., 2023) (Equation 3.16).

$$BW_b = \frac{Biomass\ Production \times HI}{ET_a} \quad 3.16$$

The harvest index (HI), the harvested portion of the accumulated dry matter (Bastiaanssen and Steduto, 2017) of wheat, is 0.3008 for the *Kekeba* variety in the area (Sewenet et al., 2021). The results were compared with two-season land and water productivity data from 41 wheat fields collected from the *Kebele* Agriculture Office following Islam et al. (2023) (Equation 3.17).

$$CWP = \frac{Crop\ yield\ (kg\ ha^{-1})}{10 \times ET_{as}} \quad 3.17$$

The crop yield is defined as the harvested yield recorded, and the ETas is the evapotranspiration from the start of the season (SOS) to the end of the season (EOS). The conversion factor, 10^{-1}, converts ETa from mm to $m^3\ ha^{-1}$.

4. RESULTS AND DISCUSSION

4.1. Smallholder Irrigated Area Mapping using Google Earth Engine

4.1.1. Relative importance of inputs

The variable importance results revealed that, for the CART classifier, the top three key features are the third principal component (pc3) (16.36%), followed by the blue band (B2) (11.08%), and the NDVI in March (ndviMar) (10.18%) is of relative importance. For the GTB model, the NDRE in December (ndreDec) was the most important with 7.38%, followed by the SAVI in January (saviJan), with 7.18% and the pc3, with 6.93%. For the RF model, the most important feature was the NDWI in December (ndwiDec), with a value of 4.11%, followed by the NDRE in December (ndreDec) and pc3, with values of 3.58% and 3.51%, respectively (Table 4.1). The full list of importance values is presented in Figure 4.1.

Table 4.1. Top 15 important variables for the CART, GTB, and RF classifiers

Rank	CART		GTB		RF	
	Bands	Importance (%)	Bands	Importance (%)	Bands	Importance (%)
1	pc3	16.36	ndreDec	7.38	ndwiDec	4.11
2	B2	11.08	saviJan	7.18	ndreDec	3.58
3	ndviMar	10.18	pc3	6.93	pc3	3.51
4	ndviMay	8.55	B5	6.29	B12	3.12
5	ndwiApr	8.44	B4	5.83	B3	2.98
6	ndreFeb	7.06	ndviNov	5.62	B2	2.80
7	B6	7.00	ndwiDec	5.02	B11	2.66
8	ndreDec	5.65	ndwiNov	3.54	ndwiJan	2.57
9	ndviNov	5.42	ndreMar	3.49	ndviDec	2.41
10	B12	4.40	B2	3.09	saviJan	2.30
11	VVmay	4.03	saviApr	3.07	saviApr	2.26
12	ndwiDec	3.97	VH	2.81	ndwiMar	2.16
13	saviJan	2.76	B11	2.67	ndwiNov	2.07
14	ndwiMar	2.06	B12	2.60	ndviNov	2.07
15	saviApr	1.81	ndviApr	2.15	B5	2.06

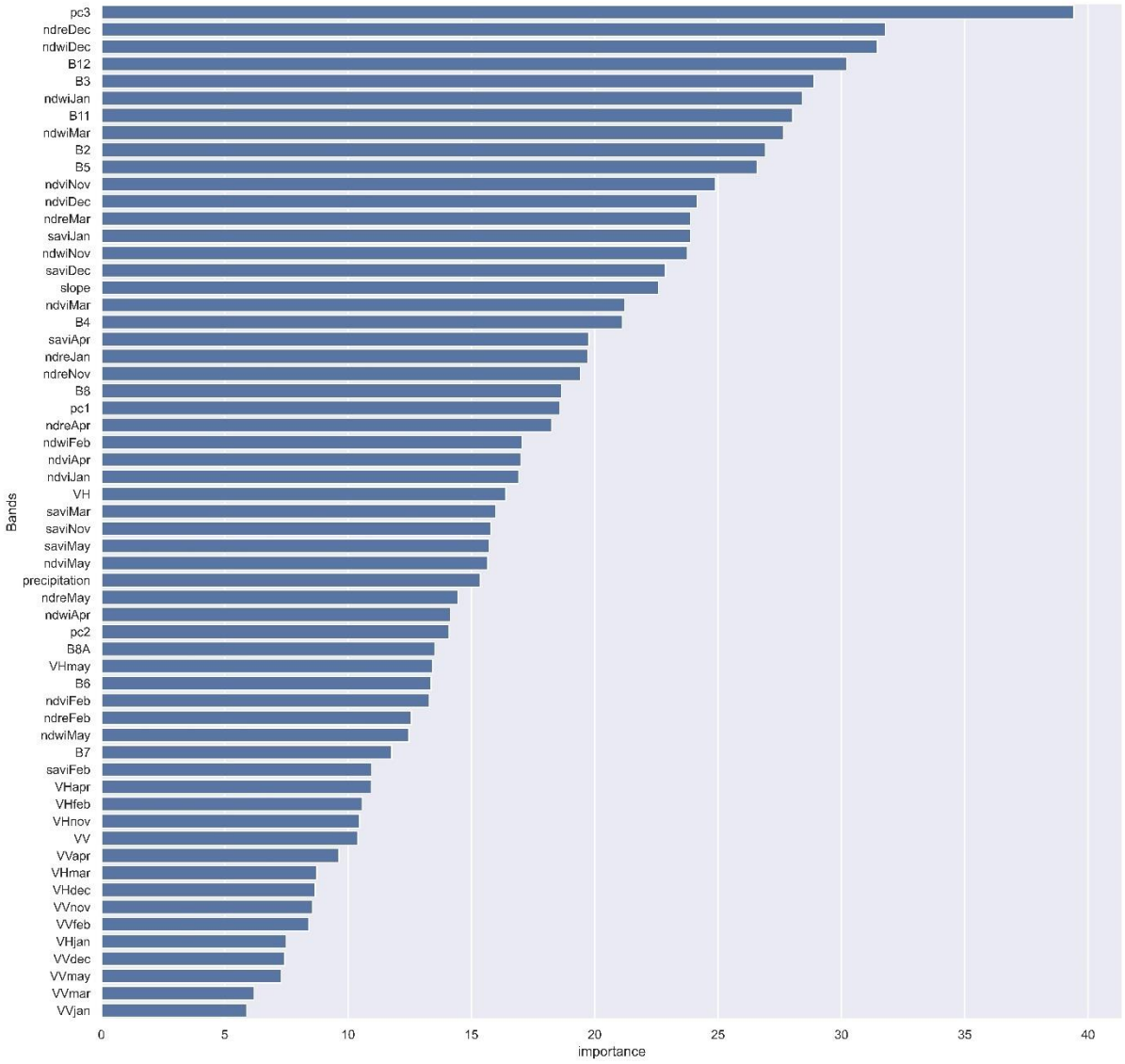

Figure 4-1. Chart of RF algorithm variable importance.

4.1.2. Accuracy comparison among classifiers

The accuracy metrics (Table 4.3), derived from the error matrix presented in Table 4.2, indicate that the RF algorithm performed the best, followed by the SVM, GTB, and CART algorithms, which use optical, SAR, vegetation indices, and auxiliary data composites. PCA on Sentinel-2 optical bands resulted in significant improvements in the accuracy of classification. The first three algorithms produced nearly similar maps representing the area well (Figure 4.2). The RF classification algorithm had an OA of 0.89 and a kappa coefficient of 0.86, with both the UA and PA for all LULC classes exceeding 0.80 except for the “built-up” class (PA = 0.74). The GTB

classification also achieved an OA of 0.89 with a 0.86 kappa coefficient, and the UA and PA were above 0.80 for all classes except “rangeland” (PA = 0.75). The SVM algorithm showed high classification accuracy, with an OA and a kappa coefficient of 0.88 and 0.85, respectively. The PAs for all classes were above 0.80 except for the “bare land” and “built-up” classes (0.78), and the UA for all classes was above 0.80. The CART algorithm is the least accurate among the tested algorithms, with an OA of 0.86. It also had a lower PA for “built-up” land (0.74) and a low UA for “bare land” (0.60) (Table 3.4). In the “irrigated area” class (Figure 4.4), the PA of the RF, SVM, and GTB algorithms was 0.91, whereas CART (0.82) performed the lowest. The UA is the RF (0.95), followed by the GTB (0.92), SVM (0.91), and CART (0.90). The code generated to classify irrigated areas can be used with minimum effort to modify them at small-scale or large-scale levels.

Table 4.2. Confusion matrix of classification for the 2021/22 irrigation season

CART							
Class	1	2	3	4	5	6	7
1	27	0	2	0	1	2	0
2	2	20	5	0	0	0	0
3	6	1	100	1	2	10	0
4	0	0	0	97	0	6	0
5	5	0	1	6	104	11	0
6	5	0	0	11	8	136	0
7	0	0	0	0	0	0	7

GTB							
Class	1	2	3	4	5	6	7
1	26	0	2	0	2	2	0
2	0	23	3	0	0	1	0
3	2	1	100	2	3	12	0
4	0	0	0	89	1	13	0
5	2	0	1	5	107	12	0
6	0	0	4	9	0	147	0
7	0	0	0	0	0	0	7

RF							
Class	1	2	3	4	5	6	7
1	27	0	1	0	2	2	0
2	0	22	4	0	0	1	0
3	2	1	101	1	4	11	0
4	0	0	0	93	1	9	0
5	2	0	1	5	114	5	0
6	0	0	3	9	2	146	0
7	0	0	0	0	0	0	7

SVM							
Class	1	2	3	4	5	6	7
1	25	0	1	0	5	1	0
2	1	21	4	0	0	1	0
3	2	1	103	2	2	10	0
4	0	0	1	93	3	6	0
5	1	0	1	4	116	5	0
6	0	0	4	11	2	143	0
7	0	0	0	0	0	0	7

The distribution of irrigated areas is uneven, where most of the irrigated land is in the middle-altitude areas of the Debre Elias, Machakel, and Gozamin districts. Compared with other districts, Senan District has limited irrigation activity, as the watershed area in the district is mountainous and frosty afro alpine. Approximately half of the watershed’s total area is used for agriculture, and 5.7% is currently irrigated (Table 4.3).

Table 4.3. Comparison of the accuracies of the classification algorithms used

ML Algorithm	Class	PA (%)	UA (%)	Area (ha)	Weight (%)
	1	0.84	0.60	8922	10.29
	2	0.74	0.95	1433	1.65
CART	3	0.83	0.93	33036	38.08
OA (%) = 0.85	4	0.94	0.84	7806	9.00
Kappa coefficient = 0.81	5	0.82	0.90	4477	5.16
	6	0.85	0.82	31013	35.75
	7	1.00	1.00	56	0.06
	1	0.75	0.92	1460	1.68
	2	0.89	0.96	821	0.95
GTB	3	0.85	0.91	39746	45.82
OA (%) = 0.87	4	0.92	0.87	7936	9.15
Kappa coefficient = 0.84	5	0.91	0.92	5141	5.93
	6	0.92	0.85	31465	36.27
	7	1.00	1.00	174	0.20
	1	0.84	0.84	2181	2.51
	2	0.81	0.96	642	0.74
RF	3	0.84	0.91	38029	43.84
OA (%) = 0.89	4	0.90	0.87	7367	8.49
Kappa coefficient = 0.86	5	0.91	0.95	4976	5.74
	6	0.92	0.84	33488	38.61
	7	1.00	1.00	62	0.07
	1	0.78	0.86	2509	2.89
	2	0.78	0.95	590	0.68
SVM	3	0.86	0.90	42540	49.04
OA (%) = 0.88	4	0.90	0.85	8267	9.53
Kappa coefficient = 0.85	5	0.91	0.91	4201	4.84
	6	0.89	0.86	28571	32.94
	7	1.00	1.00	66	0.08

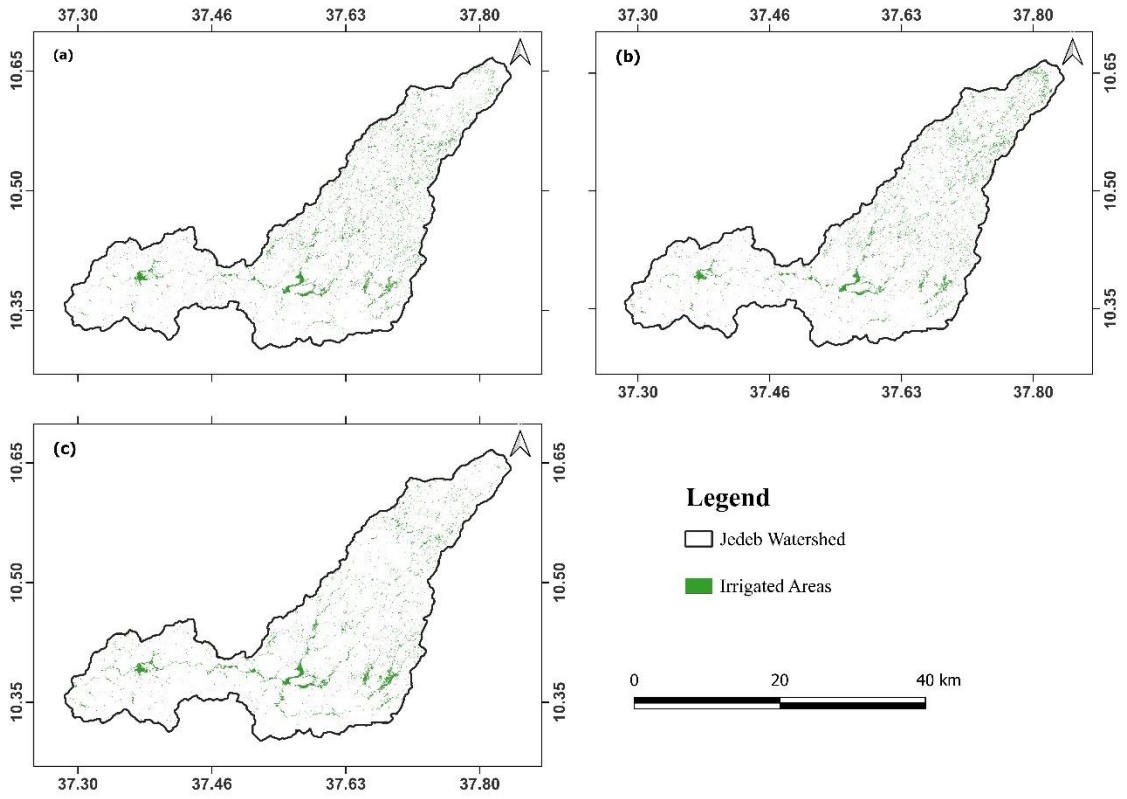

Figure 4-2. Irrigated area map of the Jedeb watershed (a) GTB, (b) RF, and (c) SVM.

4.1.3. Effect of inputs on accuracy of classification

Table 4.5 presents the performance of four classification methods (CART, GTB, RF, and SVM) on four different sets of data. The classification with ‘‘optical only” is the least accurate, whereas “optical, SAR, vegetation indices, and auxiliary data” resulted in the best accuracy. The OA slightly improved when optical and SAR images were combined. However, the use of temporally aggregated vegetation indices improves accuracy and is more important than the use of SAR data (Table 4.4). It has been reported that the integration of temporally aggregated SAR, multispectral data, and vegetation indices improved the accuracy of classification (Bazzi et al., 2021; Carrasco et al., 2019; Vizzari, 2022). Our findings align with similar studies conducted in the basin, as demonstrated by Abera et al. (2021). Dense temporal vegetation indices are valuable because of the noticeable differences in greenness between irrigated land and other land uses (Xie and Lark, 2021). The incorporation of auxiliary data, i.e., rainfall and slope data, slightly improved the accuracy of all the algorithms. Overall, the RF classifier is a consistent and best-performing algorithm with various sets of inputs for mapping smallholder irrigated areas.

Table 4.4. Accuracy of different sets of inputs used.

Classifier	Optical only		Optical and SAR		Optical and Vegetation Indices		Optical, SAR, VI Vegetation Indices, and Auxiliary Data	
	OA	Kappa	OA	Kappa	OA	Kappa	OA	Kappa
CART	0.74	0.67	0.78	0.72	0.85	0.82	0.86	0.82
GTB	0.80	0.75	0.83	0.78	0.88	0.85	0.89	0.86
RF	0.81	0.76	0.81	0.77	0.88	0.85	0.89	0.86
SVM	0.66	0.56	0.69	0.60	0.87	0.83	0.88	0.85

Figure 4.3 shows the NDVI patterns of forests, rainfed crops, and irrigated land during the 2021/2022 irrigation season. As the transition month from rainfed to irrigation, November served as a baseline, and the forest class was used as a reference to understand the variations between rainfed and irrigated lands. The values for irrigated areas increase (lemon green color) at the end of December (planting) and begin to decline in April (harvest month for the first-round irrigation). The NDVI of the rainfed cropland (brown color) remains low and increases slightly in April due to small amounts of rain that allow herbaceous plants grow and disappear due to plowing in May.

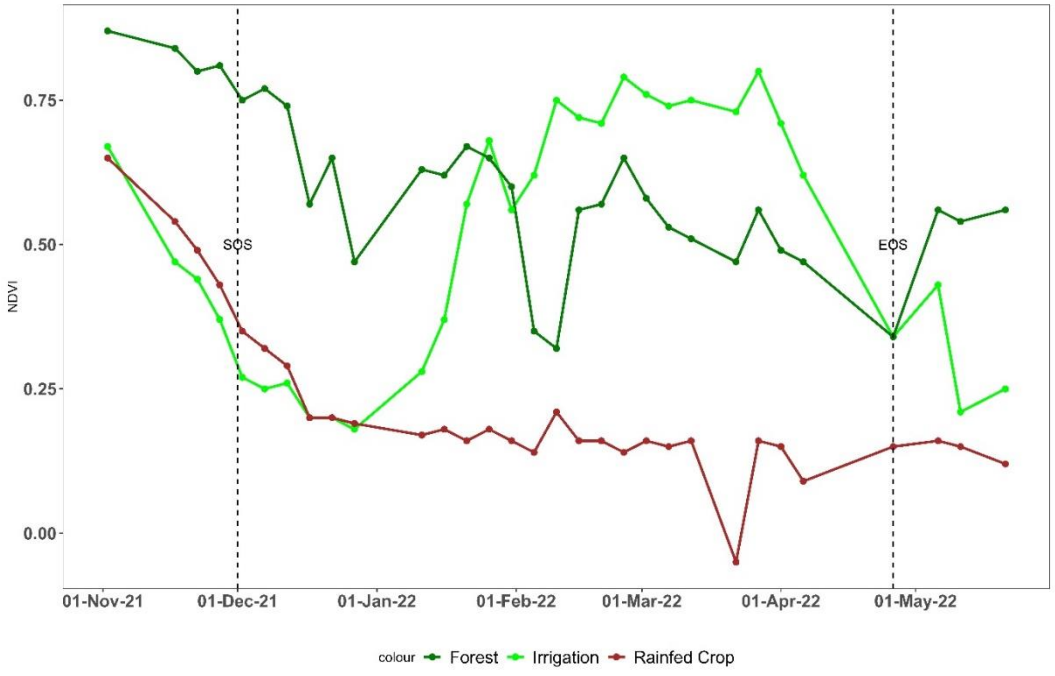

Figure 4-3. Temporal NDVI profile for the rainfed crop, irrigation, and forest classes in the 2021/22 irrigation season (SOS is the start of the season, and EOS is the end of the season).

4.1.4. Effect of agroecology on the accuracy of classification

The rainfed crop growing period in *Dega* and the irrigation calendar in *Woyna Dega* usually overlap. Thus, the classifiers were tested using two major agroecology zones where irrigation and rainfed seasons are expected to be distinct within the same zone. The results indicated that the RF classifier performed best in the *Dega* (OA = 0.83) region, whereas the GTB was superior for *Woyna Dega* (OA = 0.88). This observation implies that the accuracy of different algorithms varies across agroecological zones. In general, better results were achieved with *Woyna Dega* than *Dega* because of the high impact of cloud cover on high-altitude areas (Conlon et al., 2022) (Table 4.5).

Table 4.5. Overall accuracy and kappa coefficient agroecology.

Classifier	*Woyna Dega*		*Dega*	
	OA	Kappa	OA	Kappa
CART	0.73	0.66	0.72	0.65
GTB	0.89	0.86	0.84	0.79
RF	0.83	0.78	0.83	0.79
SVM	0.84	0.79	0.81	0.76

4.1.5. Challenges in mapping smallholder irrigated areas

Detecting irrigated areas at high altitudes is difficult because of high cloud cover and differences in species grown with different irrigation calendars due to high variability in elevation (different crop types) (Khatami et al., 2020; Vogels et al., 2019a). The crop residues collected as fodder and fuel by farmers and rainfed croplands become bare surfaces, and rangelands are highly degraded, resulting in greater errors in accuracy than other classes (Getnet and Mulu, 2021; Tekleab et al., 2014). The ‘built-up’ class had the lowest PA across all four algorithms due to the small size of the objects and was composed of heterogeneous surfaces (Osgouei et al., 2019). For example, the rocks exposed at quarry sites were classified as built-up rocks. Gully rehabilitation plantations are classified as irrigation in degraded *Dega* areas; seedlings of eucalyptus; afro-alpine areas (irrigated grass for forage due to crop damage by frost); and rainfed crop growing periods that overlap with the irrigation calendar at medium altitudes, leading to overestimations of irrigated areas. Similar challenges were reported where the valley bottoms were classified as irrigation (Chandrasekharan et al., 2021). Moreover, object-based image analysis and neural networks could result in better results (Basukala et al., 2017; Conlon et al., 2022; Vizzari, 2022; Vogels et al., 2019b).

The accuracy of classification algorithms may be affected by training and validation data quality and quantity limitations in terms of the representativeness of the training data (Magidi et al., 2021; Zurqani et al., 2021). Another critical factor is the optimal selection of months to include in the composite (Weitkamp et al., 2023). The data used were limited to the dry season only due to computational resource limitations where per-user memory limitations affected dimensionality reduction, such as PCA over large datasets (Zurqani et al., 2021). High-resolution imagery could achieve better accuracy (Vogels et al., 2019a). The lack of reported statistics on irrigated areas at the watershed level limits the accuracy of these methods.

4.2. SEBALI Model for Estimating Smallholder Irrigation ETa

4.2.1. Validation of SEBALIGEE and SEBALIGEEpy ETa against EC data

The data from all the EC stations were combined, and SEBALIGEEpy yielded lower RMSE (39.52 mm/month) and MAE (29.93 mm/month) compared to SEBALIGEE (RMSE of 43.03 mm/month and MAE of 30.99 mm/month), indicating more accurate ETa estimation (Figure 4.4). The percentage of missing records at the validation sites was 9–11% when the improved version (SEBALIGEEpy) was used and 14–29% when the SEBALIGEE model was used.

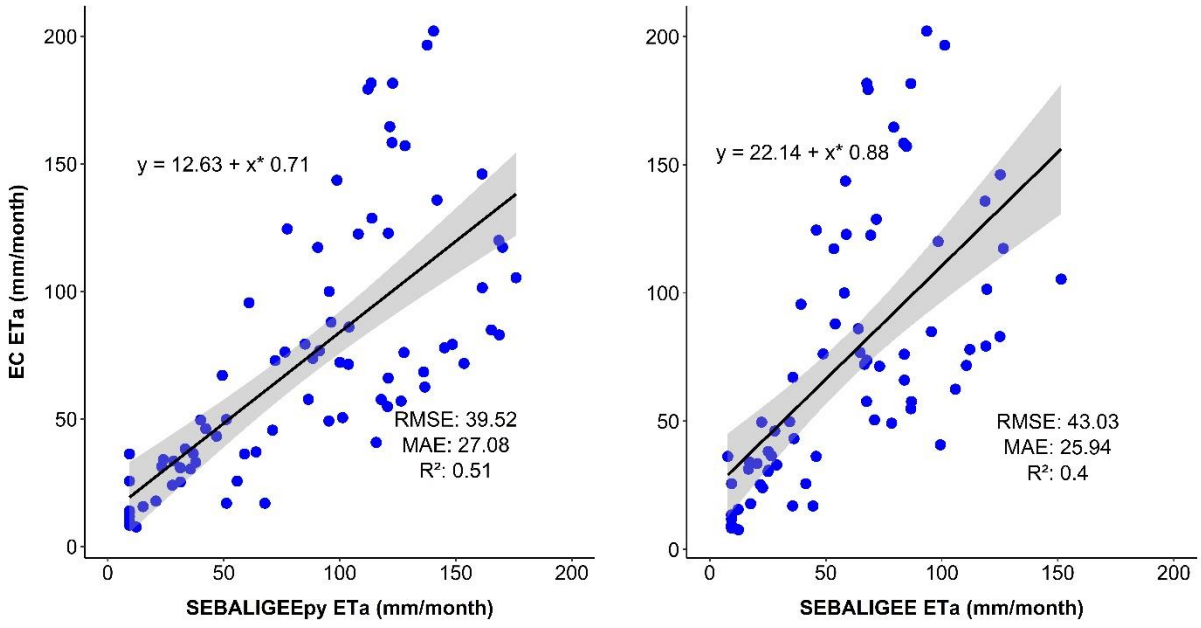

Figure 4.4. Comparison between estimated (SEBALIGEEpy (left) and SEBALIGEE (right) models) and measured (EC) actual evapotranspiration (ETa).

Moreover, the distribution of SEBALIGEEpy estimates is generally narrower than that of EC Flux ETa but wider than that of SEBALIGEE, indicating a balance between capturing variability and providing consistent estimates (Figure 4.5). SEBALIGEEpy also performed better across different seasons, with 11.95% more images processed as Tier 1 in Collection 2 than in Collection 1 Tier 1, which was used by SEBALIGEE (Crawford et al., 2023). This minimized the impact of clouds, as the median monthly Landsat 8 data were used for the LST and vegetation parameters that could be masked due to clouds. However, the results suggest that the impact of LULC data resolution varies across different sites. Higher-resolution land cover data lead to more accurate estimations, whereas coarser-resolution data may perform better in flat areas, with less variability in LULC. Considerable variability was observed in performance across different sites and seasons. The seasonal analysis highlights the sensitivity of the model to temporal changes. The best performance of the SEBALIGEEpy model was observed at the US-Bi2 EC flux tower site in spring, with an RMSE of 14.79 mm/month, an MAE of 5.85 mm/month, and an R^2 of 1.00. The worst performance of the model was observed at the US-Ro5 site in the winter season, with an RMSE of 73.34 mm/month, an MAE of 42.04 mm/month, and an R^2 of 0.66 (Table 4.6).

Table 4.6. Validation results of the SEBALIGEEpy and SEBALIGEE models in comparison with AmeriFlux data

Site ID	SEBALIGEEpy (10 m LULC)			SEBALIGEE (Original)		
	RMSE (mm/month)	MAE (mm/month)	R^2	RMSE (mm/month)	MAE (mm/month)	R^2
US-Bi1	30.17	21.00	0.86	58.61	48.66	0.86
US-Bi2	39.86	32.86	0.61	48.10	32.95	0.63
US-Ro5	36.27	27.16	0.80	21.89	15.79	0.75
US-Ro6	51.82	40.80	0.79	28.35	22.39	0.78

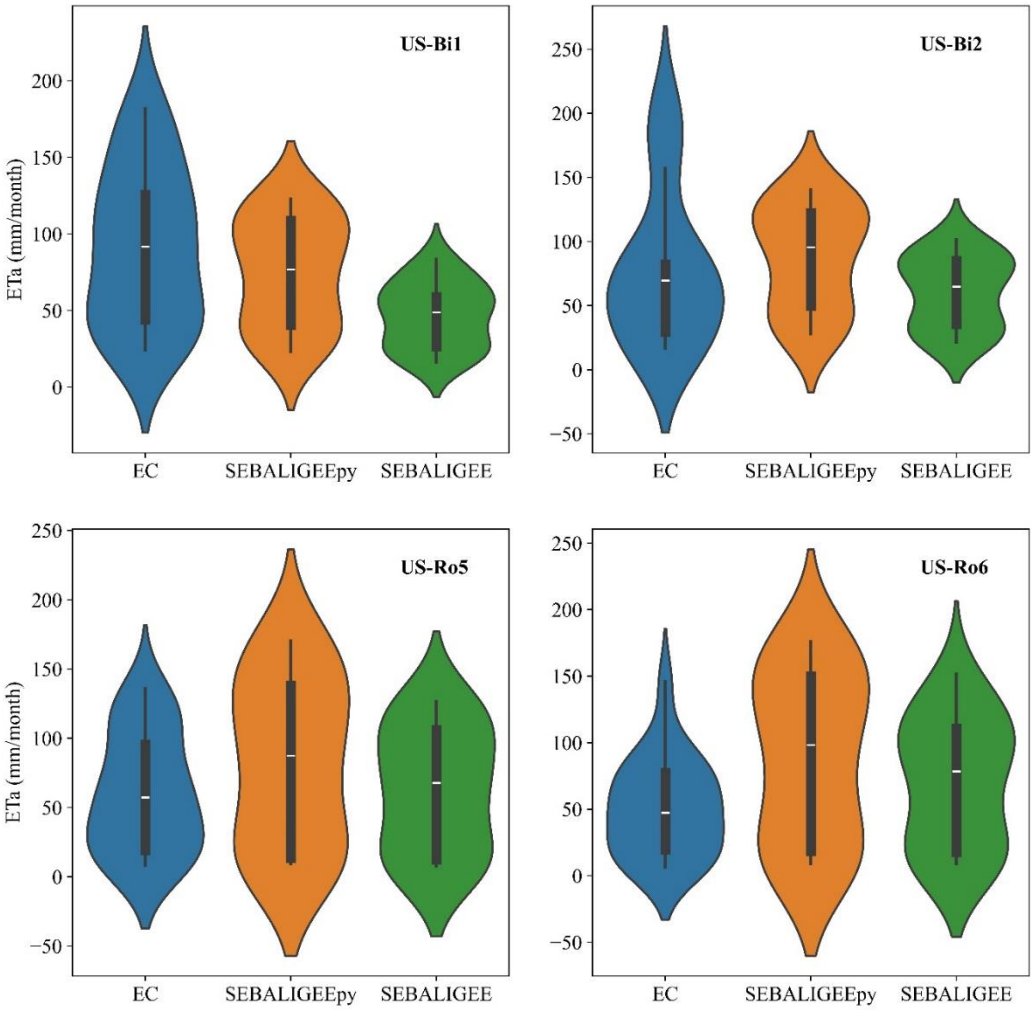

Figure 4.5. Violin plots representing the comparison of measured (EC) and modeled (SEBALIGEE and SEBALIGEEpy) actual evapotranspiration (ET_a). The vertical black line indicates the interquartile range, and the white horizontal line indicates median values.

4.2.2. Evaluating SEBALIGEEpy-based ETa in smallholder areas

SEBALIGEEpy achieved an RMSE of 48.58 mm/month, an MAE of 47.98 mm/month, and an R^2 of 0.86 compared with SWAT+ simulated ETa at the Jedeb watershed. These results suggest that SEBALIGEEpy performs well compared with the established models, showing its potential for accurate ETa estimation. In December and January, ETa was low due to minimal precipitation, whereas in April and May, the vegetation greened, and crops grew, gradually increasing ETa as

irrigated crops reached the optimal height. The average seasonal ETa for the agroecological zones is 555.25 mm for Woyna Dega, 492.21 mm for Dega, and 344.69 mm for Wurch.

The sample points used for land cover classification in the Jedeb watershed for seven different LULC classes (Mekonnen et al., 2024) were used to assess the levels of variability in ETa. The average ETa of bare soil was 457.46 mm (±30.08 mm), that of towns and settlements was 448.52 mm (±50.08 mm), rainfed croplands had the lowest at 416.73 mm (±49.69 mm), that of forests was 514.36 mm (±54.92 mm), that of irrigated areas was 508.37 mm (±39.23 mm), that of grazing lands was 449.10 mm (±56.76 mm), and that of water bodies was the highest at 623.62 mm (±30.36 mm).

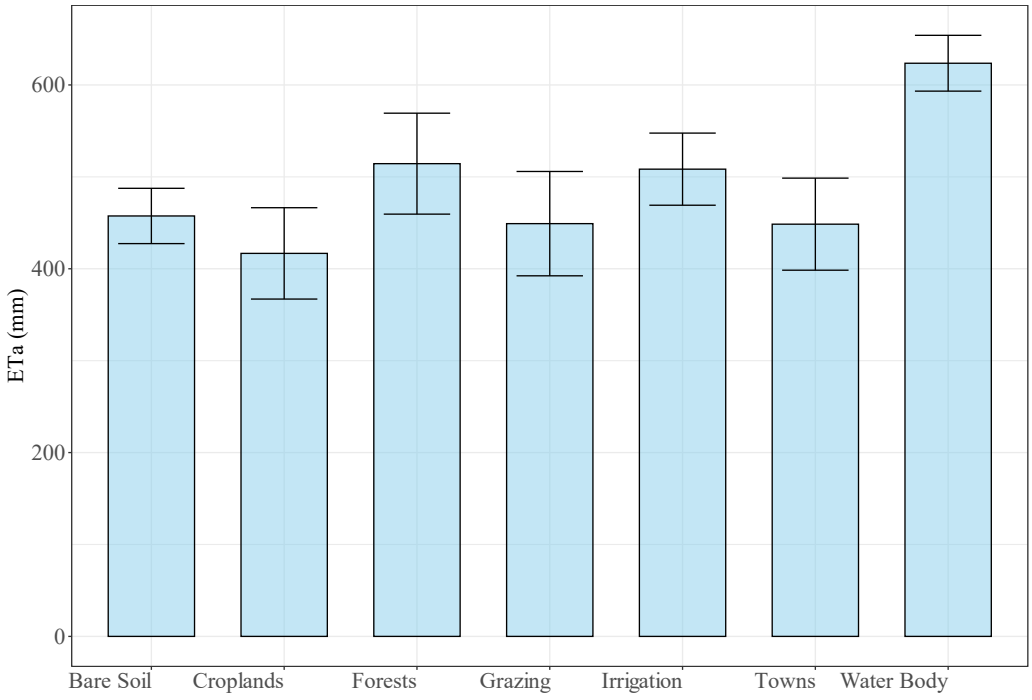

Figure 4.6. Mean seasonal ETa (2016--2022) of different land uses estimated using the SEBALIGEEpy model in the Jedeb watershed, Upper Blue Nile.

SEBALIGEEpy resulted in an RMSE of 24.57 mm/month, an MAE of 18.51 mm/month, and an R^2 of 0.64 compared with WaPOR-L3 for seven consecutive irrigation seasons (2016--2022) in the Koga irrigation scheme. In the seasonal comparison, the RMSE was 66.94 mm/season, the MAE was 63.06 mm/season, and the R^2 was 0.92. Using the WaPOR decadal land cover classification, the crops grown using irrigation were wheat, maize, potato, vegetables, and mixed

crops. The mean seasonal water consumption estimated using SEBALIGEEpy for wheat, maize, potato, vegetables, and mixed crops was 576 mm, 565 mm, 556 mm, 533 mm, and 567 mm, respectively. In the 2016/17 season, May data was missing because of high cloud cover. The mean seasonal water consumption estimated using WaPOR data for wheat, maize, potato, vegetables, and mixed crops was 569 mm, 683 mm, 663 mm, 664 mm, and 589 mm, respectively.

Across the seven seasons considered, both datasets show relatively consistent patterns in the ETa values for each crop; slight fluctuations are noticeable, indicating potential variations in the input data, model parameters, and processing methodologies. Generally, SEBALIGEEpy ETa tends to have slightly lower values than does WaPOR ETa for most crops and seasons. The WaPOR-estimated ETa also exhibited high variability among fields with high standard deviations (Figure 4.7).

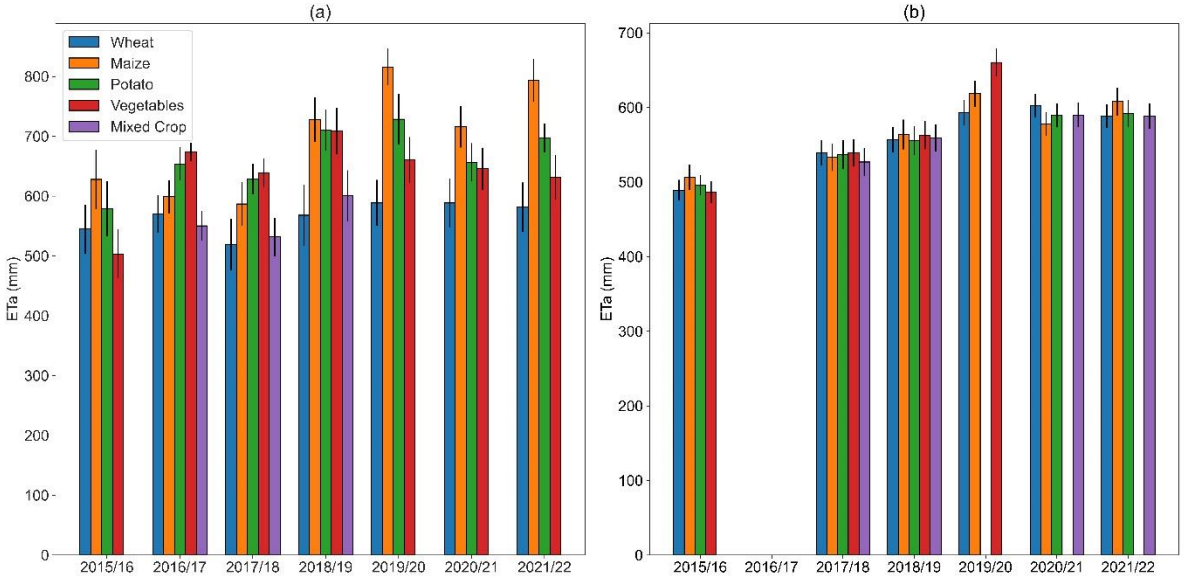

Figure 4.7. Seasonal water consumption (a) WaPOR and (b) SEBALIGEEpy ETa from six years (2016--2022) during the irrigation season (December--May) in the Koga Irrigation Project.

4.2.3. Effectiveness of remote sensing-based ETa estimation

Evapotranspiration models inherently contain some degree of uncertainty that can arise from numerous factors, including limitations of remote sensing instruments, resolution of data, methods used for data processing, spatial and temporal variations, cloud cover, and inaccuracies in climatic data (Doherty et al., 2022; Li et al., 2021; Senay et al., 2022). Land cover is an important parameter

for the SEBALIGEEpy and SWAT+ models, as it determines the values allocated to the biophysical properties (Abiodun et al., 2018; Dile et al., 2020). Sensor-derived parameters from satellite images may also have uncertainties (Cheng et al., 2023). The differences in the ETa values in the current study between the water balance and energy balance models resulted from the differences in the climate parameter inputs and land cover datasets used. ERA5 is a model-based dataset, so it may not always perfectly match the observations (Munoz-Sabater et al., 2021). Reanalysis products are viable alternatives to climate data in data-scarce locations. However, limitations exist due to the spatial resolution and observations used for reanalysis model development (Gleixner et al., 2020).

The water balance model ETa estimates rely on rainfall processes because it is the major model driver, capturing only rainfall-based (green) ETa while capturing only rainfall-based (green) ETa. In contrast, the energy balance models capture both rainfall-based ET (green) and rainfall-independent ET (blue) using land surface temperature to partition the radiant energy at the surface into heat and ET fluxes, regardless of the source type (Velpuri and Senay, 2017). As a result, the SEBALIGEEpy ETa estimate was greater than the SWAT+ model-simulated ETa estimate. Water balance methods are also sensitive to errors in precipitation data (Zhang et al., 2016). Uncertainties also arise from the lack of recent ground truth data for SWAT+ model calibration and validation. The limitations of the SWAT+ model for estimating ETa, including errors in weather data, can lead to errors in ETa estimates, and a simplified representation of vegetation may not accurately capture the complex interactions between vegetation and the environment (Parajuli et al., 2022). The other variation arises from the contrasting algorithms employed by WaPOR and SEBALI, with WaPOR utilizing a two-source algorithm sensitive to soil moisture, whereas the SEBALI model adopts a one-source algorithm sensitive to LST (Javadian et al., 2019).

The ETa estimates are assumed to represent predominantly vegetation systems in the study area (Allen et al., 2011). The higher spatial resolution of the land cover data likely provides a more detailed and accurate representation of the heterogeneous surface characteristics in the area, aiding in the selection of hot and cold pixels and resulting in good model performance (Alawi and Ozkul, 2023). The choice of land cover resolution is crucial, as it affects the accuracy and model fit and should be aligned with the specific requirements and topography.

Despite its minor limitations, SEBALIGEEpy can be used for water resource management for

smallholder irrigation systems. With minimal ground data, it can be used to assess irrigation performance and water productivity at the field and scheme levels. This assessment could help identify areas with water scarcity and inefficiencies for improving irrigation infrastructure and practices and support the sustainable expansion of irrigation. The model outputs can be used for advisory services by estimating irrigation water requirements and identifying yield and productivity gaps so that smallholder farmers can make more informed decisions, monitor drought conditions by detecting changes in ETa patterns, and advise farmers on irrigation adjustments during dry periods to prevent crop stress and yield losses.

4.3. Evaluation of Irrigation Performance and Water Productivity

4.3.1. Analysis of ET and crop water use

The seasonal ETa and precipitation for wheat over two seasons, 2021/22 and 2022/23, are presented in Table 4.7. It shows variations between seasons, with a slight decrease in ETa and an increase in precipitation. At the scheme level, in the 2021/22 irrigation season, ETa was 441.2 ± 48.74 mm, and it was 432 ± 4.68 mm in the 2022/23 irrigation season. For wheat fields, specifically, in the 2021/22 season, the ETa was 441.2 ± 5.39 mm, suggesting less variability among wheat-growing farmers. During the 2022/23 season, ETa was 432 ± 4.68 mm, a slightly lower mean and standard deviation, suggesting a more consistent pattern of evapotranspiration due to cluster farming on irrigated wheat (Table 5.1). Water consumption has decreased due to rainfall availability in the 2022/23 season. The maximum ETa occurred in March in both seasons when the wheat fully developed, and the minimum ETa and high variability occurred in December. The planting month and less variability occurred in February, indicating more consistent water consumption (Figure 5.3).

Table 4.7. Monthly actual evapotranspiration (ETa), reference evapotranspiration (ETo), precipitation (P), and effective precipitation (Pe) for the 01/12/2021 to 30/04/2022 and 01/12/2022 to 30/04/2023 irrigation seasons

Month	ETa (mm)	ETo (mm)	ETc (mm)	P (mm)	Pe (mm)
Dec-21	69.9 ± 4.16	103.5	31.04	10.5	10.3
Jan-22	76.9 ± 2.51	112.2	85.30	22.9	22.1
Feb-22	78.6 ± 1.65	112.5	128.26	16.7	16.3
Mar-22	108.5 ± 2.62	140.6	132.15	41.4	38.7
Apr-22	100.9 ± 2.78	151.8	62.24	41.9	39.1
Season Total	441.2 ± 5.39	621.9	438.99	133.3	126.5
Dec-22	69.9 ± 2.71	104.2	31.26	14.1	13.1
Jan-23	76.9 ± 1.91	106.5	80.93	11.9	11.7
Feb-23	78.6 ± 1.49	109.5	124.81	12.1	11.9
Mar-23	108.5 ± 2.73	142.2	133.64	64.8	58.1
Apr-23	100.9 ± 2.58	146.6	60.10	84.5	73.1
Season Total	432 ± 4.68	609.9	430.73	187.3	167.9

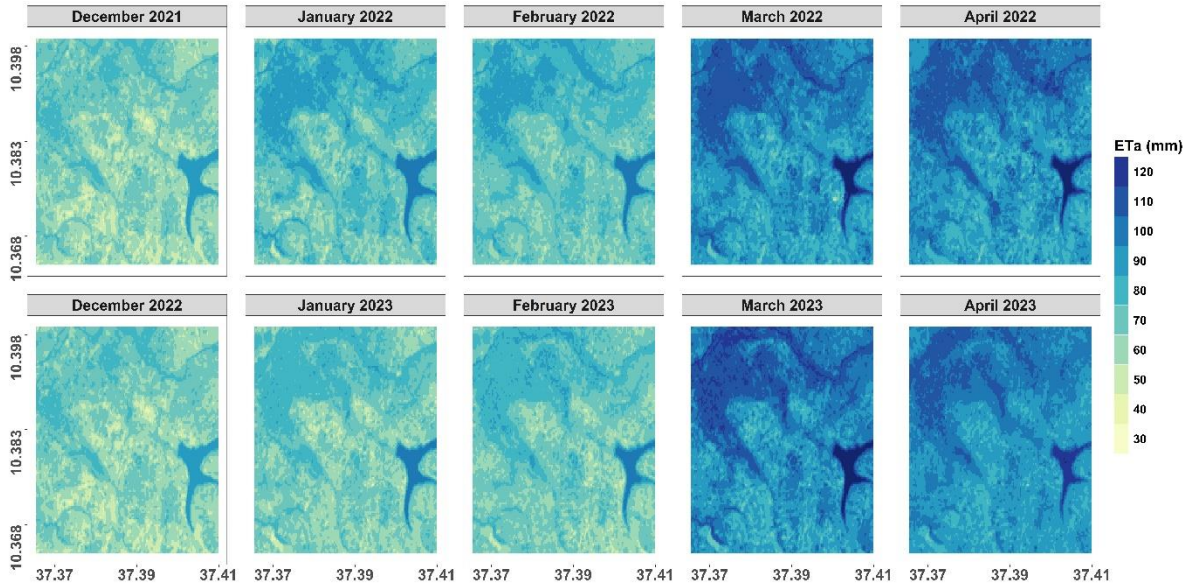

Figure 4.8. Actual evapotranspiration (ETa) for the 2021/22 and 2022/23 irrigation seasons at the Shimburit Irrigation Scheme

4.3.2. Analysis of performance indicators

In the 2021/22 irrigation season, the coefficient of variation (CV) ranged from a minimum of 2.01% to a maximum of 6.34%, with an average value of 1.90%, and from 1.90% to 3.89%, with an average value of 1.63%, for the 2022/23 irrigation season at the scheme level. For the wheat fields sampled in the 2021/22 season, the coefficient of variation (CV) ranged from a minimum of 0.26% to a maximum of 3.46%, with an average value of 1.23%, and from 0.20% to 4.82%, with an average value of 1.09%, for the 2022/23 season. The highest variability is recorded in December of both irrigation seasons due to differences in the planting dates between farmers. The seasonal time scale CV has decreased compared with the monthly scale because of the aggregated variability arising from planting dates. This shows less variability in evapotranspiration rates, suggesting that water use efficiency does not vary significantly during this season between wheat growers and within the field. The seasonal RET was 1.00 on 2021/22 and 1.04 on 2022/23, indicating that the scheme has an adequate water supply (Figure 4.9). The maximum RET is also in December in both irrigation seasons. The RWSs were 1.56 and 1.73 for the two consecutive seasons, implying an excess water supply in both seasons. The slight increase in the RET and RWS values was due to increased rainfall in the 2022/23 irrigation season (Table 4.9). The DF values were 0.65 and 0.60 for the two seasons, indicating stable water storage.

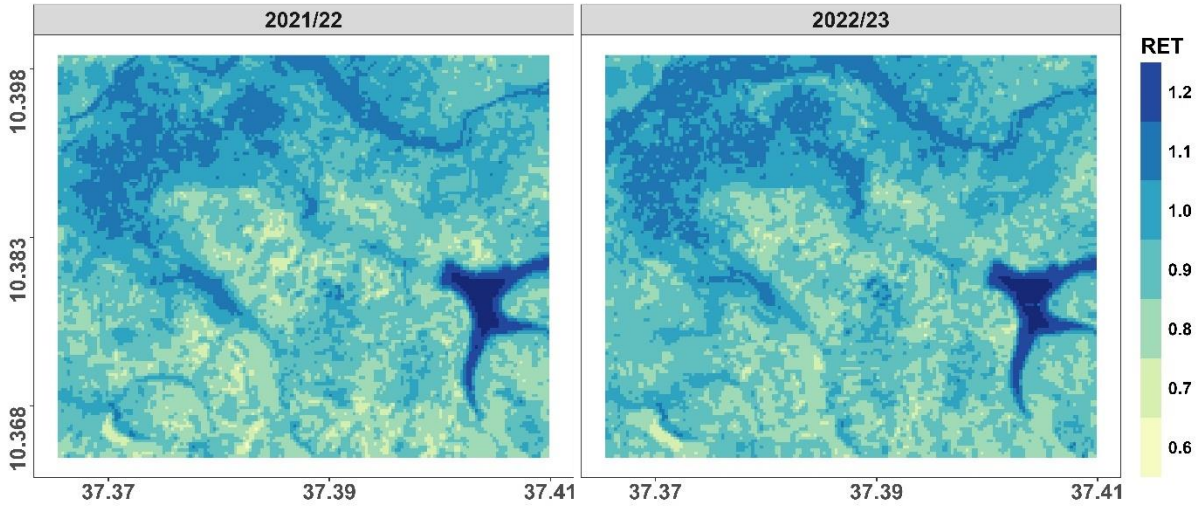

Figure 4.9. Relative evapotranspiration (RET) during the 2021/22 and 2022/23 irrigation seasons

The OCR was low at 0.54 and 0.43 for the 2021/22 and 2022/23 irrigation seasons, respectively. Conveyance losses accompany this; the conveyance efficiency is 62% for the main canal. The OCR (efficiency) varied highly between months. It was low at the start of the season (December and January) and in the middle of the season (February), when water was consumed efficiently at the vegetative stage. The OCR is high when the wheat is in its vegetative stage (February and March). In the 2022/23 season, the OCR was low (especially in April), resulting from the release of similar amounts of water from the dam throughout the season without an analysis of the monthly crop water requirements, even when rainfall was available. The monthly fluctuations in precipitation contributed to these variations in the two seasons. The analysis reveals dynamic patterns in water consumption efficiency and supply adequacy across months. A lot of tail-water runoff was observed at the tails of the fields, implying that the crop needs to be using a significant portion of the inflow (Vc). Concerns arise about efficiencies and depleted fractions during certain months, emphasizing the necessity for sustainable water management strategies. The issue in the Shimburit scheme is that a constant amount of water is released every month during the irrigation season regardless of the crop water requirements (Table 4.8).

Table 4.8. Performance metrics, including the coefficient of variation (CV), relative evapotranspiration (RET), relative water supply (RWS), depleted fraction (DF), and overall consumed ratio (OCR), for the 2021/22 and 2022/23 irrigation seasons

Month	CV (%)	RET	RWS	DF	OCR
Dec-21	6.3	2.12	1.41	1.50	0.58
Jan-22	3.0	0.99	1.83	0.54	0.45
Feb-22	2.0	0.64	1.07	0.60	0.91
Mar-22	2.5	0.80	1.32	0.61	0.66
Apr-22	2.7	1.64	2.75	0.60	0.14
Seasonal Average	1.90	0.71	1.56	0.65	0.54
Dec-22	3.9	2.31	1.53	1.51	0.48
Jan-23	2.5	0.98	1.80	0.55	0.50
Feb-23	1.9	0.65	1.07	0.61	0.92
Mar-23	2.5	0.84	1.50	0.56	0.49
Apr-23	2.6	1.73	3.60	0.48	-0.20
Seasonal Average	1.63	0.74	1.73	0.60	0.43

In the 2021/22 season, the crop water productivity (CWP) of wheat estimated from harvested data collection ranged from a minimum of 0.30 kg/m^3 to a maximum of 1.25 kg/m^3, with a mean value

of 0.74 kg/m^3, whereas the CWP estimated from the SEBALI biomass estimate ranged from a minimum of 0.39 kg/m^3 to a maximum of 1.07 kg/m^3, with a mean value of 2.49 kg/m^3. Similarly, for the 2022/23 season, the CWP from the harvested data varied between 0.14 kg/m^3 (minimum) and 0.86 kg/m^3 (maximum), with a mean value of 0.48 kg/m^3. The CWP estimated using the SEBALI model ranged from a minimum of 0.34 kg/m^3 to a maximum of 2.25 kg/m^3, with a mean of 0.96 kg/m^3.

The water productivity analysis suggested good water productivity and water management practices by farmers producing wheat, even though the SEBALIGEEpy model overestimated it due to some outliers had high CWP estimates (Figure 4.10). In the 2021/22 season, the land productivity of the sample fields ranged from a minimum of 1.33 tons/ha to a maximum of 5.53 tons/ha, with an average value of 3.25 tons/ha. In the 2022/23 season, land productivity ranged from 0.6 tons/ha to 3.73 tons/ha, with an average of 2.08 tons/ha. Wheat production (tons/ha) has declined due to untimely rainfall during harvest, whereas the CWP has been relatively consistent.

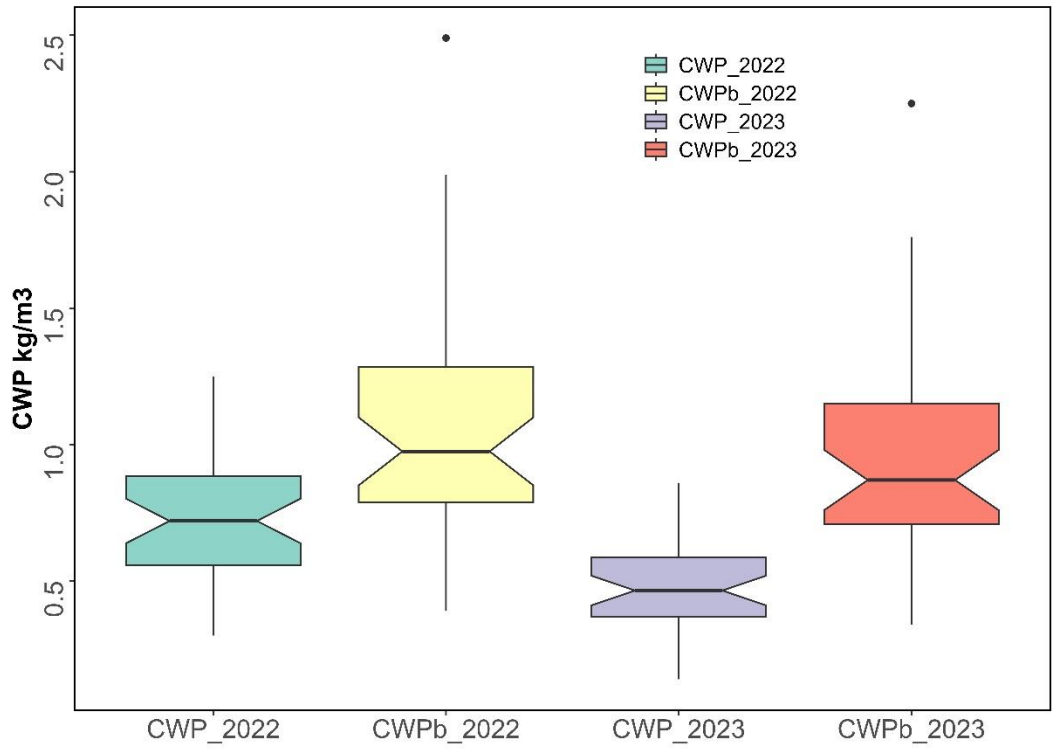

Figure 4.10. Box plot showing the crop water productivity estimated from remote sensing and field measurements

where CWPb_2022 and CWPb_2023 represent CWP estimated using remote sensing, and CWP_2022 and CWP_2023 represent the CWP estimated from yield collected from the field for the 2021/22 and 2022/23 seasons, respectively.

4.3.3. Effectiveness and limitations of remote sensing in irrigation performance assessment

The remote sensing method employed to evaluate spatiotemporal irrigation performance and water productivity at the field level with minimal ground-based measurements was found to be efficient. Remote sensing provides useful information to decision-makers, water managers, and farmers to improve the management of water resources and realize food security in smallholder farming systems (Bashe et al., 2023). Compared with ground-based performance assessments, remote sensing-based methods reduce the cost of evaluating irrigation performance and have the potential for scalability (Chukalla et al., 2022; Karimi et al., 2019).

The analysis of the irrigation performance indicators revealed that the Shimburit irrigation scheme had good equity and adequate water distribution among different fields and crops. However, the OCR and DF values were low due to excessive water release during the land preparation and harvest periods, indicating that the water from the irrigation supply was not fully consumed (Bastiaanssen et al., 2001). This is also attributed to excessive water release from the dam throughout the irrigation season due to the absence of a properly functioning distribution system. The scheme faces issues of excessive water loss, especially during the start of the irrigation season, and necessitates infrastructure development and management to mitigate losses and enhance overall efficiency, which is a common problem among schemes in the area (Abera et al., 2019; Bashe et al., 2023). The increase in crop water productivity (CWP) and the decrease in reported land productivity are due to extreme weather conditions (rain damage) during the harvest period in the area.

The OCR quantifies the degree to which crop irrigation requirements are met by irrigation water (Abera et al., 2019; Bos et al., 2005). The OCR (efficiency) values of the schemes were 0.54 and 0.43 in the 2021/22 and 2022/23 irrigation seasons, respectively, indicating that water was released in excess of the CWR. The results are relatively similar to those of other related irrigation performance assessment studies in the area (Alemie et al., 2023; Ayele et al., 2021; Belay et al., 2022; Yihune et al., 2022). Alemie et al. (2023) reported that the efficiency of the scheme was

44%. Similarly, Ayele et al. (2021) reported that the overall efficiency was 51.75% for the Lower Fetam scheme and 47.71% for the Leza scheme. Overall performances of 50% and 51% were reported for the small-scale irrigation schemes of Mugie and Fesas (Belay et al., 2022). The overall efficiency of the Inguti unit in the Koga irrigation scheme was found to be 46.3% (Yihune et al., 2022). The global CWP of wheat categories is low (≤ 0.75 kg/m³), medium (> 0.75 to < 1.10 kg/m³), and high (≥ 1.10 kg/m³) (Foley et al., 2020). The Shimburit irrigation scheme had a low to medium good CWP during the 2021/22 and 2022/23 irrigation seasons and had room for improvement if well managed.

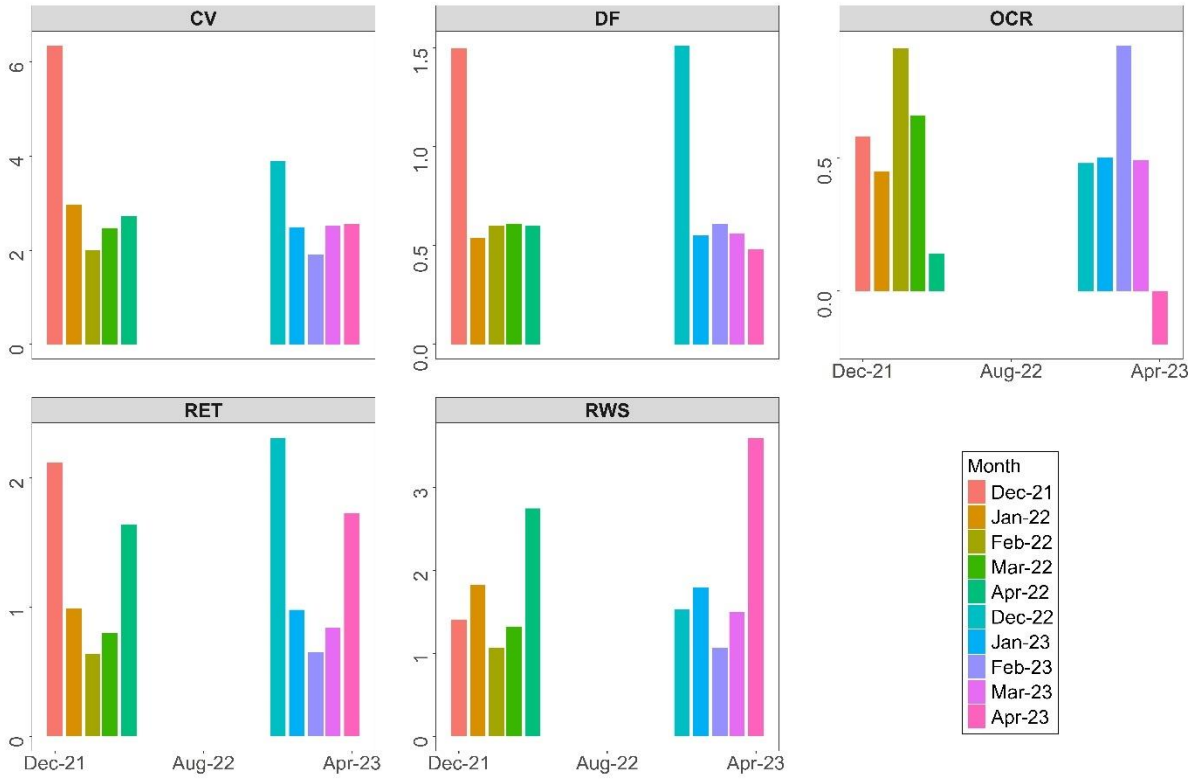

Figure 4.11. Monthly coefficient of variation (CV), depleted fraction (DF), overall consumed ratio (OCR), relative ET (RET), and relative water supply (RWS) for the 2021/22 and 2022/23 irrigation seasons

Despite the many benefits of using remote sensing techniques for irrigation performance assessment, there is still a gap between research projects and practical applications (Taghvaeian et al., 2018). Data collected at the scheme or field level are often sparse, and when available, they are frequently unreliable or difficult to access (Nikam et al., 2020). Limitations in the remote

sensing method applied include variations in planting dates among farmers, which have led to inconsistencies in the values of the performance indicator. The spatial resolution of climate data, such as CHIRPS (5 km) and ERA5 (11 km) data, may also introduce errors. Under different field management conditions by farmers, crop-specific parameters, such as the harvest index, can significantly vary (Chukalla et al., 2022). Generally, the accuracy of irrigation performance indicators relies on the availability and quality of data, and data scarcity may result in less robust results (Fernández et al., 2020). Thus, higher-resolution satellite images are favored for local-scale applications despite accessibility and cost constraints. The accuracy of the evapotranspiration model for estimating biomass can also be affected by the complexity of the study area and the accuracy of the parameters derived from remote sensing datasets (Mingxing et al., 2020).

The project is facing and will face challenges that will reduce its performance. The mean annual irrigation water demand is expected to increase due to climate change-induced decreases in future precipitation and temperature increases (Worku et al., 2023b). Over the past six years, the Shimburit reservoir has experienced a 7.5% decrease in capacity due to excessive sedimentation (Endalew and Mulu, 2022). Weak institutional, technical, and human capacity to manage the scheme and preparedness for high variability in space and time conditions, such as untimely rainfall, affects water use efficiency (Eshete et al., 2020; Nakawuka et al., 2017). These challenges necessitate urgent attention and strategic interventions to ensure project sustainability and effectiveness under changing climatic and environmental conditions.

5. CONCLUSION AND RECOMMENDATION

5.1. Conclusion

Remote sensing has proven effective in addressing hydrological applications, particularly in filling data gaps and providing reliable information for water resource management. However, challenges such as limited validation datasets and regional variability in satellite rainfall estimates persist. There is a need for further exploration of alternative models and continuous improvement in remote sensing technology to increase accuracy and applicability.

Research on smallholder irrigation mapping has demonstrated the effectiveness of fusing multitemporal and multispectral data, particularly using multitemporal synthetic aperture radar (SAR) and machine learning algorithms. However, mapping smallholder irrigation remains challenging because of the fragmentation of land and varied management practices. Careful input data and algorithm selection are crucial for accurately mapping irrigated areas.

The operationalization of the SEBALI model using Python and high-resolution land cover data shows promising results in estimating evapotranspiration rates, albeit with limitations in data frequency. Continuous refinement and integration of multiple data sources are necessary to mitigate uncertainties.

Assessment of small-scale irrigation scheme performance using remote sensing reveals insights into water resource management and identifies areas for improvement. While schemes such as Shimburit provide an adequate water supply, efficiency improvements are needed to ensure sustainability. Remote sensing offers valuable information for decision-making and continuous evaluation of irrigation schemes.

In conclusion, remote sensing and machine learning algorithms and advanced modeling techniques present valuable tools for addressing hydrological challenges and improving irrigation management in Ethiopian highlands. Continuous research and technological advancements are necessary to further harness the potential of remote sensing for sustainable water resource management and agricultural development.

5.2. Recommendations

On the basis of the findings of this study, the following recommendations are suggested:

i. Efforts should be made to improve the coverage and quality of validation datasets for remote sensing products, including streamflow measurement stations and the establishment of flux towers for ETa monitoring.

ii. To mitigate the uncertainties associated with remote sensing-based models, there is a need to integrate data from multiple sources, including ground-based observations and model simulations. This integrated approach can help improve the accuracy and reliability of remote sensing-derived estimates.

iii. Irrigation mapping using machine learning should be performed frequently to evaluate the extent of irrigation in the schemes built and the sustainability of irrigation development.

iv. Continuous performance evaluation is critical for the sustainability of small-scale irrigation schemes. The developed framework can be applied in a time series manner.

v. Investment in canal infrastructure development and the implementation of soil and water conservation measures can reduce sedimentation and increase water use efficiency.

vi. Efforts should be made to increase the capacity of stakeholders, including researchers, water managers, and decision makers, in the utilization of remote sensing technologies for hydrological and irrigation management. In this context, collaboration between academia, government agencies, and international organizations can facilitate knowledge exchange and technology transfer.

References

Abdelmoneim, H., Soliman, M.R., Moghazy, H.M., 2020. Evaluation of TRMM 3B42v7 and CHIRPS Satellite Precipitation Products as an Input for Hydrological Model Over Eastern Nile Basin. Earth Syst. Environ. 4, 685–698. https://doi.org/10.1007/s41748-020-00185-3

Abdelwares, M., Lelieveld, J., Zittis, G., Haggag, M., Wagdy, A., 2020. A Comparison of Gridded Datasets of Precipitation and Temperature Over the Eastern Nile Basin Region. Euro-Mediterr. J. Environ. Integr. 5, 3. https://doi.org/10.1007/s41207-019-0140-y

Abebe, W.B., Tilahun, S.A., Moges, M.M., Wondie, A., Dersseh, M.G., Assefa, W.W., Mhiret, D.A., Adem, A.A., Zimale, F.A., Abera, W., Steenhuis, T.S., McClain, M.E., 2021. Ecological Status as the Basis for the Holistic Environmental Flow Assessment of a Tropical Highland River in Ethiopia. Water 13, 1913. https://doi.org/10.3390/w13141913

Abera, A., Verhoest, N.E.C., Tilahun, S., Inyang, H., Nyssen, J., 2021. Assessment of irrigation expansion and implications for water resources by using RS and GIS techniques in the Lake Tana Basin of Ethiopia. Environ. Monit. Assess. 193, 13. https://doi.org/10.1007/s10661-020-08778-1

Abera, A., Verhoest, N.E.C., Tilahun, S.A., Alamirew, T., Adgo, E., Moges, M.M., Nyssen, J., 2019. Performance of small-scale irrigation schemes in Lake Tana Basin of Ethiopia: technical and socio-political attributes. Phys. Geogr. 40, 227–251. https://doi.org/10.1080/02723646.2018.1516445

Abera, W., Brocca, L., Rigon, R., 2016. Comparative Evaluation of Different Satellite Rainfall Estimation Products and Bias Correction in the Upper Blue Nile (UBN) Basin. Atmospheric Res. 178–179, 471–483. https://doi.org/10.1016/j.atmosres.2016.04.017

Abera, W., Formetta, G., Brocca, L., Rigon, R., 2017. Modeling the Water Budget of the Upper Blue Nile Basin Using the Jgrass-Newage Model System and Satellite Data. Hydrol. Earth Syst. Sci. 21, 3145–3165. https://doi.org/10.5194/hess-21-3145-2017

Abiodun, O.O., Guan, H., Post, V.E.A., Batelaan, O., 2018. Comparison of MODIS and SWAT evapotranspiration over a complex terrain at different spatial scales. Hydrol. Earth Syst. Sci. 22, 2775–2794. https://doi.org/10.5194/hess-22-2775-2018

Abiy, A.Z., Melesse, A.M., 2017. Evaluation of Watershed Scale Changes in Groundwater and Soil Moisture Storage with the Application of Grace Satellite Imagery Data. CATENA 153, 50–60. https://doi.org/10.1016/j.catena.2017.01.036

Abunnasr, Y., Mhawej, M., Chrysoulakis, N., 2022. SEBU: A novel fully automated Google Earth Engine surface energy balance model for urban areas. Urban Clim. 44, 101187. https://doi.org/10.1016/j.uclim.2022.101187

Ademe, D., Zaitchik, B.F., Tesfaye, K., Simane, B., Alemayehu, G., Adgo, E., 2021. Analysis of agriculturally relevant rainfall characteristics in a tropical highland region: An agroecosystem perspective. Agric. For. Meteorol. https://doi.org/10.1016/j.agrformet.2021.108697

Agide, Z., Haileslassie, A., Sally, H., Erkossa, T., Schmitter, P.S., Langan, S.J., Hoekstra, D., 2016. Analysis of water delivery performance of smallholder irrigation schemes in

Ethiopia: Diversity and lessons across schemes, typologies and reaches. International Livestock Research Institute.

Agutu, N.O., Awange, J.L., Ndehedehe, C., Kirimi, F., Kuhn, M., 2019. GRACE-Derived Groundwater Changes Over Greater Horn of Africa: Temporal Variability and the Potential for Irrigated Agriculture. Sci. Total Environ. 693, 133467. https://doi.org/10.1016/j.scitotenv.2019.07.273

Ahadi, R., Samani, Z., Skaggs, R., 2013. Evaluating on-farm irrigation efficiency across the watershed: A case study of New Mexico's Lower Rio Grande Basin. Agric. Water Manag. 124, 52–57. https://doi.org/10.1016/j.agwat.2013.03.010

Ahmad, I., Dar, M.A., Andualem, T.G., Teka, A.H., 2020. GIS-Based Multi-Criteria Evaluation of Groundwater Potential of the Beshilo River Basin, Ethiopia. J. Afr. Earth Sci. 164, 103747. https://doi.org/10.1016/j.jafrearsci.2019.103747

Ahmad, M.-D., Turral, H., Nazeer, A., 2009. Diagnosing irrigation performance and water productivity through satellite remote sensing and secondary data in a large irrigation system of Pakistan. Agric. Water Manag. 96, 551–564. https://doi.org/10.1016/j.agwat.2008.09.017

Ahmed, M., Sultan, M., Wahr, J., Yan, E., Milewski, A., Sauck, W., Becker, R., Welton, B., 2011. Integration of GRACE (Gravity Recovery and Climate Experiment) Data with Traditional Data Sets for a Better Understanding of the Time-Dependent Water Partitioning in African Watersheds. Geology 39, 479–482. https://doi.org/10.1130/G31812.1

Ajaz, A., Karimi, P., Cai, X., De Fraiture, C., Akhter, M.S., 2019. Statistical Data Collection Methodologies of Irrigated Areas and Their Limitations: A Review. Irrig. Drain. 68, 702–713. https://doi.org/10.1002/ird.2365

Akhtar, F., Awan, U.K., Tischbein, B., Liaqat, U.W., 2018. Assessment of Irrigation Performance in Large River Basins Under Data Scarce Environment - a Case of Kabul River Basin, Afghanistan. Remote Sens. https://doi.org/10.3390/rs10060972

Alawi, S.A., Ozkul, S., 2023. Evaluation of land use/land cover datasets in hydrological modelling using the SWAT model. H2Open J. 6, 63–74. https://doi.org/10.2166/h2oj.2023.062

Aldiansyah, S., Wardani, F., 2024. Spatiotemporal dynamic of soil erosion in the Roraya River Basin based on RUSLE model and Google Earth Engine. J. Hydroinformatics jh2024219. https://doi.org/10.2166/hydro.2024.219

Alemie, B.T., Defersha, D.T., Tesfaye, A.T., Moges, M.M., 2023. Physical performance of small-scale irrigation scheme: a case study of Tilku Fetam irrigation scheme, Awi zone, Amhara region, Ethiopia. Sustain. Water Resour. Manag. 9, 11. https://doi.org/10.1007/s40899-022-00789-9

Alemu, A.M., Seleshi, Y., Meshesha, T.W., 2022. Modeling the spatial and temporal availability of water resources potential over Abbay river basin, Ethiopia. J. Hydrol. Reg. Stud. 44, 101280. https://doi.org/10.1016/j.ejrh.2022.101280

Alemu, H., Kaptué, A., Senay, G., Wimberly, M., Henebry, G., 2015a. Evapotranspiration in the Nile Basin: Identifying Dynamics and Drivers, 2002–2011. Water 7, 4914–4931. https://doi.org/10.3390/w7094914

Alemu, H., Kaptué, A.T., Senay, G.B., Wimberly, M.C., Henebry, G.M., 2015b. Evapotranspiration in the Nile Basin: Identifying Dynamics and Drivers, 2002–2011. Water. https://doi.org/10.3390/w7094914

Alemu, H., Senay, G., Kaptue, A., Kovalskyy, V., 2014. Evapotranspiration Variability and Its Association with Vegetation Dynamics in the Nile Basin, 2002–2011. Remote Sens. 6, 5885–5908. https://doi.org/10.3390/rs6075885

Allam, M., Mhawej, M., Meng, Q., Faour, G., Abunnasr, Y., Fadel, A., Xinli, H., 2021. Monthly 10-m evapotranspiration rates retrieved by SEBALI with Sentinel-2 and MODIS LST data. Agric. Water Manag. https://doi.org/10.1016/j.agwat.2020.106432

Allam, M.M., Jain Figueroa, A., McLaughlin, D.B., Eltahir, E.A.B., 2016. Estimation of Evaporation Over the Upper Blue Nile Basin by Combining Observations from Satellites and River Flow Gauges. Water Resour. Res. 52, 644–659. https://doi.org/10.1002/2015WR017251

Allen, R.G., Irmak, A., Trezza, R., Hendrickx, J.M.H., Bastiaanssen, W.G.M., Kjaersgaard, J., 2011. Satellite-based ET estimation in agriculture using SEBAL and METRIC. Hydrol. Process. https://doi.org/10.1002/hyp.8408

Allen, R.G., Morton, C., Baburao Kamble, Kilic, A., Huntington, J., Thau, D., Gorelick, N., Erickson, T., Moore, R., Trezza, R., Ratcliffe, I., Robison, C., 2015. EEFlux: A Landsat-based Evapotranspiration mapping tool on the Google Earth Engine, in: 2015 ASABE / IA Irrigation Symposium: Emerging Technologies for Sustainable Irrigation - A Tribute to the Career of Terry Howell, Sr. Conference Proceedings. Presented at the 2015 ASABE / IA Irrigation Symposium: Emerging Technologies for Sustainable Irrigation - A Tribute to the Career of Terry Howell, Sr. Conference Proceedings, American Society of Agricultural and Biological Engineers, pp. 1–11. https://doi.org/10.13031/irrig.20152143511

Allen, R.G., Pereira, L.S., Raes, D., Smith, M., 1998. Crop evapotranspiration-Guidelines for computing crop water requirements-FAO Irrigation and drainage paper 56. FAO, Rome.

Allen, R.G., Tasumi, M., Morse, A., Trezza, R., Wright, J.L., Bastiaanssen, W.G.M., Kramber, W.J., Lorite, I.J., Robison, C.W., 2007. Satellite-Based Energy Balance for Mapping Evapotranspiration with Internalized Calibration (METRIC)—Applications. J. Irrig. Drain. Eng.-Asce. https://doi.org/10.1061/(asce)0733-9437(2007)133:4(395)

Alquraish, M.M., Khadr, M., 2021. Remote-Sensing-Based Streamflow Forecasting Using Artificial Neural Network and Support Vector Machine Models. Remote Sens. 13, 4147. https://doi.org/10.3390/rs13204147

Amani, M., Ghorbanian, A., Ahmadi, S.A., Kakooei, M., Moghimi, A., Moghaddam, S.H.A., Mahdavi, S., Ghahremanloo, M., Parsian, S., Wu, Q., Wu, Q., Wu, Q., Brisco, B., 2020. Google Earth Engine Cloud Computing Platform for Remote Sensing Big Data Applications: A Comprehensive Review. IEEE J. Sel. Top. Appl. Earth Obs. Remote Sens. https://doi.org/10.1109/jstars.2020.3021052

Amede, T., 2015. Technical and institutional attributes constraining the performance of small-scale irrigation in Ethiopia. Water Resour. Rural Dev. 6, 78–91. https://doi.org/10.1016/j.wrr.2014.10.005

Anapalli, S.S., Fisher, D.K., Reddy, K.N., Rajan, N., Pinnamaneni, S.R., 2019. Modeling evapotranspiration for irrigation water management in a humid climate. Agric. Water Manag. 225, 105731. https://doi.org/10.1016/j.agwat.2019.105731

Andualem, T.G., Demeke, G.G., 2019. Groundwater Potential Assessment Using GIS and Remote Sensing: A Case Study of Guna Tana Landscape, Upper Blue Nile Basin, Ethiopia. J. Hydrol. Reg. Stud. 24, 100610. https://doi.org/10.1016/j.ejrh.2019.100610

Andualem, T.G., Malede, D.A., Ejigu, M.T., 2020. Performance Evaluation of Integrated Multi-Satellite Retrieval for Global Precipitation Measurement Products Over Gilgel Abay Watershed, Upper Blue Nile Basin, Ethiopia. Model. Earth Syst. Environ. 6, 1853–1861. https://doi.org/10.1007/s40808-020-00795-w

Angelini, L.P., Biudes, M.S., Machado, N.G., Geli, H.M.E., Vourlitis, G.L., Ruhoff, A., Nogueira, J. de S., 2021. Surface Albedo and Temperature Models for Surface Energy Balance Fluxes and Evapotranspiration Using SEBAL and Landsat 8 over Cerrado-Pantanal, Brazil. Sensors 21, 7196. https://doi.org/10.3390/s21217196

Anteneh, Z.L., Alemu, M.M., Bawoke, G.T., Kehali, A.T., Fenta, M.C., Desta, M.T., 2022. Appraising Groundwater Potential Zones Using Geospatial and Multi-Criteria Decision Analysis (MCDA) Techniques in Andasa-Tul Watershed, Upper Blue Nile Basin, Ethiopia. Environ. Earth Sci. 81, 14. https://doi.org/10.1007/s12665-021-10083-0

Asrade, T.M., Tadesse, K.B., Kerebih, M.S., Ayinalem, S.B., 2024. Assessment of Groundwater Recharge Using WetSpass-M and MODFLOW Coupling in Jedeb Watershed, Upper Blue Nile Basin, Ethiopia. Air Soil Water Res. 17, 11786221241253325. https://doi.org/10.1177/11786221241253325

Assefa, W.W., Eneyew, B.G., Wondie, A., 2022. The Driving Forces of Wetland Degradation in Bure and Wonberma Woredas, Upper Blue Nile Basin, Ethiopia. Environ. Monit. Assess. 194, 838. https://doi.org/10.1007/s10661-022-10516-8

Awan, U.K., Tischbein, B., Conrad, C., Martius, C., Hafeez, M., 2011. Remote Sensing and Hydrological Measurements for Irrigation Performance Assessments in a Water User Association in the Lower Amu Darya River Basin. Water Resour. Manag. 25, 2467–2485. https://doi.org/10.1007/s11269-011-9821-2

Awulachew, S.B., Ayana, M., 2011. Performance of Irrigation: An Assessment at Different Scales in Ethiopia. Exp. Agric. 47, 57–69. https://doi.org/10.1017/S0014479710000955

Awulachew, S.B., Yilma, A.D., Loulseged, M., Loiskandl, W., Ayana, M., Alamirew, T., 2007. Water resources and irrigation development in Ethiopia (Working Paper No. 123). IWMI.

Ayana, E.K., Srinivasan, R., 2019. Impact of the Grand Ethiopian Renaissance Dam (GERD) and Climate Change on Water Availability in Sudan, in: Extreme Hydrology and Climate Variability. Elsevier, pp. 137–149. https://doi.org/10.1016/B978-0-12-815998-9.00012-9

Ayehu, G., Tadesse, T., Gessesse, B., 2020. Monitoring Residual Soil Moisture and Its Association to the Long-Term Variability of Rainfall Over the Upper Blue Nile Basin in Ethiopia. Remote Sens. 12, 2138. https://doi.org/10.3390/rs12132138

Ayehu, G., Tadesse, T., Gessesse, B., Yigrem, Y., 2019. Soil Moisture Monitoring Using Remote Sensing Data and a Stepwise-Cluster Prediction Model: The Case of Upper Blue Nile Basin, Ethiopia. Remote Sens. 11, 125. https://doi.org/10.3390/rs11020125

Ayehu, G.T., Tadesse, T., Gessesse, B., Dinku, T., 2018. Validation of New Satellite Rainfall Products Over the Upper Blue Nile Basin, Ethiopia. Atmospheric Meas. Tech. 11, 1921–1936. https://doi.org/10.5194/amt-11-1921-2018

Ayele, W.T., Ayele, Z.T., Shumey, E.E., Demessie, S.A., 2021. Performance evaluation of Lower Fetam and Leza small-scale irrigation schemes by using internal and external process indicators: case study in west gojjam zone, Amhara, Ethiopia. Sustain. Water Resour. Manag. 7, 70. https://doi.org/10.1007/s40899-021-00554-4

Bai, P., 2023. Comparison of remote sensing evapotranspiration models: Consistency, merits, and pitfalls. J. Hydrol. 617, 128856. https://doi.org/10.1016/j.jhydrol.2022.128856

Bartsotas, N.S., Anagnostou, E.N., Nikolopoulos, E.I., Kallos, G., 2018. Investigating Satellite Precipitation Uncertainty Over Complex Terrain. J. Geophys. Res. Atmospheres 123, 5346–5359. https://doi.org/10.1029/2017JD027559

Bashe, T., Alamirew, T., Dejen, Z.A., 2023. Evaluating Performance of Community-Based Irrigation Schemes Using Remote-Sensing Technologies to Enhance Sustainable Irrigation Water Management. Water Conserv. Sci. Eng. 8, 45. https://doi.org/10.1007/s41101-023-00222-y

Bashe, T., Alamirew, T., Dejen, Z.A., 2022. Estimating the economic value and economic return of irrigation water as a sustainable water resource management mechanism. Sustain. Water Resour. Manag. 8, 175. https://doi.org/10.1007/s40899-022-00764-4

Basheer, S., Wang, X., Farooque, A.A., Nawaz, R.A., Liu, K., Adekanmbi, T., Liu, S., 2022. Comparison of Land Use Land Cover Classifiers Using Different Satellite Imagery and Machine Learning Techniques. Remote Sens. 14, 4978. https://doi.org/10.3390/rs14194978

Bastiaanssen, W., Karimi, P., Rebelo, L.-M., Duan, Z., Senay, G., Muthuwatte, L., Smakhtin, V., 2014. Earth Observation Based Assessment of the Water Production and Water Consumption of Nile Basin Agro-Ecosystems. Remote Sens. 6, 10306–10334. https://doi.org/10.3390/rs61110306

Bastiaanssen, W.G.M., Bos, M.G., 1999. Irrigation Performance Indicators Based on Remotely Sensed Data: A Review of Literature. Irrig. Drain. Syst. https://doi.org/10.1023/a:1006355315251

Bastiaanssen, W.G.M., Brito, R.A.L., Bos, M.G., Souza, R.A., Cavalcanti, E.B., Bakker, M.M., 2001. Low Cost Satellite Data for Monthly Irrigation Performance Monitoring: Benchmarks from Nilo Coelho, Brazil. Irrig. Drain. Syst. 15, 53–79. https://doi.org/10.1023/A:1017967021198

Bastiaanssen, W.G.M., Menenti, M., Feddes, R.A., Holtslag, A.A.M., 1998a. A remote sensing surface energy balance algorithm for land (SEBAL)-1. Formulation. J. Hydrol. https://doi.org/10.1016/s0022-1694(98)00253-4

Bastiaanssen, W.G.M., Pelgrum, H., Wang, J., Ma, Y., Moreno, J.F., Roerink, G.J., Wal, T. van der, 1998b. A remote sensing surface energy balance algorithm for land (SEBAL). J. Hydrol. https://doi.org/10.1016/s0022-1694(98)00254-6

Bastiaanssen, W.G.M., Steduto, P., 2017. The Water Productivity Score (WPS) at Global and Regional Level: Methodology and First Results from Remote Sensing Measurements of Wheat, Rice and Maize. Sci. Total Environ. 575, 595–611. https://doi.org/10.1016/j.scitotenv.2016.09.032

Basukala, A.K., Oldenburg, C., Schellberg, J., Sultanov, M., Dubovyk, O., 2017. Towards improved land use mapping of irrigated croplands: performance assessment of different image classification algorithms and approaches. Eur. J. Remote Sens. 50. https://doi.org/10.1080/22797254.2017.1308235

Bathe, K.D., Patil, N.S., 2024. Assessment of land use-land cover dynamics and its future projection through Google Earth Engine, machine learning and QGIS-MOLUSCE: A case study in Jagatsinghpur district, Odisha, India. J. Earth Syst. Sci. 133, 111. https://doi.org/10.1007/s12040-024-02305-3

Bayissa, Y., Moges, S., Melesse, A., Tadesse, T., Abiy, A.Z., Worqlul, A., 2021. Multi-Dimensional Drought Assessment in Abbay/Upper Blue Nile Basin: The Importance of Shared Management and Regional Coordination Efforts for Mitigation. Remote Sens. 13, 1835. https://doi.org/10.3390/rs13091835

Bayissa, Y., Tadesse, T., Demisse, G., 2019. Building a High-Resolution Vegetation Outlook Model to Monitor Agricultural Drought for the Upper Blue Nile Basin, Ethiopia. Remote Sens. 11, 371. https://doi.org/10.3390/rs11040371

Bayissa, Y., Tadesse, T., Demisse, G., Shiferaw, A., 2017. Evaluation of Satellite-Based Rainfall Estimates and Application to Monitor Meteorological Drought for the Upper Blue Nile Basin, Ethiopia. Remote Sens. 9, 669. https://doi.org/10.3390/rs9070669

Bazzi, H., Baghdadi, N., Amin, G., Fayad, I., Zribi, M., Demarez, V., Belhouchette, H., 2021. An Operational Framework for Mapping Irrigated Areas at Plot Scale Using Sentinel-1 and Sentinel-2 Data. Remote Sens. https://doi.org/10.3390/rs13132584

Belayneh, A., Sintayehu, G., Gedam, K., Muluken, T., 2020. Evaluation of Satellite Precipitation Products Using HEC-HMS Model. Model. Earth Syst. Environ. 6, 2015–2032. https://doi.org/10.1007/s40808-020-00792-z

Belete, M., Deng, J., Wang, K., Zhou, M., Zhu, E., Shifaw, E., Bayissa, Y., 2020. Evaluation of Satellite Rainfall Products for Modeling Water Yield Over the Source Region of Blue Nile Basin. Sci. Total Environ. 708, 134834. https://doi.org/10.1016/j.scitotenv.2019.134834

Bewket, W., 2002. Land Cover Dynamics Since the 1950s in Chemoga Watershed, Blue Nile Basin, Ethiopia. Mt. Res. Dev. 22, 263–269. https://doi.org/10.1659/0276-4741(2002)022[0263:LCDSTI]2.0.CO;2

Bieger, K., Jeffrey G. Arnold, Jeffrey G. Arnold, Hendrik Rathjens, Michael J. White, Michael J. White, David D. Bosch, Peter M. Allen, Martin Volk, Raghavan Srinivasan, 2017. Introduction to SWAT+, A Completely Restructured Version of the Soil and Water Assessment Tool. J. Am. Water Resour. Assoc. https://doi.org/10.1111/1752-1688.12482

Biswas, J., Jobaer, M.A., Haque, S.F., Islam Shozib, M.S., Limon, Z.A., 2023. Mapping and monitoring land use land cover dynamics employing Google Earth Engine and machine learning algorithms on Chattogram, Bangladesh. Heliyon 9, e21245. https://doi.org/10.1016/j.heliyon.2023.e21245

Bitew, M.M., Gebremichael, M., 2011. Assessment of Satellite Rainfall Products for Streamflow Simulation in Medium Watersheds of the Ethiopian Highlands. Hydrol. Earth Syst. Sci. 15, 1147–1155. https://doi.org/10.5194/hess-15-1147-2011

Blatchford, M.L., Mannaerts, C.M., Njuki, S.M., Nouri, H., Zeng, Y., Pelgrum, H., Wonink, S., Karimi, P., 2020a. Evaluation of WaPOR V2 evapotranspiration products across Africa. Hydrol. Process. 34, 3200–3221. https://doi.org/10.1002/hyp.13791

Blatchford, M.L., Mannaerts, C.M., Zeng, Y., Nouri, H., Karimi, P., 2020b. Influence of Spatial Resolution on Remote Sensing-Based Irrigation Performance Assessment Using WaPOR Data. Remote Sens. https://doi.org/10.3390/rs12182949

Breiman, L., 2001. Random Forests. Mach. Learn. https://doi.org/10.1023/a:1010933404324

Breiman, L., Friedman, J.H., Olshen, R.A., Stone, C.J., 1984. Classification And Regression Trees, 1st ed. Routledge. https://doi.org/10.1201/9781315139470

Brown, C.F., Brumby, S.P., Guzder-Williams, B., Birch, T., Hyde, S.B., Mazzariello, J., Czerwinski, W., Pasquarella, V.J., Haertel, R., Ilyushchenko, S., Schwehr, K., Weisse, M., Stolle, F., Hanson, C., Guinan, O., Moore, R., Tait, A.M., 2022. Dynamic World, Near real-time global 10 m land use land cover mapping. Sci. Data 9, 251. https://doi.org/10.1038/s41597-022-01307-4

Bwambale, E., Naangmenyele, Z., Iradukunda, P., Agboka, K.M., Houessou-Dossou, E.A.Y., Akansake, D.A., Bisa, M.E., Hamadou, A.-A.H., Hakizayezu, J., Onofua, O.E., Chikabvumbwa, S.R., 2022. Towards precision irrigation management: A review of GIS, remote sensing and emerging technologies. Cogent Eng. 9, 2100573. https://doi.org/10.1080/23311916.2022.2100573

Carrasco, L., Carrasco, L., Carrasco, L.R., Aneurin W. O'Neil, Morton, R.D., Rowland, C.S., 2019. Evaluating Combinations of Temporally Aggregated Sentinel-1, Sentinel-2 and Landsat 8 for Land Cover Mapping with Google Earth Engine. Remote Sens. https://doi.org/10.3390/rs11030288

Chandrasekharan, K.M., Subasinghe, C., Haileslassie, A., 2021. Mapping irrigated and rainfed agriculture in Ethiopia (2015-2016) using remote sensing methods. International Water Management Institute (IWMI). https://doi.org/10.5337/2021.206

Chawla, I., Karthikeyan, L., Mishra, A.K., 2020. A Review of Remote Sensing Applications for Water Security: Quantity, Quality, and Extremes. J. Hydrol. 585, 124826. https://doi.org/10.1016/j.jhydrol.2020.124826

Cheng, M., Yin, D., Wu, W., Cui, N., Nie, C., Shi, L., Liu, S., Yu, X., Bai, Y., Liu, Y., Zhu, Y., Jin, X., 2023. A review of remote sensing estimation of crop water productivity: definition, methodology, scale, and evaluation. Int. J. Remote Sens. 44, 5033–5068. https://doi.org/10.1080/01431161.2023.2240523

Chu, H., Luo, X., Ouyang, Z., Chan, W.S., Dengel, S., Biraud, S.C., Torn, M.S., Metzger, S., Kumar, J., Arain, M.A., Arkebauer, T.J., Baldocchi, D., Bernacchi, C., Billesbach, D., Black, T.A., Blanken, P.D., Bohrer, G., Bracho, R., Brown, S., Brunsell, N.A., Chen, J., Chen, X., Clark, K., Desai, A.R., Duman, T., Durden, D., Fares, S., Forbrich, I., Gamon, J.A., Gough, C.M., Griffis, T., Helbig, M., Hollinger, D., Humphreys, E., Ikawa, H., Iwata, H., Ju, Y., Knowles, J.F., Knox, S.H., Kobayashi, H., Kolb, T., Law, B., Lee, X., Litvak, M., Liu, H., Munger, J.W., Noormets, A., Novick, K., Oberbauer, S.F., Oechel, W., Oikawa, P., Papuga, S.A., Pendall, E., Prajapati, P., Prueger, J., Quinton, W.L., Richardson, A.D., Russell, E.S., Scott, R.L., Starr, G., Staebler, R., Stoy, P.C., Stuart-Haëntjens, E., Sonnentag, O., Sullivan, R.C., Suyker, A., Ueyama, M., Vargas, R., Wood, J.D., Zona, D., 2021. Representativeness of Eddy-Covariance flux footprints for areas surrounding AmeriFlux sites. Agric. For. Meteorol. 301–302, 108350. https://doi.org/10.1016/j.agrformet.2021.108350

Chukalla, A.D., Mul, M.L., van der Zaag, P., van Halsema, G., Mubaya, E., Muchanga, E., den Besten, N., Karimi, P., 2022. A framework for irrigation performance assessment using WaPOR data: the case of a sugarcane estate in Mozambique. Hydrol. Earth Syst. Sci. 26, 2759–2778. https://doi.org/10.5194/hess-26-2759-2022

Congalton, R.G., 1991. A review of assessing the accuracy of classifications of remotely sensed data. Remote Sens. Environ. 37, 35–46. https://doi.org/10.1016/0034-4257(91)90048-B

Conlon, T., Small, C., Modi, V., 2022. A Multiscale Spatiotemporal Approach for Smallholder Irrigation Detection. Front. Remote Sens. 3. https://doi.org/10.3389/frsen.2022.871942

Cortes, C., Vapnik, V., 1995. Support-vector networks. Mach. Learn. 20, 273–297. https://doi.org/10.1007/BF00994018

Crawford, C.J., Roy, D.P., Arab, S., Barnes, C., Vermote, E., Hulley, G., Gerace, A., Choate, M., Engebretson, C., Micijevic, E., Schmidt, G., Anderson, C., Anderson, M., Bouchard, M., Cook, B., Dittmeier, R., Howard, D., Jenkerson, C., Kim, M., Kleyians, T., Maiersperger, T., Mueller, C., Neigh, C., Owen, L., Page, B., Pahlevan, N., Rengarajan, R., Roger, J.-C., Sayler, K., Scaramuzza, P., Skakun, S., Yan, L., Zhang, H.K., Zhu, Z., Zahn, S., 2023. The 50-year Landsat collection 2 archive. Sci. Remote Sens. 8, 100103. https://doi.org/10.1016/j.srs.2023.100103

Damtie, B.B., Mengistu, D.A., Waktola, D.K., Meshesha, D.T., 2022. Impacts of Soil and Water Conservation Practice on Soil Moisture in Debre Mewi and Sholit Watersheds, Abbay Basin, Ethiopia. Agriculture 12, 417. https://doi.org/10.3390/agriculture12030417

Deines, J.M., Kendall, A.D., Crowley, M.A., Rapp, J., Cardille, J.A., Hyndman, D.W., 2019. Mapping three decades of annual irrigation across the US High Plains Aquifer using Landsat and Google Earth Engine. Remote Sens. Environ. 233, 111400. https://doi.org/10.1016/j.rse.2019.111400

Demarez, V., Helen, F., Marais-Sicre, C., Baup, F., 2019. In-Season Mapping of Irrigated Crops Using Landsat 8 and Sentinel-1 Time Series. Remote Sens. https://doi.org/10.3390/rs11020118

Deng, Y., Jiang, W., Tang, Z., Ling, Z., Wu, Z., 2019. Long-Term Changes of Open-Surface Water Bodies in the Yangtze River Basin Based on the Google Earth Engine Cloud Platform. Remote Sens. https://doi.org/10.3390/rs11192213

Dile, Y.T., Ayana, E.K., Worqlul, A.W., Xie, H., Srinivasan, R., Lefore, N., You, L., Clarke, N., 2020. Evaluating satellite-based evapotranspiration estimates for hydrological applications in data-scarce regions: A case in Ethiopia. Sci. Total Environ. 743, 140702. https://doi.org/10.1016/j.scitotenv.2020.140702

Dile, Y.T., Tekleab, S., Ayana, E.K., Gebrehiwot, S.G., Worqlul, A.W., Bayabil, H.K., Yimam, Y.T., Tilahun, S.A., Daggupati, P., Karlberg, L., Srinivasan, R., 2018. Advances in Water Resources Research in the Upper Blue Nile Basin and the Way Forward: A Review. J. Hydrol. 560, 407–423. https://doi.org/10.1016/j.jhydrol.2018.03.042

Doherty, C.T., Johnson, L.F., Volk, J., Mauter, M.S., Bambach, N., McElrone, A.J., Alfieri, J.G., Hipps, L.E., Prueger, J.H., Castro, S.J., Alsina, M.M., Kustas, W.P., Melton, F.S., 2022. Effects of meteorological and land surface modeling uncertainty on errors in winegrape ET calculated with SIMS. Irrig. Sci. 40, 515–530. https://doi.org/10.1007/s00271-022-00808-9

Dubeau, P., King, D., Unbushe, D., Rebelo, L.-M., 2017. Mapping the Dabus Wetlands, Ethiopia, Using Random Forest Classification of Landsat, Palsar and Topographic Data. Remote Sens. 9, 1056. https://doi.org/10.3390/rs9101056

Duguma, T.A., Duguma, G.A., 2022. Assessment of Groundwater Potential Zones of Upper Blue Nile River Basin Using Multi-Influencing Factors Under GIS and RS Environment: A Case Study on Guder Watersheds, Abay Basin, Oromia Region, Ethiopia. Geofluids 2022, 1–26. https://doi.org/10.1155/2022/1172039

Elnashar, A., Zeng, H., Wu, B., Fenta, A.A., Nabil, M., Duerler, R., 2021. Soil erosion assessment in the Blue Nile Basin driven by a novel RUSLE-GEE framework. Sci. Total Environ. 793, 148466. https://doi.org/10.1016/j.scitotenv.2021.148466

Elnmer, A., Khadr, M., Allam, A., Kanae, S., Tawfik, A., 2018. Assessment of Irrigation Water Performance in the Nile Delta Using Remotely Sensed Data. Water. https://doi.org/10.3390/w10101375

Elsayed, H., Ibrahim, H., Farag, H., Sobeih, M.F., 2022. Remote sensing-based techniques for water management in small-scale farms in arid climate. Water Supply 22, 6692–6714. https://doi.org/10.2166/ws.2022.288

Elshaikh, A.E., Jiao, X., Yang, S., 2018. Performance evaluation of irrigation projects: Theories, methods, and techniques. Agric. Water Manag. https://doi.org/10.1016/j.agwat.2018.02.034

Eshete, D.G., Sinshaw, B.G., Legesse, K.G., 2020. Critical review on improving irrigation water use efficiency: Advances, challenges, and opportunities in the Ethiopia context. Water-Energy Nexus. https://doi.org/10.1016/j.wen.2020.09.001

FAO, World Bank, 2022. Irrigating from space: Using remote sensing for agricultural water management. https://doi.org/10.4060/cc3745en

Farhan, M., Wu, T., Amin, M., Tariq, A., Guluzade, R., Alzahrani, H., 2024. Monitoring and prediction of the LULC change dynamics using time series remote sensing data with Google Earth Engine. Phys. Chem. Earth Parts ABC 103689. https://doi.org/10.1016/j.pce.2024.103689

Fenta, A.A., Rientjes, T., Haile, A.T., Reggiani, P., 2014. Satellite Rainfall Products and Their Reliability in the Blue Nile Basin, in: Melesse, A.M., Abtew, W., Setegn, S.G. (Eds.), Nile River Basin. Springer International Publishing, Cham, pp. 51–67. https://doi.org/10.1007/978-3-319-02720-3_4

Fernandez, E., 2023. Editorial note on terms for crop evapotranspiration, water use efficiency and water productivity. Agric. Water Manag. 289, 108548. https://doi.org/10.1016/j.agwat.2023.108548

Fernandez, J.E., Alcon, F., Diaz-Espejo, A., Hernandez-Santana, V., Cuevas, M.V., 2020. Water use indicators and economic analysis for on-farm irrigation decision: A case study of a super high density olive tree orchard. Agric. Water Manag. 237, 106074. https://doi.org/10.1016/j.agwat.2020.106074

Ferreira, S., Sanchéz, J.M., Gonçalves, J.M., 2021. Exploring the Potential of Remote Sensing in Irrigation Management at District Scale. Study on Lis Valley, Portugal, in: da Costa Sanches Galvão, J.R., Duque de Brito, P.S., dos Santos Neves, F., da Silva Craveiro, F.G., de Amorim Almeida, H., Correia Vasco, J.O., Pires Neves, L.M., de Jesus Gomes, R., de Jesus Martins Mourato, S., Santos Ribeiro, V.S. (Eds.), Proceedings of the 1st International Conference on Water Energy Food and Sustainability (ICoWEFS 2021). Springer International Publishing, Cham, pp. 806–811. https://doi.org/10.1007/978-3-030-75315-3_85

Foody, G.M., 2002. Status of land cover classification accuracy assessment. Remote Sens. Environ. 80, 185–201. https://doi.org/10.1016/S0034-4257(01)00295-4

Foster, T., Mieno, T., Brozovic, N., 2020. Satellite-Based Monitoring of Irrigation Water Use: Assessing Measurement Errors and Their Implications for Agricultural Water Management Policy. Water Resour. Res. https://doi.org/10.1029/2020wr028378

Friedman, J.H., 2001. Greedy function approximation: A gradient boosting machine. Ann. Stat. 29. https://doi.org/10.1214/aos/1013203451

Gao, B., 1996. NDWI—A normalized difference water index for remote sensing of vegetation liquid water from space. Remote Sens. Environ. https://doi.org/10.1016/s0034-4257(96)00067-3

Gao, Q., Zribi, M., Escorihuela, M.J., Baghdadi, N., Seguí, P.Q., 2018. Irrigation Mapping Using Sentinel-1 Time Series at Field Scale. Remote Sens. https://doi.org/10.3390/rs10091495

Gebremichael, M., Anagnostou, E.N., Bitew, M.M., 2010. Critical Steps for Continuing Advancement of Satellite Rainfall Applications for Surface Hydrology in the Nile River Basin. JAWRA J. Am. Water Resour. Assoc. 46, 361–366. https://doi.org/10.1111/j.1752-1688.2010.00428.x

Gebul, M.A., 2021. Trend, Status, and Challenges of Irrigation Development in Ethiopia—A Review. Sustainability 13, 5646. https://doi.org/10.3390/su13105646

Getachew, B., Manjunatha, B.R., Gangadhara Bhat, H., 2020. Spatio-Temporal Distribution of Aerosol Optical Depth and Cloud Properties Over Lake Tana Basin, Upper Blue Nile River Basin, Ethiopia. Remote Sens. Appl. Soc. Environ. 20, 100401. https://doi.org/10.1016/j.rsase.2020.100401

Getnet, T., Mulu, A., 2021. Assessment of soil erosion rate and hotspot areas using RUSLE and multi-criteria evaluation technique at Jedeb watershed, Upper Blue Nile, Amhara Region, Ethiopia. Environ. Chall. https://doi.org/10.1016/j.envc.2021.100174

Ghorbanpour, A.K., Kisekka, I., Afshar, A., Hessels, T., Taraghi, M., Hessari, B., Tourian, M.J., Duan, Z., 2022. Crop Water Productivity Mapping and Benchmarking Using Remote Sensing and Google Earth Engine Cloud Computing. Remote Sens. 14, 4934. https://doi.org/10.3390/rs14194934

Gill, M.A., 1978. Flood routing by the Muskingum method. J. Hydrol. 36, 353–363. https://doi.org/10.1016/0022-1694(78)90153-1

Gitelson, A., Merzlyak, M.N., 1994. Quantitative estimation of chlorophyll-a using reflectance spectra: Experiments with autumn chestnut and maple leaves. J. Photochem. Photobiol. B 22, 247–252. https://doi.org/10.1016/1011-1344(93)06963-4

Gleixner, S., Demissie, T., Diro, G.T., 2020. Did ERA5 Improve Temperature and Precipitation Reanalysis over East Africa? Atmosphere 11, 996. https://doi.org/10.3390/atmos11090996

Gorelick, N., Hancher, M., Dixon, M.J., Ilyushchenko, S., Thau, D., Moore, R., 2017. Google Earth Engine: Planetary-scale geospatial analysis for everyone. Remote Sens. Environ. https://doi.org/10.1016/j.rse.2017.06.031

Gumindoga, W., Rientjes, T.H.M., Haile, A.T., Dube, T., 2014. Predicting Streamflow for Land Cover Changes in the Upper Gilgel Abay River Basin, Ethiopia: A TOPMODEL Based Approach. Phys. Chem. Earth Parts ABC 76–78, 3–15. https://doi.org/10.1016/j.pce.2014.11.012

Gupta, A., Singh, R.K., Kumar, M., Sawant, C.P., Gaikwad, B.B., 2022. On-farm irrigation water management in India: Challenges and research gaps*. Irrig. Drain. 71, 3–22. https://doi.org/10.1002/ird.2637

Gupta, H.V., Kling, H., Yilmaz, K.K., Martinez, G.F., 2009. Decomposition of the mean squared error and NSE performance criteria: Implications for improving hydrological modelling. J. Hydrol. https://doi.org/10.1016/j.jhydrol.2009.08.003

Habib, E., Haile, A., Sazib, N., Zhang, Y., Rientjes, T., 2014. Effect of Bias Correction of Satellite-Rainfall Estimates on Runoff Simulations at the Source of the Upper Blue Nile. Remote Sens. 6, 6688–6708. https://doi.org/10.3390/rs6076688

Haileslassie, A., Agide, Z., Erkossa, T., Hoekstra, D., Schmitter, P., Langan, S.J., 2016. On-farm smallholder irrigation performance in Ethiopia: From water use efficiency to equity and sustainability.

Haj-Amor, Z., Ritzema, H., Hashemi, H., Bouri, S., 2018. Surface irrigation performance of date palms under water scarcity in arid irrigated lands. Arab. J. Geosci. 11, 27. https://doi.org/10.1007/s12517-017-3374-5

Higginbottom, T.P., Adhikari, R., Dimova, R., Redicker, S., Foster, T., 2021. Performance of large-scale irrigation projects in sub-Saharan Africa. Nat. Sustain. https://doi.org/10.1038/s41893-020-00670-7

Hird, J.N., DeLancey, E.R., McDermid, G.J., Kariyeva, J., 2017. Google Earth Engine, Open-Access Satellite Data, and Machine Learning in Support of Large-Area Probabilistic Wetland Mapping. Remote Sens. https://doi.org/10.3390/rs9121315

Hu, S., Mo, X., 2022. Diversified Evapotranspiration Responses to Climatic Change and Vegetation Greening in Eight Global Great River Basins. J. Hydrol. 613, 128411. https://doi.org/10.1016/j.jhydrol.2022.128411

Huete, A.R., 1988. A soil-adjusted vegetation index (SAVI). Remote Sens. Environ. 25, 295–309. https://doi.org/10.1016/0034-4257(88)90106-X

Ibrahim, A., Wayayok, A., Shafri, H.Z.M., Toridi, N.M., 2024. Remote Sensing Technologies for Unlocking New Groundwater Insights: A Comprehensive Review. J. Hydrol. X 23, 100175. https://doi.org/10.1016/j.hydroa.2024.100175

Irving, D., 2019. Python for Atmosphere and Ocean Scientists. J. Open Source Educ. 2, 37. https://doi.org/10.21105/jose.00037

Islam, A.T., Islam, A.S., Islam, G.T., Bala, S.K., Salehin, M., Choudhury, A.K., Dey, N.C., Mahboob, M.G., 2023. Simulation of water productivity of wheat in northwestern Bangladesh using multi-satellite data. Agric. Water Manag. 281, 108242. https://doi.org/10.1016/j.agwat.2023.108242

Jaafar, H.H., Mourad, R.M., Kustas, W.P., Anderson, M.C., 2022. A Global Implementation of Single- and Dual-Source Surface Energy Balance Models for Estimating Actual Evapotranspiration at 30-m Resolution Using Google Earth Engine. Water Resour. Res. 58, e2022WR032800. https://doi.org/10.1029/2022WR032800

Javadian, M., Behrangi, A., Gholizadeh, M., Tajrishy, M., 2019. METRIC and WaPOR Estimates of Evapotranspiration over the Lake Urmia Basin: Comparative Analysis and Composite Assessment. Water 11, 1647. https://doi.org/10.3390/w11081647

Jiang, D., Wang, K., 2019. The Role of Satellite-Based Remote Sensing in Improving Simulated Streamflow: A Review. Water 11, 1615. https://doi.org/10.3390/w11081615

Jorge, J., Vallbé, M., Soler, J.A., 2019. Detection of irrigation inhomogeneities in an olive grove using the NDRE vegetation index obtained from UAV images. Eur. J. Remote Sens. 52, 169–177. https://doi.org/10.1080/22797254.2019.1572459

Kansara, P., Li, W., El-Askary, H., Lakshmi, V., Piechota, T., Struppa, D., Abdelaty Sayed, M., 2021. An Assessment of the Filling Process of the Grand Ethiopian Renaissance Dam and Its Impact on the Downstream Countries. Remote Sens. 13, 711. https://doi.org/10.3390/rs13040711

Karatas, B.S., Akkuzu, E., Unal, H.B., Asik, S., Avci, M., 2009. Using satellite remote sensing to assess irrigation performance in Water User Associations in the Lower Gediz Basin, Turkey. Agric. Water Manag. 96, 982–990. https://doi.org/10.1016/j.agwat.2009.01.010

Karimi, P., Bongani, B., Blatchford, M., de Fraiture, C., 2019. Global Satellite-Based ET Products for the Local Level Irrigation Management: An Application of Irrigation Performance

Assessment in the Sugarbelt of Swaziland. Remote Sens. 11, 705. https://doi.org/10.3390/rs11060705

Ketchum, D., Jencso, K., Maneta, M.P., Melton, F., Jones, M.O., Jones, M.O., Huntington, J.L., 2020. IrrMapper: A Machine Learning Approach for High Resolution Mapping of Irrigated Agriculture Across the Western U.S. Remote Sens. https://doi.org/10.3390/rs12142328

Khaki, M., Awange, J., 2020. Altimetry-Derived Surface Water Data Assimilation Over the Nile Basin. Sci. Total Environ. 735, 139008. https://doi.org/10.1016/j.scitotenv.2020.139008

Khan, R., Gilani, H., Gilani, H., 2021. Global drought monitoring with big geospatial datasets using Google Earth Engine. Environ. Sci. Pollut. Res. https://doi.org/10.1007/s11356-020-12023-0

Kharrou, M.H., Page, M.L., Chehbouni, A., Simonneaux, V., Er-Raki, S., Jarlan, L., Ouzine, L., Khabba, S., Chehbouni, G., 2013. Assessment of Equity and Adequacy of Water Delivery in Irrigation Systems Using Remote Sensing-Based Indicators in Semi-Arid Region, Morocco. Water Resour. Manag. https://doi.org/10.1007/s11269-013-0438-5

Khatami, R., Southworth, J., Muir, C., Caughlin, T., Ayana, A.N., Brown, D.G., Liao, C., Agrawal, A., 2020. Operational Large-Area Land-Cover Mapping: An Ethiopia Case Study. Remote Sens. 12, 954. https://doi.org/10.3390/rs12060954

Laipelt, L., Kayser, R.H.B., Fleischmann, A.S., Ruhoff, A.L., Bastiaanssen, W.G.M., Bastiaanssen, W., Erickson, T.A., Melton, F., 2021. Long-term monitoring of evapotranspiration using the SEBAL algorithm and Google Earth Engine cloud computing. Isprs J. Photogramm. Remote Sens. https://doi.org/10.1016/j.isprsjprs.2021.05.018

Lakew, H.B., 2020. Investigating the Effectiveness of Bias Correction and Merging MSWEP with Gauged Rainfall for the Hydrological Simulation of the Upper Blue Nile Basin. J. Hydrol. Reg. Stud. 32, 100741. https://doi.org/10.1016/j.ejrh.2020.100741

Lakew, H.B., Moges, S.A., Asfaw, D.H., 2020. Hydrological Performance Evaluation of Multiple Satellite Precipitation Products in the Upper Blue Nile Basin, Ethiopia. J. Hydrol. Reg. Stud. 27, 100664. https://doi.org/10.1016/j.ejrh.2020.100664

Lakew, H.B., Moges, S.A., Asfaw, D.H., 2017. Hydrological Evaluation of Satellite and Reanalysis Precipitation Products in the Upper Blue Nile Basin: A Case Study of Gilgel Abbay. Hydrology 4, 39. https://doi.org/10.3390/hydrology4030039

Leroux, L., Jolivot, A., Bégué, A., Seen, D., Zoungrana, B., 2014. How Reliable is the MODIS Land Cover Product for Crop Mapping Sub-Saharan Agricultural Landscapes? Remote Sens. 6, 8541–8564. https://doi.org/10.3390/rs6098541

Leta, M.K., Demissie, T.A., Tränckner, J., 2022. Optimal Operation of Nashe Hydropower Reservoir under Land Use Land Cover Change in Blue Nile River Basin. Water 14, 1606. https://doi.org/10.3390/w14101606

Lewoyehu, M., Fentahun, D., Addisu, S., 2023. Evaluation of Koga irrigation water in Mecha district, Amhara Region, as an example of irrigation water quality in Northwestern Ethiopia. Appl. Water Sci. 13, 196. https://doi.org/10.1007/s13201-023-01997-0

Li, T., Johansen, K., McCabe, M.F., 2022. A machine learning approach for identifying and delineating agricultural fields and their multi-temporal dynamics using three decades of

Landsat data. ISPRS J. Photogramm. Remote Sens. 186, 83–101. https://doi.org/10.1016/j.isprsjprs.2022.02.002

Li, X., Xu, X., Wang, X., Xu, S., Tian, W., Tian, J., He, C., 2021. Assessing the Effects of Spatial Scales on Regional Evapotranspiration Estimation by the SEBAL Model and Multiple Satellite Datasets: A Case Study in the Agro-Pastoral Ecotone, Northwestern China. Remote Sens. 13, 1524. https://doi.org/10.3390/rs13081524

Liu, C.-C., Shieh, M.C., Ke, M.S., Wang, K.H., 2018. Flood prevention and emergency response system powered by Google Earth Engine. Remote Sens. https://doi.org/10.3390/rs10081283

Long, X., Li, X., Lin, H., Zhang, M., 2021. Mapping the vegetation distribution and dynamics of a wetland using adaptive-stacking and Google Earth Engine based on multi-source remote sensing data. Int. J. Appl. Earth Obs. Geoinformation. https://doi.org/10.1016/j.jag.2021.102453

Lubczynski, M.W., Leblanc, M., Batelaan, O., 2024. Remote sensing and hydrogeophysics give a new impetus to integrated hydrological models: A review. J. Hydrol. 633, 130901. https://doi.org/10.1016/j.jhydrol.2024.130901

Magidi, J., Nhamo, L., Mpandeli, S., Mabhaudhi, T., 2021. Application of the random forest classifier to map irrigated areas using google earth engine. Remote Sens. https://doi.org/10.3390/rs13050876

Malede, D.A., Agumassie, T.A., Kosgei, J.R., Pham, Q.B., Andualem, T.G., 2022a. Evaluation of Satellite Rainfall Estimates in a Rugged Topographical Basin Over South Gojjam Basin, Ethiopia. J. Indian Soc. Remote Sens. 50, 1333–1346. https://doi.org/10.1007/s12524-022-01530-x

Malede, D.A., Alamirew, T., Andualem, T.G., 2022b. Integrated and Individual Impacts of Land Use Land Cover and Climate Changes on Hydrological Flows over Birr River Watershed, Abbay Basin, Ethiopia. Water 15, 166. https://doi.org/10.3390/w15010166

Malede, D.A., Alamirew, T., Andualem, T.G., 2022c. Integrated and Individual Impacts of Land Use Land Cover and Climate Changes on Hydrological Flows over Birr River Watershed, Abbay Basin, Ethiopia. Water 15, 166. https://doi.org/10.3390/w15010166

Mamba, M.P., Shongwe, M.I., 2022. Spatial variability assessment of irrigation performance in the Lower Usuthu Smallholder Irrigation Project (LUSIP) in Eswatini. Model. Earth Syst. Environ. https://doi.org/10.1007/s40808-022-01368-9

Manderso, T.M., Mekonnen, Y.A., Worku, T.A., 2023. Application of GIS Based Analytical Hierarchy Process and Multicriteria Decision Analysis Methods to Identify Groundwater Potential Zones in Jedeb Watershed, Ethiopia. J. Groundw. Sci. Eng. 11, 221–236. https://doi.org/10.26599/JGSE.2023.9280019

Manivasagam, V.S., 2024. Remote sensing of irrigation: Research trends and the direction to next-generation agriculture through data-driven scientometric analysis. Water Secur. 21, 100161. https://doi.org/10.1016/j.wasec.2023.100161

Massari, C., Modanesi, S., Dari, J., Gruber, A., Gabrielle De Lannoy, Gabrielle J. M. De Lannoy, Manuela Girotto, Pere Quintana-Seguí, Michel Le Page, Lionel Jarlan, Mehrez Zribi,

Nadia Ouaadi, Mariette Vreugdenhil, Luca Zappa, Wouter Dorigo, Wolfgang Wagner, Joost Brombacher, Henk Pelgrum, Pauline Jaquot, Vahid Freeman, Espen Volden, Diego Fernandez Prieto, Angelica Tarpanelli, Silvia Barbetta, Luca Brocca, 2021. A Review of Irrigation Information Retrievals from Space and Their Utility for Users. Remote Sens. https://doi.org/10.3390/rs13204112

Maxwell, A.E., Warner, T.A., Fang, F., 2018. Implementation of machine-learning classification in remote sensing: an applied review. Int. J. Remote Sens. 39, 2784–2817. https://doi.org/10.1080/01431161.2018.1433343

McNamara, I., Baez-Villanueva, O.M., Zomorodian, A., Ayyad, S., Zambrano-Bigiarini, M., Zaroug, M., Mersha, A., Nauditt, A., Mbuliro, M., Wamala, S., Ribbe, L., 2021. How Well Do Gridded Precipitation and Actual Evapotranspiration Products Represent the Key Water Balance Components in the Nile Basin? J. Hydrol. Reg. Stud. 37, 100884. https://doi.org/10.1016/j.ejrh.2021.100884

Mekonnen, D.F., Duan, Z., Rientjes, T., Disse, M., 2018. Analysis of combined and isolated effects of land-use and land-cover changes and climate change on the upper Blue Nile River basin's streamflow. Hydrol. Earth Syst. Sci. https://doi.org/10.5194/hess-22-6187-2018

Mekonnen, Y.G., Alamirew, T., Chukalla, A.D., Hunegnaw, A.T., Malede, D.A., 2024. Comparison of Google Earth Engine Machine Learning Algorithms for Mapping Smallholder Irrigated Areas in a Mountainous Watershed, Upper Blue Nile Basin, Ethiopia. J. Indian Soc. Remote Sens. 52. https://doi.org/10.1007/s12524-024-01846-w

Mhawej, M., Caiserman, A., Nasrallah, A., Dawi, A., Bachour, R., Faour, G., 2020a. Automated evapotranspiration retrieval model with missing soil-related datasets: The proposal of SEBALI. Agric. Water Manag. https://doi.org/10.1016/j.agwat.2019.105938

Mhawej, M., Elias, G., Nasrallah, A., Faour, G., 2020b. Dynamic calibration for better SEBALI ET estimations: Validations and recommendations. Agric. Water Manag. https://doi.org/10.1016/j.agwat.2019.105955

Mhawej, M., Faour, G., 2020. Open-source Google Earth Engine 30-m evapotranspiration rates retrieval: The SEBALIGEE system. Environ. Model. Softw. https://doi.org/10.1016/j.envsoft.2020.104845

Mhawej, M., Gao, X., Reilly, J., Abunnasr, Y., 2022. SEBALIGEE v2: Global Evapotranspiration Estimation Replacing Hot/Cold Pixels with Machine Learning (preprint). Agricultural, Veterinary and Food Sciences. https://doi.org/10.1002/essoar.10512468.1

Modanesi, S., Massari, C., Bechtold, M., Lievens, H., Tarpanelli, A., Brocca, L., Zappa, L., De Lannoy, G.J.M., 2022. Challenges and benefits of quantifying irrigation through the assimilation of Sentinel-1 backscatter observations into Noah-MP. Hydrol. Earth Syst. Sci. 26, 4685–4706. https://doi.org/10.5194/hess-26-4685-2022

Mohammedshum, A.A., Maathuis, B.H.P., Mannaerts, C.M., Teka, D., 2023. Mapping Small-Scale Irrigation Areas Using Expert Decision Rules and the Random Forest Classifier in Northern Ethiopia. Remote Sens. 15, 5647. https://doi.org/10.3390/rs15245647

Moriasi, D.N., Arnold, J.G., Liew, M.W.V., Bingner, R.L., Harmel, R.D., Veith, T.L., 2007. Model Evaluation Guidelines for Systematic Quantification of Accuracy in Watershed Simulations. Trans. ASABE 50, 885–900. https://doi.org/10.13031/2013.23153

Mpakairi, K.S., Dube, T., Sibanda, M., Mutanga, O., 2023. Fine-scale characterization of irrigated and rainfed croplands at national scale using multi-source data, random forest, and deep learning algorithms. ISPRS J. Photogramm. Remote Sens. 204, 117–130. https://doi.org/10.1016/j.isprsjprs.2023.09.006

Mu, Q., Zhao, M., Running, S.W., 2011. Improvements to a MODIS global terrestrial evapotranspiration algorithm. Remote Sens. Environ. 115, 1781–1800. https://doi.org/10.1016/j.rse.2011.02.019

Mullissa, A.G., Vollrath, A., Vollrath, A., Odongo-Braun, C., Slagter, B., Balling, J., Gou, Y., Gorelick, N., Reiche, J., 2021. Sentinel-1 SAR Backscatter Analysis Ready Data Preparation in Google Earth Engine. Remote Sens. https://doi.org/10.3390/rs13101954

Munoz-Sabater, J., Dutra, E., Agustí-Panareda, A., Albergel, C., Arduini, G., Balsamo, G., Boussetta, S., Choulga, M., Harrigan, S., Hersbach, H., Martens, B., Miralles, D.G., Piles, M., Rodríguez-Fernández, N.J., Zsoter, E., Buontempo, C., Thépaut, J.-N., 2021. ERA5-Land: a state-of-the-art global reanalysis dataset for land applications. Earth Syst. Sci. Data 13, 4349–4383. https://doi.org/10.5194/essd-13-4349-2021

Nash, J.E., Sutcliffe, J.V., 1970. River flow forecasting through conceptual models part I — A discussion of principles☆. J. Hydrol. https://doi.org/10.1016/0022-1694(70)90255-6

Neale, C.M.U., Gonzalez-Dugo, M.P., Serrano-Perez, A., Campos, I., Mateos, L., 2021. Cotton canopy reflectance under variable solar zenith angles: Implications of use in evapotranspiration models. Hydrol. Process. 35, e14162. https://doi.org/10.1002/hyp.14162

Neitsch, S.L., Arnold, J.G., Kiniry, J.R., Williams, J.R., 2011. Soil and water assessment tool theoretical documentation version 2009. Texas Water Resources Institute.

Nooni, I.K., Wang, G., Hagan, D.F.T., Lu, J., Ullah, W., Li, S., 2019. Evapotranspiration and its Components in the Nile River Basin Based on Long-Term Satellite Assimilation Product. Water 11, 1400. https://doi.org/10.3390/w11071400

Norman, J.M., Kustas, W.P., Humes, K.S., 1995. Source approach for estimating soil and vegetation energy fluxes in observations of directional radiometric surface temperature. Agric. For. Meteorol. https://doi.org/10.1016/0168-1923(95)02265-y

Nourani, V., Gökçekuş, H., Gichamo, T., 2021. Ensemble Data-Driven Rainfall-Runoff Modeling Using Multi-Source Satellite and Gauge Rainfall Data Input Fusion. Earth Sci. Inform. 14, 1787–1808. https://doi.org/10.1007/s12145-021-00615-4

NRCS, 2004. NRCS national engineering handbook. Part 630: Hydrology.

Osgouei, P.E., Kaya, S., Sertel, E., Alganci, U., 2019. Separating Built-Up Areas from Bare Land in Mediterranean Cities Using Sentinel-2A Imagery. Remote Sens. 11, 345. https://doi.org/10.3390/rs11030345

Ouattara, B., Forkuor, G., Zoungrana, B.J.-B., Dimobe, K., Danumah, J., Saley, B.M., Tondoh, J.E., 2020. Crops monitoring and yield estimation using sentinel products in semi-arid smallholder irrigation schemes. Int. J. Remote Sens. https://doi.org/10.1080/01431161.2020.1739355

Pageot, Y., Baup, F., Inglada, J., Baghdadi, N., Baghdadi, N., Demarez, V., 2020. Detection of Irrigated and Rainfed Crops in Temperate Areas Using Sentinel-1 and Sentinel-2 Time Series. Remote Sens. https://doi.org/10.3390/rs12183044

Pan, Z., Yang, S., Ren, X., Lou, H., Zhou, B., Wang, H., Zhang, Y., Li, H., Li, J., Dai, Y., 2023. GEE can prominently reduce uncertainties from input data and parameters of the remote sensing-driven distributed hydrological model. Sci. Total Environ. 870, 161852. https://doi.org/10.1016/j.scitotenv.2023.161852

Parajuli, P.B., Risal, A., Ouyang, Y., Thompson, A., 2022. Comparison of SWAT and MODIS Evapotranspiration Data for Multiple Timescales. Hydrology 9, 103. https://doi.org/10.3390/hydrology9060103

Pereira, L.S., Cordery, I., Iacovides, I., 2012. Improved indicators of water use performance and productivity for sustainable water conservation and saving. Agric. Water Manag. 108, 39–51. https://doi.org/10.1016/j.agwat.2011.08.022

Poudel, U., Stephen, H., Ahmad, S., 2021. Evaluating Irrigation Performance and Water Productivity Using EEFlux ET and NDVI. Sustainability. https://doi.org/10.3390/su13147967

Redicker, S., Dimova, R., Foster, T., 2022. Synthesising evidence on irrigation scheme performance in West Africa. J. Hydrol. 610, 127919. https://doi.org/10.1016/j.jhydrol.2022.127919

Ren, J., Shao, Y., Wan, H., Xie, Y., Campos, A., 2021. A two-step mapping of irrigated corn with multi-temporal MODIS and Landsat analysis ready data. ISPRS J. Photogramm. Remote Sens. 176, 69–82. https://doi.org/10.1016/j.isprsjprs.2021.04.007

Safi, C., Pareeth, S., Yalew, S., Van Der Zaag, P., Mul, M., 2023. Estimating agricultural water productivity using remote sensing derived data. Model. Earth Syst. Environ. https://doi.org/10.1007/s40808-023-01841-z

Sahlu, D., Nikolopoulos, E.I., Moges, S.A., Anagnostou, E.N., Hailu, D., 2016. First Evaluation of the Day-1 IMERG over the Upper Blue Nile Basin. J. Hydrometeorol. 17, 2875–2882. https://doi.org/10.1175/JHM-D-15-0230.1

Salama, A., ElGabry, M., El-Qady, G., Moussa, H.H., 2022. Evaluation of Grand Ethiopian Renaissance Dam Lake Using Remote Sensing Data and GIS. Water 14, 3033. https://doi.org/10.3390/w14193033

Santos, C., Lorite, I.J., Tasumi, M., Tasumi, M., Allen, R.G., Fereres, E., 2010. Performance assessment of an irrigation scheme using indicators determined with remote sensing techniques. Irrig. Sci. https://doi.org/10.1007/s00271-010-0207-7

Sawadogo, A., Kouadio, L., Traore, F., Zwart, S.J., Hessels, T., Gundogdu, K.S., 2020. Spatiotemporal Assessment of Irrigation Performance of the Kou Valley Irrigation Scheme

in Burkina Faso Using Satellite Remote Sensing-Derived Indicators. ISPRS Int. J. Geo-Inf. https://doi.org/10.3390/ijgi9080484

Senay, G.B., Asante, K., Artan, G., 2009. Water balance dynamics in the Nile Basin. Hydrol. Process. 23, 3675–3681. https://doi.org/10.1002/hyp.7364

Senay, G.B., Bohms, S., Singh, R., Gowda, P.H., Velpuri, N.M., Alemu, H., Verdin, J.P., 2013. Operational Evapotranspiration Mapping Using Remote Sensing and Weather Datasets: A New Parameterization for the SSEB Approach. J. Am. Water Resour. Assoc. https://doi.org/10.1111/jawr.12057

Senay, G.B., Budde, M.E., Verdin, J.P., Melesse, A.M., 2007. A Coupled Remote Sensing and Simplified Surface Energy Balance Approach to Estimate Actual Evapotranspiration from Irrigated Fields. Sensors. https://doi.org/10.3390/s7060979

Senay, G.B., Friedrichs, M., Morton, C., Parrish, G.E.L., Schauer, M., Khand, K., Kagone, S., Boiko, O., Huntington, J., 2022. Mapping actual evapotranspiration using Landsat for the conterminous United States: Google Earth Engine implementation and assessment of the SSEBop model. Remote Sens. Environ. 275, 113011. https://doi.org/10.1016/j.rse.2022.113011

Senay, G.B., Velpuri, N.M., Bohms, S., Demissie, Y., Gebremichael, M., 2014. Understanding the Hydrologic Sources and Sinks in the Nile Basin Using Multisource Climate and Remote Sensing Data Sets. Water Resour. Res. 50, 8625–8650. https://doi.org/10.1002/2013WR015231

Sentani, A., Niam, M.F., Boogaard, F.C., 2024. Probability of Erosion Utilizing Google Earth Engine and the RUSLE Method in the Tuntang Watershed. IOP Conf. Ser. Earth Environ. Sci. 1321, 012001. https://doi.org/10.1088/1755-1315/1321/1/012001

Sewenet, H.K., Anley, A.M., Getie, M.A., 2021. Performance evaluation and participatory varietal selection of improved bread wheat (Triticum aestivum L.) varieties, the case of Debre Elias District, Northwestern Ethiopia. Ecol. Genet. Genomics 19, 100086. https://doi.org/10.1016/j.egg.2021.100086

Seyoum, W.M., 2018. Characterizing Water Storage Trends and Regional Climate Influence Using Grace Observation and Satellite Altimetry Data in the Upper Blue Nile River Basin. J. Hydrol. 566, 274–284. https://doi.org/10.1016/j.jhydrol.2018.09.025

Sheffield, J., Wood, E.F., Pan, M., Beck, H., Coccia, G., Serrat-Capdevila, A., Verbist, K., 2018. Satellite Remote Sensing for Water Resources Management: Potential for Supporting Sustainable Development in Data-Poor Regions. Water Resour. Res. 54, 9724–9758. https://doi.org/10.1029/2017WR022437

Simane, B., Zaitchik, B.F., Ozdogan, M., 2013. Agroecosystem Analysis of the Choke Mountain Watersheds, Ethiopia. Sustainability. https://doi.org/10.3390/su5020592

Singh, R.K., Khand, K., Kagone, S., Schauer, M., Senay, G.B., Wu, Z., 2020. A novel approach for next generation water-use mapping using Landsat and Sentinel-2 satellite data. Hydrol. Sci. J.-J. Sci. Hydrol. https://doi.org/10.1080/02626667.2020.1817461

Sinshaw, B.G., Moges, M.A., Tilahun, S.A., Dokou, Z., Moges, S., Anagnostou, E., Eshete, D.G., Kindie, A.T., Bekele, E., Asese, M., Getie, W.A., 2020. Integration of SWAT and Remote

Sensing Techniques to Simulate Soil Moisture in Data Scarce Micro-watersheds: A Case of Awramba Micro-watershed in the Upper Blue Nile Basin, Ethiopia, in: Habtu, N.G., Ayele, D.W., Fanta, S.W., Admasu, B.T., Bitew, M.A. (Eds.), Advances of Science and Technology, Lecture Notes of the Institute for Computer Sciences, Social Informatics and Telecommunications Engineering. Springer International Publishing, Cham, pp. 294–314. https://doi.org/10.1007/978-3-030-43690-2_20

Stacke, T., Hagemann, S., 2021. HydroPy (v1.0): a new global hydrology model written in Python. Geosci. Model Dev. 14, 7795–7816. https://doi.org/10.5194/gmd-14-7795-2021

Su, Z., 2002. The Surface Energy Balance System (SEBS) for estimation of turbulent heat fluxes. Hydrol. Earth Syst. Sci. https://doi.org/10.5194/hess-6-85-2002

Sud, A., Sajan, B., Kanga, S., Singh, S.K., Singh, S., Durin, B., Kumar, P., Meraj, G., Sahariah, D., Debnath, J., Chand, K., 2024. Integrating RUSLE Model with Cloud-Based Geospatial Analysis: A Google Earth Engine Approach for Soil Erosion Assessment in the Satluj Watershed. Water 16, 1073. https://doi.org/10.3390/w16081073

Svoboda, J., Štych, P., Laštovička, J., Paluba, D., Kobliuk, N., 2022. Random Forest Classification of Land Use, Land-Use Change and Forestry (LULUCF) Using Sentinel-2 Data—A Case Study of Czechia. Remote Sens. 14, 1189. https://doi.org/10.3390/rs14051189

Taghvaeian, S., Neale, C.M.U., Osterberg, J., Sritharan, S.I., Watts, D.R., 2018. Remote sensing and GIS techniques for assessing irrigation performance: Case study in southern California. J. Irrig. Drain. Eng.-Asce. https://doi.org/10.1061/(asce)ir.1943-4774.0001306

Tamiru, H., Wagari, M., 2022. Comparison of ANN Model and GIS Tools for Delineation of Groundwater Potential Zones, Fincha Catchment, Abay Basin, Ethiopia. Geocarto Int. 37, 6736–6754. https://doi.org/10.1080/10106049.2021.1946171

Taye, M., Mengistu, D., Sahlu, D., 2023. Performance Evaluation of Multiple Satellite Rainfall Data Sets in Central Highlands of Abbay Basin, Ethiopia. Eur. J. Remote Sens. 56, 2233686. https://doi.org/10.1080/22797254.2023.2233686

Taye, M., Sahlu, D., Zaitchik, B.F., Neka, M., 2020. Evaluation of Satellite Rainfall Estimates for Meteorological Drought Analysis over the Upper Blue Nile Basin, Ethiopia. Geosciences 10, 352. https://doi.org/10.3390/geosciences10090352

Teferi, E., Uhlenbrook, S., Bewket, W., Wenninger, J., Simane, B., 2010. The Use of Remote Sensing to Quantify Wetland Loss in the Choke Mountain Range, Upper Blue Nile Basin, Ethiopia. Hydrol. Earth Syst. Sci. 14, 2415–2428. https://doi.org/10.5194/hess-14-2415-2010

Tegegne, E.B., Ma, Y., Chen, X., Ma, W., Wang, B., Ding, Z., Zhu, Z., 2021. Estimation of the Distribution of the Total Net Radiative Flux from Satellite and Automatic Weather Station Data in the Upper Blue Nile Basin, Ethiopia. Theor. Appl. Climatol. 143, 587–602. https://doi.org/10.1007/s00704-020-03397-9

Tekleab, S., Mohamed, Y.A., Uhlenbrook, S., Jochen Wenninger, 2014. Hydrologic responses to land cover change: the case of Jedeb mesoscale catchment, Abay/Upper Blue Nile basin, Ethiopia. Hydrol. Process. https://doi.org/10.1002/hyp.9998

Tekleab, S., Uhlenbrook, S., Savenije, H.H.G., Mohamed, Y.A., Wenninger, J., 2015. Modelling rainfall–runoff processes of the Chemoga and Jedeb meso-scale catchments in the Abay/Upper Blue Nile basin, Ethiopia. Hydrol. Sci. J.-J. Sci. Hydrol. https://doi.org/10.1080/02626667.2015.1032292

Tesfaye, A.T., Moges, M.A., Moges, M.M., Worqlul, A.W., Defersha, D.T., Wassie, A.B., 2023. Reservoir Sedimentation Evaluation Using Remote Sensing and GIS Approaches for the Reservoirs in the Upper Blue Nile Basin. Sustain. Water Resour. Manag. 9, 23. https://doi.org/10.1007/s40899-022-00792-0

Tucker, C.J., 1979. Red and photographic infrared linear combinations for monitoring vegetation. Remote Sens. Environ. 8, 127–150. https://doi.org/10.1016/0034-4257(79)90013-0

Usman, M., Mahmood, T., Conrad, C., Bodla, H.U., 2020. Remote sensing and modelling based framework for valuing irrigation system efficiency and steering indicators of consumptive water use in an irrigated region. Sustainability. https://doi.org/10.3390/su12229535

Velpuri, N.M., Senay, G.B., 2017. Partitioning Evapotranspiration into Green and Blue Water Sources in the Conterminous United States. Sci. Rep. 7, 6191. https://doi.org/10.1038/s41598-017-06359-w

Vidal, R., Ma, Y., Sastry, S.S., 2016. Principal Component Analysis, in: Vidal, R., Ma, Y., Sastry, S.S. (Eds.), Generalized Principal Component Analysis, Interdisciplinary Applied Mathematics. Springer, New York, NY, pp. 25–62. https://doi.org/10.1007/978-0-387-87811-9_2

Vizzari, M., 2022. PlanetScope, Sentinel-2, and Sentinel-1 Data Integration for Object-Based Land Cover Classification in Google Earth Engine. Remote Sens. 14, 2628. https://doi.org/10.3390/rs14112628

Vogels, M.F.A., De Jong, S.M., Sterk, G., Wanders, N., Bierkens, M.F.P., Addink, E.A., 2020. An object-based image analysis approach to assess irrigation-water consumption from MODIS products in Ethiopia. Int. J. Appl. Earth Obs. Geoinformation 88, 102067. https://doi.org/10.1016/j.jag.2020.102067

Vogels, M.F.A., Jong, S.M. de, Sterk, G., Addink, E.A., 2019a. Mapping irrigated agriculture in complex landscapes using SPOT6 imagery and object-based image analysis – A case study in the Central Rift Valley, Ethiopia –. Int. J. Appl. Earth Obs. Geoinformation. https://doi.org/10.1016/j.jag.2018.07.019

Vogels, M.F.A., Jong, S.M. de, Sterk, G., Douma, H., Addink, E.A., 2019b. Spatio-temporal patterns of smallholder irrigated agriculture in the horn of Africa using GEOBIA and Sentinel-2 imagery. Remote Sens. https://doi.org/10.3390/rs11020143

Volk, J.M., Huntington, J.L., Melton, F., Minor, B., Wang, T., Anapalli, S., Anderson, R.G., Evett, S., French, A., Jasoni, R., Bambach, N., Kustas, W.P., Alfieri, J., Prueger, J., Hipps, L., McKee, L., Castro, S.J., Alsina, M.M., McElrone, A.J., Reba, M., Runkle, B., Saber, M., Sanchez, C., Tajfar, E., Allen, R., Anderson, M., 2023. Post-processed data and graphical tools for a CONUS-wide eddy flux evapotranspiration dataset. Data Brief 48, 109274. https://doi.org/10.1016/j.dib.2023.109274

Wamala, F., Gidudu, A., Wanyama, J., Nakawuka, P., Bwambale, E., Chukalla, A.D., 2023. Assessment of irrigation water distribution using remotely sensed indicators: A case study of Doho Rice Irrigation Scheme, Uganda. Smart Agric. Technol. 4, 100184. https://doi.org/10.1016/j.atech.2023.100184

Wang, H., Zhao, H., 2020. Dynamic Changes of Soil Erosion in the Taohe River Basin Using the RUSLE Model and Google Earth Engine. Water 12, 1293. https://doi.org/10.3390/w12051293

Wanniarachchi, S., Sarukkalige, R., 2022. A Review on Evapotranspiration Estimation in Agricultural Water Management: Past, Present, and Future. Hydrology 9, 123. https://doi.org/10.3390/hydrology9070123

Weerasinghe, I., Bastiaanssen, W., Mul, M., Jia, L., Van Griensven, A., 2020. Can We Trust Remote Sensing Evapotranspiration Products Over Africa? Hydrol. Earth Syst. Sci. 24, 1565–1586. https://doi.org/10.5194/hess-24-1565-2020

Wegayehu, E.B., Muluneh, F.B., 2023. Super Ensemble Based Streamflow Simulation Using Multi-Source Remote Sensing and Ground Gauged Rainfall Data Fusion. Heliyon 9, e17982. https://doi.org/10.1016/j.heliyon.2023.e17982

Weitkamp, T., Jan Veldwisch, G., Karimi, P., De Fraiture, C., 2023. Mapping irrigated agriculture in fragmented landscapes of sub-Saharan Africa: An examination of algorithm and composite length effectiveness. Int. J. Appl. Earth Obs. Geoinformation 122, 103418. https://doi.org/10.1016/j.jag.2023.103418

Woldesenbet, T.A., Elagib, N.A., Ribbe, L., Heinrich, J., 2017. Hydrological Responses to Land Use/Cover Changes in the Source Region of the Upper Blue Nile Basin, Ethiopia. Sci. Total Environ. 575, 724–741. https://doi.org/10.1016/j.scitotenv.2016.09.124

Worqlul, A.W., Ayana, E.K., Maathuis, B.H.P., MacAlister, C., Philpot, W.D., Leyton, J.M.O., Steenhuis, T.S., 2018. Performance of bias corrected MPEG rainfall estimate for rainfall-runoff simulation in the upper Blue Nile Basin, Ethiopia. J. Hydrol. https://doi.org/10.1016/j.jhydrol.2017.01.058

Worqlul, A.W., Yen, H., Collick, A.S., Tilahun, S.A., Langan, S., Steenhuis, T.S., 2017. Evaluation of CFSR, TMPA 3B42 and Ground-Based Rainfall Data as Input for Hydrological Models, in Data-Scarce Regions: The Upper Blue Nile Basin, Ethiopia. CATENA 152, 242–251. https://doi.org/10.1016/j.catena.2017.01.019

Wu, D.D., Anagnostou, E.N., Wang, G., Moges, S., Zampieri, M., 2014. Improving the surface-ground water interactions in the Community Land Model: Case study in the Blue Nile Basin. Water Resour. Res. 50, 8015–8033. https://doi.org/10.1002/2013WR014501

Wu, Q., 2020. Geemap: A Python package for interactive mapping with Google Earth Engine. J. Open Source Softw. https://doi.org/10.21105/joss.02305

Wulder, M.A., Roy, D.P., Radeloff, V.C., Loveland, T.R., Anderson, M.C., Johnson, D.M., Healey, S., Zhu, Z., Scambos, T.A., Pahlevan, N., Hansen, M., Gorelick, N., Crawford, C.J., Masek, J.G., Hermosilla, T., White, J.C., Belward, A.S., Schaaf, C., Woodcock, C.E., Huntington, J.L., Lymburner, L., Hostert, P., Gao, F., Lyapustin, A., Pekel, J.-F., Strobl,

P., Cook, B.D., 2022. Fifty years of Landsat science and impacts. Remote Sens. Environ. 280, 113195. https://doi.org/10.1016/j.rse.2022.113195

Xiang, K., Ma, M., Liu, W., Dong, J., Zhu, X., Yuan, W., 2019. Mapping Irrigated Areas of Northeast China in Comparison to Natural Vegetation. Remote Sens. 11, 825. https://doi.org/10.3390/rs11070825

Xie, Y., Lark, T.J., 2021. Mapping annual irrigation from Landsat imagery and environmental variables across the conterminous United States. Remote Sens. Environ. https://doi.org/10.1016/j.rse.2021.112445

Xu, H., Duan, H., Li, Q., Han, C., 2024. Identification of Actual Irrigated Areas in Tropical Regions Based on Remote Sensing Evapotranspiration. Atmosphere 15, 492. https://doi.org/10.3390/atmos15040492

Xu, T., Deines, J., Kendall, A., Basso, B., Hyndman, D., 2019. Addressing Challenges for Mapping Irrigated Fields in Subhumid Temperate Regions by Integrating Remote Sensing and Hydroclimatic Data. Remote Sens. 11, 370. https://doi.org/10.3390/rs11030370

Yihune, W.N., Abera, A., Zewdie, M., Kibret, E.A., 2022. Assessing Farm Water Management and Performance of Koga Irrigation Scheme: a Case Study of Inguti Unit, Amhara Regional State, Ethiopia. Water Conserv. Sci. Eng. 7, 545–560. https://doi.org/10.1007/s41101-022-00162-z

Yimer, A.K., Haile, A.T., Hatiye, S.D., Ragettli, S., Taye, M.T., 2024. Comparative evaluation of the accuracy of mapping irrigated areas using sentinel 1 images in the Bilate and Gumara watersheds, Ethiopia. Cogent Eng. 11, 2357728. https://doi.org/10.1080/23311916.2024.2357728

Yuan, W., Liu, S., Zhou, Guangsheng, Zhou, Guoyi, Tieszen, L.L., Baldocchi, D., Bernhofer, C., Gholz, H., Goldstein, A.H., Goulden, M.L., Hollinger, D.Y., Hu, Y., Law, B.E., Stoy, P.C., Vesala, T., Wofsy, S.C., 2007. Deriving a light use efficiency model from eddy covariance flux data for predicting daily gross primary production across biomes. Agric. For. Meteorol. 143, 189–207. https://doi.org/10.1016/j.agrformet.2006.12.001

Zappa, L., Schlaffer, S., Bauer-Marschallinger, B., Nendel, C., Nendel, C., Nendel, C., Zimmerman, B., Dorigo, W., 2021. Detection and Quantification of Irrigation Water Amounts at 500 m Using Sentinel-1 Surface Soil Moisture. Remote Sens. https://doi.org/10.3390/rs13091727

Zeng, F., Song, C., Cao, Z., Xue, K., Lu, S., Chen, T., Liu, K., 2023. Monitoring Inland Water Via Sentinel Satellite Constellation: A Review and Perspective. ISPRS J. Photogramm. Remote Sens. 204, 340–361. https://doi.org/10.1016/j.isprsjprs.2023.09.011

Zeng, H., Elnashar, A., Wu, B., Zhang, M., Zhu, W., Tian, F., Ma, Z., 2022. A Framework for Separating Natural and Anthropogenic Contributions to Evapotranspiration of Human-Managed Land Covers in Watersheds Based on Machine Learning. Sci. Total Environ. 823, 153726. https://doi.org/10.1016/j.scitotenv.2022.153726

Zhang, C., Dong, J., Xie, Y., Zhang, X., Ge, Q., 2022. Mapping irrigated croplands in China using a synergetic training sample generating method, machine learning classifier, and Google

Earth Engine. Int. J. Appl. Earth Obs. Geoinformation 112, 102888. https://doi.org/10.1016/j.jag.2022.102888

Zhang, K., Kimball, J.S., Nemani, R.R., Running, S.W., 2010. A Continuous Satellite-Derived Global Record of Land Surface Evapotranspiration from 1983 to 2006: Global Record of Land Surface Evapotranspiration. Water Resour. Res. 46. https://doi.org/10.1029/2009WR008800

Zhang, K., Zhang, K., Kimball, J.S., Running, S.W., 2016. A review of remote sensing based actual evapotranspiration estimation. Wiley Interdiscip. Rev. Water. https://doi.org/10.1002/wat2.1168

Zhang, Y., Kong, D., Gan, R., Chiew, F.H.S., McVicar, T.R., Zhang, Q., Yang, Y., 2019. Coupled estimation of 500 m and 8-day resolution global evapotranspiration and gross primary production in 2002–2017. Remote Sens. Environ. 222, 165–182. https://doi.org/10.1016/j.rse.2018.12.031

Zhao, J., Huang, S., Huang, Q., Leng, G., Wang, H., Li, P., 2020. Watershed water-energy balance dynamics and their association with diverse influencing factors at multiple time scales. Sci. Total Environ. https://doi.org/10.1016/j.scitotenv.2019.135189

Zhu, X., Liu, Y., Xu, K., 2024. Study on mapping method of irrigated cultivated land–taking Nebraska as an example. Ecol. Indic. 166, 112271. https://doi.org/10.1016/j.ecolind.2024.112271

Zou, L., Zhan, C., Xia, J., Wang, T., Gippel, C.J., 2017. Implementation of evapotranspiration data assimilation with catchment scale distributed hydrological model via an ensemble Kalman Filter. J. Hydrol. 549, 685–702. https://doi.org/10.1016/j.jhydrol.2017.04.036

Zurqani, H.A., Allen, J., Post, C.J., Pellett, C.A., Walker, T., 2021. Mapping and quantifying agricultural irrigation in heterogeneous landscapes using Google Earth Engine. Remote Sens. Appl. Soc. Environ. https://doi.org/10.1016/j.rsase.2021.100590

Zwart, S.J., Leclert, L.M.C., 2010. A remote sensing-based irrigation performance assessment: a case study of the Office du Niger in Mali. Irrig. Sci. https://doi.org/10.1007/s00271-009-0199-3

Appendices

Appendix A: Meteorological Stations

Station Code	Station Name	Latitude	Longitude	Elevation	Station Description
1	Debre Markos	10.33	37.74	2440	Level 1
2	Dembecha	10.55	37.48	2117	Level 2
3	Debre Elias	10.30	37.47	2140	Level 2
4	Robgebeya	10.55	37.87	2940	Level 4

Appendix B: Monthly Stream Flow Measurement of Jedeb River at Yewula River Gauging Station

Year	Jan	Feb	Mar	Apr	May	Jun	Jul	Aug	Sep	Oct	Nov	Dec
1990	0.15	0.48	0.17	0.20	0.17	0.61	15.42	17.58	18.25	2.05	0.56	0.27
1991	0.49	0.24	0.52	2.03	0.87	4.53	25.47	44.70	32.97	4.56	1.31	0.92
1992	0.47	0.11	0.01	0.14	1.25	3.12	15.62	29.49	22.98	13.07	5.94	7.39
1993	1.02	0.75	0.46	1.92	5.10	10.72	31.67	32.19	19.15	27.37	10.32	7.56
1994	1.90	1.27	0.91	0.77	2.83	7.97	21.49	34.90	20.76	3.76	1.61	0.93
1995	2.16	0.82	0.86	1.62	3.42	6.11	20.30	16.90	15.08	4.84	2.51	1.65
1996	2.16	0.37	0.81	1.96	3.32	5.19	19.10	19.34	16.26	7.37	2.85	2.77
1997	2.42	2.08	1.88	2.56	3.22	4.26	14.89	18.60	11.13	6.01	6.99	5.14
1998	1.08	0.84	0.50	0.43	0.62	0.84	9.08	22.89	24.81	21.61	3.36	2.04
1999	1.88	1.37	0.95	0.85	1.13	3.07	12.86	19.27	11.13	8.30	2.38	1.16
2000	0.51	0.29	0.17	0.44	0.48	2.11	9.58	17.97	9.28	5.19	1.55	0.68
2001	0.34	0.10	0.20	0.30	0.27	2.11	12.67	24.76	7.44	2.08	0.73	0.21
2002	0.30	0.07	0.23	0.17	0.05	2.72	15.96	29.51	9.15	1.88	2.35	1.57
2003	1.59	1.31	1.73	1.30	0.32	3.32	19.26	34.26	10.86	1.69	3.97	2.93
2004	2.27	1.20	1.64	2.48	1.95	5.62	16.00	23.45	13.34	7.98	4.00	2.87
2005	2.23	1.72	2.58	1.84	2.00	2.96	17.04	24.56	34.59	8.605	4.02	2.78

Appendix C: Production data of farmers for 2021/22 and 2022/23 Seasons

Code	Lat	Long	Size (ha)	2021/22 Production	2022/23 Production
01	322096	1149150	0.375	9	4
02	322252	1149108	0.556	25	15.5
03	322884	1148911	0.75	38	26
04	322478	1149165	0.5	15	9
05	322901	1148768	0.41	32	20
06	322823	1148971	0.375	12	5
07	321956	1149049	0.451	19	12
08	321799	1148871	0.375	8	6
09	321937	1148961	0.5	16	7
10	322390	1149205	0.375	10	7
11	322311	1148988	0.56	22	15
12	322293	1149131	1	45	32
13	322009	1149017	0.5	22	15
14	322341	1149142	0.375	12	8
15	322514	1148856	0.5	18	10
16	321857	1148840	0.5	12	7
17	322598	1148852	0.5	12	7
18	321729	1148882	0.375	12	7
19	321629	1148974	0.375	8	5
20	322618	1148922	0.375	12	8
21	321963	1148719	0.5	12	8
22	321976	1149293	0.556	22	12
23	322184	1149187	0.375	12	8
24	322057	1149305	0.759	42	25
25	321993	1148736	0.5	10	9
26	322395	1149124	0.325	8	7
27	321755	1149401	0.375	14	10
28	321974	1149120	0.375	18	14
29	321845	1149389	0.375	18	12
30	322235	1148849	0.375	10	4
31	321604	1149004	0.556	18	14
32	321840	1149021	1	27	19
33	321968	1149177	0.75	28	19
34	322585	1149130	0.75	34	19
35	322257	1148864	0.375	8	6
36	322432	1149149	0.5	8	3
37	321922	1149316	1	27	18
38	322138	1149172	0.375	13	7
39	322065	1148860	0.375	5	3
40	322504	1148902	0.375	10	8
41	322099	1148904	0.5	16	9

About the author and List of Publications

1. Personal Information
    - Full Name: Yilkal Gebeyehu Mekonnen
    - Date of birth: 08 September 1988
    - Place of birth: Amber, East Gojjam, Ethiopia
    - Nationality: Ethiopian
    - Email address: Yilkalg3@gmail.com

      yilkal.gebeyehu@aau.edu.et
2. Educational background
    - PhD in Hydrology and Water Resource Management at Addis Ababa University (December 2020–July 2024)
    - M.Sc. in Remote Sensing and Geoinformatics from Addis Ababa University (November 2016 - July 2018)
    - B.Sc. in Natural Resource Management, Debre Markos University (November 2007–July 2010)
3. Work Experience
    - Lecturer at Debre Markos University for GIS and remote sensing (July 2018–November 2020), Debre Markos, Ethiopia.
    - Assistant Lecturer at Debre Markos University for GIS and remote sensing, Fundamentals of soils, Introduction to Hydrology courses (July 2014–November 2016), Debre Markos, Ethiopia.
    - Instructor at Bure Agriculture Technical Vocation Education Training, Burie, West Gojjam, Ethiopia (April 2013–July 2014)
    - Junior Instructor at Agarfa Agriculture Technical Vocation Education Training, Agarfa, Bale, Ethiopia (November 2010–March 2013)

List of Publications During PhD Study

1. Wakejo, W. K., Meshesha, B. T., Habtu, N. G., & Mekonnen, Y. G. (2022). Anthropogenic nitrate contamination of water resources in Ethiopia: An overview. *Water Supply*, *22*(11), 8157–8172. https://doi.org/10.2166/ws.2022.377
2. Malede, D. A., Andualem, T. G., Yibeltal, M., Alamirew, T., Demeke, G. G., & Mekonnen, Y. G. (2024). Climate change impacts on hydroclimatic variables over Awash basin, Ethiopia: A systematic review. *Discover Applied Sciences*, *6*(1), 1–11. https://doi.org/10.1007/s42452-024-05640-8
3. Mekonnen, Y.G., Alamirew, T., Chukalla, A.D., Hunegnaw, A.T., Malede, D.A., 2024. Comparison of Google Earth Engine Machine Learning Algorithms for Mapping Smallholder Irrigated Areas in a Mountainous Watershed, Upper Blue Nile Basin, Ethiopia. Journal of the Indian Society of Remote Sensing. https://doi.org/10.1007/s12524-024-01846-w
4. Mekonnen, Y.G., Alamirew, T., Tadesse, K.B., Chukalla, A.D., 2024. Monitoring small-scale irrigation performance using remote sensing in the Upper Blue Nile Basin, Ethiopia. Agricultural Water Management 300, 108928. https://doi.org/10.1016/j.agwat.2024.108928
5. Mekonnen, Y.G., Alamirew, T., Malede, D.A., Pareeth, S., Bantider, A., Chukalla, A.D., 2024. Tailoring the surface energy balance algorithm for land-improved (SEBALI) model using high-resolution land/use land cover for monitoring actual evapotranspiration. Agricultural Water Management 303, 109058. https://doi.org/10.1016/j.agwat.2024.109058
6. Mekonnen, Y.G., Alamirew, T., Chukalla, A.D., Malede, D.A., Yalew, S.G., Mengistu, A.F., 2024. Remote sensing in hydrology: A systematic review of its applications in the upper Blue Nile Basin, Ethiopia. HydroResearch 8, 1–12. https://doi.org/10.1016/j.hydres.2024.09.002